

---

This item was submitted to [Loughborough's Research Repository](#) by the author.  
Items in Figshare are protected by copyright, with all rights reserved, unless otherwise indicated.

## **Studies of electric discharges and their interactions with gases**

PLEASE CITE THE PUBLISHED VERSION

PUBLISHER

© Qiulin Yuan

PUBLISHER STATEMENT

This work is made available according to the conditions of the Creative Commons Attribution-NonCommercial-NoDerivatives 4.0 International (CC BY-NC-ND 4.0) licence. Full details of this licence are available at:  
<https://creativecommons.org/licenses/by-nc-nd/4.0/>

LICENCE

CC BY-NC-ND 4.0

REPOSITORY RECORD

Yuan, Qiulin. 2019. "Studies of Electric Discharges and Their Interactions with Gases". figshare.  
<https://hdl.handle.net/2134/22086>.

**Pilkington Library**



Author/Filing Title ..... YUAN, Q .....

Accession/Copy No.

040152486

Vol. No. ....

Class Mark .....

LOAN COPY

**25 JUN 1999**

0401524868



BADMINTON PRESS  
UNIT 1 BROOK ST  
SYSTON  
LEICESTER, LE7 1GD  
ENGLAND  
TEL : 0116 260 2917  
FAX : 0116 269 6639



# **Studies of Electric Discharges and Their Interactions with Gases**

by

**Qiulin YUAN B.Sc. M.Sc.**


A Doctoral Thesis

Submitted in partial fulfilment of the requirements for the  
award of Ph.D. of Loughborough University, (1997).

Supervisor: Dr. J. E. Harry

Department of Electronic and Electrical Engineering

© by Qiulin YUAN 1997.

 <b>Loughborough University</b> FUNDAMENTAL	
Date	Nw 97
Class	
Acc No.	040152486

9 9099307

*To my parents, wife and son*

## Abstract

Measurements of the effect of increasing the discharge column voltage gradient were investigated using argon based mixtures with nitrogen, oxygen and sulphur hexafluoride in a plasma torch. The theoretical calculation of the voltage gradient and the electron number density was based on the Saha equation which was modified for application to the gas mixtures. The investigations showed that a mixture of Ar and SF<sub>6</sub> was most effective and increased the voltage gradient to 0.5 V/mm from 0.3 V/mm. The best mixture was 89% Ar, 10% N<sub>2</sub>, 1% SF<sub>6</sub> based on the highest increase of the voltage gradient and the least added gas. A model has been developed to illustrate the effects of dissociation, excitation, ionisation of gases and their effects on the discharge column voltage gradient.

The mode of an electric discharge in Ar was investigated using spectroscopy. The study showed that for a glow discharge the 520.0 nm line and for an arc discharge the 427.1 nm line were unique. These lines were used to investigate a Glydarc electric discharge which was shown to be a mixture of the glow and the arc discharges.

Measurements of the transition of the glow to arc in Ar with discharge current ranging from 0.1 A to 1.0 A at atmospheric pressure showed that at the lower value of discharge current (0.25 A) the spectral lines were dominated by the near infra-red lines whereas at the higher value of discharge current (1.0 A) the spectral lines were included from the near infra-red to the near UV.

The Glydarc electric discharge has been studied in still and fast air flows at atmospheric pressure over a range of discharge currents from 100 mA to 3 A. The results showed that the increase of the discharge voltage with increasing discharge current was due to increase of the discharge column length which varied with time and the air flow rate and was not due to a positive dynamic characteristic.



## Acknowledgements

It is my great pleasure to acknowledge the kind advice, encouragement and patience of my supervisor and friend, Dr. John E. Harry, throughout this work.

I am grateful to the Overseas Research Students Awards Scheme for the grant that made this work possible. Thanks are also given to the Department of Electronic and Electric Engineering, Loughborough University for the studentship to support this study.

I also give thanks to Dr. R. Angus, Rees Instruments Ltd. for the kind free loan of the optical spectrum analyser, and advice concerning the practical consideration relating to the measurement of spectral lines to support the research on the diagnostics of the electric discharge using spectroscopy, and to Dr. M. Cormier, the Department of Physics, Orlean University in France for the helpful discussion and cooperation on the study of the Glydarc electric discharge.

Finally my sincere thanks go to my wife Hong for her support, understanding and encouragement.

# Contents

Title.....	1
Abstract.....	3
Acknowledgements.....	5
Contents.....	6
List of figures.....	12
List of tables.....	16
List of symbols.....	17
<b>Chapter 1. Introduction.....</b>	<b>22</b>
§1.1 Introduction.....	23
§1.2 Present work.....	23
§1.3 The structure of the thesis.....	24
<b>Chapter 2. Review of published work on the interaction between electric discharges and gases on the voltage gradient, spectroscopy and Glydarc electric discharge .....</b>	<b>28</b>
§2.1 Introduction.....	29
§2.2 Interaction between electric discharges and gases.....	29
§2.3 Voltage gradient in electric discharges.....	34
§2.4 Measurement of the voltage gradient.....	39
§2.5 Measurement of emission lines using spectroscopy .....	42
§2.5.1 Common spectral emission lines used for the electric discharge diagnosis.....	42
§2.6 The gases used for the electric welding.....	46
§2.6.1 Gas mixtures for gas metal arc	

welding (GMAW) processes.....	46
§2.6.2 Gases for gas tungsten arc welding (GTAW) and the plasma welding.....	48
§2.7 Research on the Glydarc electric discharge.....	48
§2.8 Summary.....	53
 <b>Chapter 3. Review of the electric discharge.....</b>	<b>55</b>
 §3.1 Gases.....	56
§3.1.1 Kinetic theory of gases.....	57
§3.1.2 Excitation, ionisation and dissociation.....	58
§3.1.3 Degree of ionisation.....	61
§3.1.4 Thermal conductivity.....	63
§3.1.5 Inelastic collisions of the first kind and the second kind.....	66
§3.2 The glow electric discharge.....	67
§3.2.1 The glow discharge column, the anode and the cathode.....	67
§3.2.2 The mobilities of particles.....	70
§3.2.3 The density of the discharge current.....	72
§3.3 Arc discharge.....	72
§3.3.1 The arc cathode, the anode and the discharge column.....	72
§3.3.2 The condition for stabilising electric discharge.....	74
§3.3.3 Excitation of spectra.....	75
§3.4 Summary.....	77
 <b>Chapter 4. Investigation of a Glydarc electric discharge.....</b>	<b>78</b>
 §4.1 Introduction.....	79
§4.2 Experimental arrangement of a Glydarc	

electric discharge and power supplies.....	80
§4.3 Characteristic of the discharge voltage and the discharge current in a Glydarc electric discharge.....	85
§4.3.1 A Glydarc electric discharge with an AC power supply with stabilising resistor only.....	85
§4.3.2 A Glydarc electric discharge with an AC power supply with an inductor.....	88
§4.3.3 A Glydarc electric discharge with a DC power supply.....	88
§4.4 Discussion.....	91
§4.5 Computer simulation of the gas profile of a Glydarc electric discharge.....	93
§4.5.1 Optimum shape of the Glydarc electrodes.....	94
§4.6 Measurement of the discharge voltage in an AC Glydarc electric discharge.....	95
§4.7 Simulation of the discharge voltage and the discharge current for a Glydarc electric discharge.....	99
§4.8 Summary of the results.....	100

<b>Chapter 5. Gas mixtures and their effect on increasing the discharge column voltage gradient in a plasm torch.....</b>	<b>104</b>
§5.1 Introduction.....	105
§5.2 The mobilities of electrons and positive ions.....	106
§5.3 Electric field strength in a plasma torch.....	108
§5.4 Tailoring the electric discharge gases for a plasma torch.....	109
§5.4.1 Mean free path of electrons.....	111
§5.4.2 Electronegativity of gases.....	112
§5.4.3 Ionisation and excitation potentials.....	113

§5.5 The Saha equation.....	114
§5.5.1 Degree of ionisation for gases.....	116
§5.5.2 Number density of electrons in the mixtures of gases.....	117
§5.5.3 Equation for the mixture of Ar and O <sub>2</sub> .....	119
§5.6 Numerical procedures.....	121
§5.7 Theoretical calculation.....	121
§5.7.1 The number density of electrons in different gas mixtures.....	122
§5.7.2 The calculation of the electric field strength.....	122
§5.8 Experimental arrangement.....	122
§5.9 Measurements of the discharge column voltage gradient.....	128
§5.9.1 The mixture of Ar and N <sub>2</sub> .....	128
§5.9.2 Free burning plasma in the mixture of Ar and O <sub>2</sub> surrounded by air at atmospheric pressure.....	134
§5.9.3 Mixtures of Ar, N <sub>2</sub> and SF <sub>6</sub> .....	138
§5.10 Discussion.....	138
§5.10.1 Effects of gas mixtures .....	138
§5.10.2 Collisions between electrons and atoms in mixtures of different gases.....	143
§5.10.3 Temperature effect.....	144
§5.10.3.1 Power dissipation.....	144
§5.10.3.2 Thermal conductivity in the plasma column.....	145
§5.10.3.3 Variation of temperature.....	146
§5.10.4 The discharge current density.....	146
§5.11 The summary.....	147

## **Chapter 6. Distinction between a glow discharge and an arc discharge using spectroscopy..... 150**

§6.1 Introduction.....	151
§6.1.1 Spectral lines used as a diagnostics	

for electric discharges.....	151
§6.2 Preliminary investigation.....	153
§6.2.1 Silicon photodiode monochromator.....	154
§6.2.2 Rofin monochromator using a photomultiplier tube.....	155
§6.2.3 Photodiodes array monochromator.....	158
§6.3 Computer-based scanning monochromator with a photomultiplier tube detector .....	160
§6.4 Calibration of the monochromator.....	160
§6.5 Experimental arrangement.....	161
§6.6 Experimental procedure.....	164
§6.6.1 Operating procedure for the glow discharge .....	164
§6.6.2 Operating procedure for the arc discharge.....	165
§6.6.3 Operating procedure for the Glydarc discharge .....	166
§6.7 Measurement of the discharge column voltage gradient.....	166
§6.8 Emission lines from a glow discharge.....	168
§6.9 Emission lines from an arc discharge with low discharge current.....	171
§6.10 Emission lines from an arc discharge with high discharge current .....	172
§6.11 Emission lines from the Glydarc electric discharge.....	176
§6.12 Comparison of the emission lines.....	178
§6.13 Discussion.....	178
§6.14 Summary.....	181

<b>Chapter 7. Conclusion and recommendations for further work.....</b>	<b>182</b>
--	------------

§7.1 Conclusion.....	183
§7.2 Further work.....	186

References.....	187
Appendices.....	201
Appendix A The programme of the PSPICE simulation for an electric discharge.....	202
Appendix B The program for the calculation of the number density of electrons and the electric field.....	203
Appendix C Number density of electrons in a single ionised gas.....	211
Appendix D Specification of MultiSpect™ 1/8 M monochromator.....	214

## List of figures

### Chapter 1

Fig. 1.1 The structure of the thesis.....	27
---	----

### Chapter 2

Fig. 2.1 The characteristic of the discharge voltage and the discharge current (Harry, 1993).....	35
Fig. 2.2 Dependence of the voltage gradient and the discharge current of an arc in air and nitrogen (King, 1961).....	37
Fig. 2.3 The voltage gradient as a function of current in different configuration of gas flows (King, 1964).....	38
Fig. 2.4 Schematic diagram of measuring the voltage gradient after Francis (1965).....	41
Fig. 2.5 The voltage gradient in a glow discharge ( $p=80$ Pa, discharge current= $6$ mA) (Barbeau, et al. 1991).....	43
Fig. 2.6 The basic configuration of a Glydarc electric discharge.....	49

### Chapter 3

Fig. 3.1 Degree of ionisation of Ar (one atmospheric pressure) (Cambel, 1963).....	62
Fig. 3.2a Thermal conductivity of Ar and He and their mixtures at one atmospheric pressure (Mondain-Monval, 1973).....	64
Fig. 3.2b Thermal conductivity of Ar and $N_2$ and $O_2$ at one atmospheric pressure (Cambel, 1963).....	65
Fig. 3.3 The voltage-current characteristic of an electric discharge at about $100$ Pa (Guile, 1986).....	68



Fig. 3.4 The general appearance of the glow discharge at a few hundred Pa (Beynon, 1972).....	69
---	----

**Chapter 4**

Fig. 4.1 Glydarc electrodes.....	81
Fig. 4.2 A schematic circuit of the Glydarc electric discharge.....	83
Fig. 4.3 The schematic diagram of the experimental arrangement.....	84
Fig. 4.4 Variation of discharge voltage and current using AC.....	86
Fig. 4.5 Waveform of the discharge voltage and current.....	87
Fig. 4.6 Variation of the discharge current and voltage using AC with a series inductance of 2 H.....	89
Fig. 4.7 Variation of discharge voltage and current using DC.....	90
Fig. 4.8 The gas profile in a Glydarc discharge.....	96
Fig. 4.9 Dependence of the discharge voltage and current measured with a stabilising resistor ( $R=2\text{ K}$ ).....	97
Fig. 4.10 Dependence of the discharge voltage and current measured with a R-L ( $R=1\text{ k}$ and $L=2\text{ H}$ ) in series.....	98
Fig. 4.11 Schematic circuit of the discharge for simulation using PSPICE.....	99
Fig. 4.12 Waveforms of the discharge voltage and current with a resistor ( $R=2\text{ k}$ ) in PSPICE.....	102
Fig 4.13 Waveforms of the discharge voltage and current with a R-L ( $R=1\text{ k}$ , $L=1\text{ H}$ ) in PSPICE.....	103

## Chapter 5

Fig. 5.1 Schematic diagram of the discharge voltage caused by effects of excitation, ionisation ( $R_{ei}$ ) and dissociation ( $R_{ds}$ ), electrodes fall ( $R_e$ ), and the heat loss ( $R_h$ ).....	110
Fig. 5.2 Calculated the number density of electrons with temperature in pure Ar and mixtures of different gases.....	123
Fig. 5.3 Calculated the discharge column voltage gradient in different gas mixtures.....	124
Fig. 5.4 Schematic of the experimental arrangement.....	125
Fig. 5.5 Schematic diagram of the orifice.....	126
Fig. 5.6 The air tight chamber.....	127
Fig. 5.7 Schematic of measurement of the discharge length.....	129
Fig. 5.8 Schematic of the cathode, the anode, the column voltages.....	130
Fig. 5.9 Dependence of the discharge column voltage gradient and the discharge current in different mixtures of Ar and $N_2$ surrounded by air at atmospheric pressure.....	132
Fig. 5.10 Variation of the discharge column voltage gradient and the addition of $N_2$ in different mixtures of Ar and $N_2$ at different currents surrounded by air.....	133
Fig 5.11 Dependence of the discharge column voltage gradient and the discharge current in the mixture of Ar and $N_2$ in the air tight chamber.....	135
Fig 5.12 Variation of the discharge column voltage gradient with the addition of $N_2$ in different mixtures of Ar and $N_2$ at different currents in the air tight chamber.....	136
Fig. 5.13 Dependence of the discharge column voltage gradient and the discharge current in the mixture of Ar and $O_2$ surrounded by air at atmospheric pressure.....	137

Fig. 5.14 Dependence of the discharge column voltage gradient and the discharge current in different mixtures of Ar and SF <sub>6</sub> .....	139
Fig. 5.15 Dependence of the discharge column voltage gradient and the discharge current in different mixtures of Ar, N <sub>2</sub> and SF <sub>6</sub> .....	140

## Chapter 6

Fig. 6.1 Schematic diagram of the monochromator Rofin 6000 series.....	156
Fig. 6.2 Spectral lines from a glow discharge (discharge current of 100 mA at 500 Pa (5 mbar)).....	157
Fig. 6.3 MultiSpec™ 1/8 M monochromator.....	159
Fig. 6.4 Schematic of the experimental arrangement using the Rees 6800 series monochromator.....	162
Fig. 6.5 Discharge tube used for a glow discharge.....	163
Fig. 6.6 Spectral lines from the glow discharge at discharge current of 150 mA, 500 Pa (5 mbar).....	169
Fig. 6.7 The energy levels of argon.....	170
Fig. 6.8 Different orders of light by a reflection grating.....	171
Fig. 6.9 Spectral lines from the glow discharge at discharge current of 150 mA, 500 Pa (5 mbar) with the filter of OG570.....	173
Fig. 6.10 Spectral lines from an arc discharge with low discharge current of 0.25 A, 0.5 A and 1.0 A.....	174
Fig. 6.11 The spectral lines from TIG arc at discharge current of 50 A.....	175
Fig. 6.12 Spectral lines from a Glydarc discharge with discharge current 1 A.....	177
Fig. 6.13 Schematic diagram of comparison of emission lines from the glow discharge and the arc discharge.....	179

## List of tables

### Chapter 2

Table 2.1 Discharge column voltage gradient in arc discharges.....	40
Table 2.2 Emission lines from a glow discharge with argon.....	44
Table 2.3 Emission lines used in the discharges.....	45
Table 2.4 The main research on the Glydarc electric discharge.....	54

### Chapter 3

Table 3.1 Ionisation potentials (eV).....	59
Table 3.2 Dissociation Energies.....	60
Table 3.3 The density of the discharge current.....	73

### Chapter 4

Table 4.1 Coefficients used in the simulation in FLUENT.....	94
--	----

## List of symbols

Symbol	Meaning	Unit
A	Atom	
A*	Excited atom	
A <sub>n</sub>	Nth level ionised particle	
a,b,c, etc.	General correlation coefficients	
D,d	Diameter	m
E	Electric field strength	Vm <sup>-1</sup>
E <sub>i</sub>	Energy interval	eV
ΔE	Difference of Energy	V
e	Electron charge	C
f	Frequency	Hz
G <sub>ij</sub>	statistic weighted constant	
HT	High voltage transformer	
h	Plank constant (6.63x10 <sup>-34</sup> Js)	
I	Electric current	A
ΔI	Difference of the current	A
i <sub>d</sub>	Instantaneous electric discharge current	A
J	Discharge current density	Am <sup>-2</sup>
K <sub>i+1</sub>	Equilibrium constant	
k	Boltsmann constant (1.38x10 <sup>-23</sup> JK <sup>-1</sup> )	
L	Inductance	H
l	Length	m
Δl	Difference of length	m

$m$	Mass	kg
$m_e$	Mass of electron	kg
$N$	Normal line	
$n$	Particle density	$m^{-3}$
$n_e$	Number density of electrons	$m^{-3}$
$n_H$	Number density of heavy particles	$m^{-3}$
$p$	Total absolute pressure	$Nm^{-2}$
$Q_e, Q_0$	Effective cross section of neutral particles	$m^2$
$Q_i$	Effective cross section of ions	$m^2$
$Q_{ie}$	Ionisation cross section	$m^2$
$R$	Electrical resistance	$\Omega$
$R$	Universal gas constant (8.31433)	$J(mol\ K)^{-1}$
$R, r$	Radial distance	m
$R_{ds}$	Corresponding resistance of dissociation	$\Omega$
$R_e$	Reynolds number	
$R_e$	Corresponding resistance of electrodes fall	$\Omega$
$R_{ei}$	Corresponding resistance of excitation and ionisation	$\Omega$
$R_h$	Corresponding resistance of heat losses	$\Omega$
$R_{neg}$	Corresponding resistance of electro-negative gas	$\Omega$
$T$	Temperature	K
$t$	Time	s
$u_d$	Electron drift velocity	$ms^{-1}$
$u, v, w$	Velocity in x, y, z directions	$ms^{-1}$
$V$	Volume	$m^3$

$V$	Voltage	V
$\Delta V$	Difference of the voltage	V
$V_a$	Anode fall voltage	V
$V_b$	Break down voltage	V
$V_c$	Cathode fall voltage	V
$V_d$	Discharge voltage	V
$V_{max}$	Magnitude of instantaneous voltage	V
$V_s$	Voltage drop along the stabilising impedance	V
$W$	Energy	eV
$x, y, z$	Co-ordinate distance	
$Z$	Partition function	

## Greek symbols

$\alpha, \alpha_i$	Degree of ionisation	
$\alpha_e$	Ratio of electrons to heavy particles	
$\alpha_n$	Angle	degree
$\Delta$	Measurement error	
$\delta$	Ratio of two different gases by volume	
$\varepsilon$	Dissipation ratio of kinetic energy of the turbulence	
$\varepsilon$	Error	
$\eta$	Efficiency	
$\theta$	Angle	degree
$\kappa$	Thermal conductivity	$\text{J (msK)}^{-1}$
$\kappa$	Kinetic energy of the turbulence	$\text{kg (ms}^{-1})^2$
$\lambda$	Wavelength	m
$\lambda$	Mean free path	m
$\lambda_e$	Electron mean free path	m
$\mu$	Mobility	$\text{m}^2 (\text{Vs})^{-1}$
$\mu$	Viscosity	$\text{Nsm}^{-2}$
$\mu_e$	Mobility of electrons	$\text{m}^2 (\text{Vs})^{-1}$
$\mu^+$	Mobility of ions	$\text{m}^2 (\text{Vs})^{-1}$
$\mu_t$	Effective turbulence viscosity	$\text{Nsm}^{-2}$
$\sigma$	Electrical conductivity	S
$\sigma_a$	Cross section of attachment	$\text{m}^2$
$v_e$	Drift velocity of electrons	$\text{ms}^{-1}$



$v_i$	Drift velocity of ions	$\text{ms}^{-1}$
$\phi$	Diameter	m
$\varphi$	Angle	degree

**Chapter One      Introduction**

## **§1.1 Introduction**

Electric discharges in gases have been known for more than a century. Understanding of the electric discharge was advanced by the study of electric discharge lamps, especially the fluorescent lamp which became a commercial reality in the 1940's in order to increase efficiency in converting electrical energy into light. The demonstration of a laser using a gas discharge to excite it was made by Javan et al in 1961. This stimulated further study of the electric discharge. There have also been dramatic improvements in understanding the basic physical phenomena on which the properties of the gas lasers depend; these improvements have made it possible to develop more compact, more powerful lasers for industrial applications. Recently more interest has developed in the use of electric discharge to destroy harmful gases at atmospheric pressure in the environment.

## **§1.2 Present work**

The initial object of this research was developed from a Glydarc electric discharge in which a third electrode (an auxiliary electrode) was inserted into the gap between the main electrodes in order to reduce the breakdown voltage. As a result the main transformer could be optimally designed to improve the effective power factor. The use of the Glydarc electric discharge was required to understand its characteristics of the discharge voltage and the discharge current and its discharge mode.

The discharge voltage and the discharge current characteristic of the Glydarc electric discharge was determined under different conditions of air flows. The discharge voltage of the Glydarc electric discharge fluctuated from time to time due to the inherent changing

length of the discharge column. This feature was strongly coupled with the fast air flows employed. The discharge voltage in the Glydarc electric discharge was difficult to be defined because the average voltage or the rms value was strongly influenced by the high peak transient discharge voltage. The measurement of the discharge voltage and the discharge current was explored.

High power input for electric discharges is necessary when it is required. In a glow discharge increasing the discharge current after a certain value causes the transition of the discharge mode from a glow to an arc, which should be avoided for example in electric discharge excited gas lasers because the arc discharge totally destroys the operation of laser output. In an arc discharge the large discharge current shortens the working life of the electrodes. The increase of the discharge voltage was preferred for high power input and directed to the use of gas and gas mixtures.

The research on using gas and gas mixtures to increase the power input was based on a plasma torch system because the higher discharge voltage would reduce the cross-section of cables and less discharge current will extend the working life of the cathode. The higher discharge voltage was explored using pure gas initially such as Ar and  $N_2$ , and  $O_2$ . The theoretical calculation was based on the Saha equation on condition that the arc discharge was in thermal equilibrium. The test results soon suggested the better gas would be a combination of different gases because the higher discharge voltage would be achieved by reducing the number density of electrons in the discharge column.

The determination of the discharge mode in a Glydarc electric discharge has led to the use of spectral analysis. The idea was based on the difference of the spectral lines

between the glow discharge and the arc discharge. The Plank's equation points out the wave length of emitted light is dependent upon the energy released from different levels of photon. Since the arc discharge and the glow discharge have bigger differences in degree of ionisation, electric field strength in the discharge column and the density of electrons, these features should be reflected from the spectral emission lines.

### **§1.3 The structure of the thesis**

Fig. 1.1 shows the structure of this thesis. Chapter 2 and chapter 3 are mainly concerned with the fundamental theory of the electric discharge and the gas, whereas chapter 4 and chapter 5 and chapter 6 are focussed on the application of the electric discharge and the interaction of the electric discharges with gases and the diagnostics of the electric discharges.

Chapter 2 is a review of published work on the interaction between electric discharge and gases, and the effect of gases on the voltage gradient and spectroscopy as well as a Glydarc electric discharge. It covers the interactions between the electric discharge and gases that occur in still and fast flows, the voltage gradient in arc discharges with different gas mediums, and spectral lines used in spectroscopy.

Chapter 3 presents a review of the electric discharge. It contains the basic theory of the glow discharge and the arc discharge, and the gas equation. The mobilities of ions and electrons are discussed. The condition for the operation of the electric discharge is given. The use of the spectral lines from the electric discharge for a method of arc diagnosis is discussed.

Chapter 4 describes the study of the Glydarc electric discharge which includes the interaction between the Glydarc electric discharge with slow and fast air flows. The characteristic of the Glydarc electric discharge in different air flows is given.

Chapter 5 describes the investigations carried out with different gases and gas mixtures on increasing the discharge column voltage gradient in a plasma torch. It contains the theoretical calculation of the number density of electrons using the Saha equation with different gases. The gradient of the discharge voltage in the plasma torch with Ar, and Ar based mixtures with  $N_2$ ,  $O_2$ , and  $SF_6$  is shown. The equivalent resistance of electric discharge gases is also described so as to increase the discharge voltage.

Chapter 6 describes the study carried out on the diagnosis of electric discharges using spectral analysis. It contains the basic spectral lines from the glow discharge and the arc discharge. The determination of the discharge mode based on the spectral lines from different discharges is given.

Chapter 7 presents the conclusion of this study and recommendation for further work.

The computer programs for simulation of the Glydarc electric discharge using PSPICE and for the calculation of the electron density using the Saha equation are given. The technical specifications for MultiSpec™ is given in the Appendices.

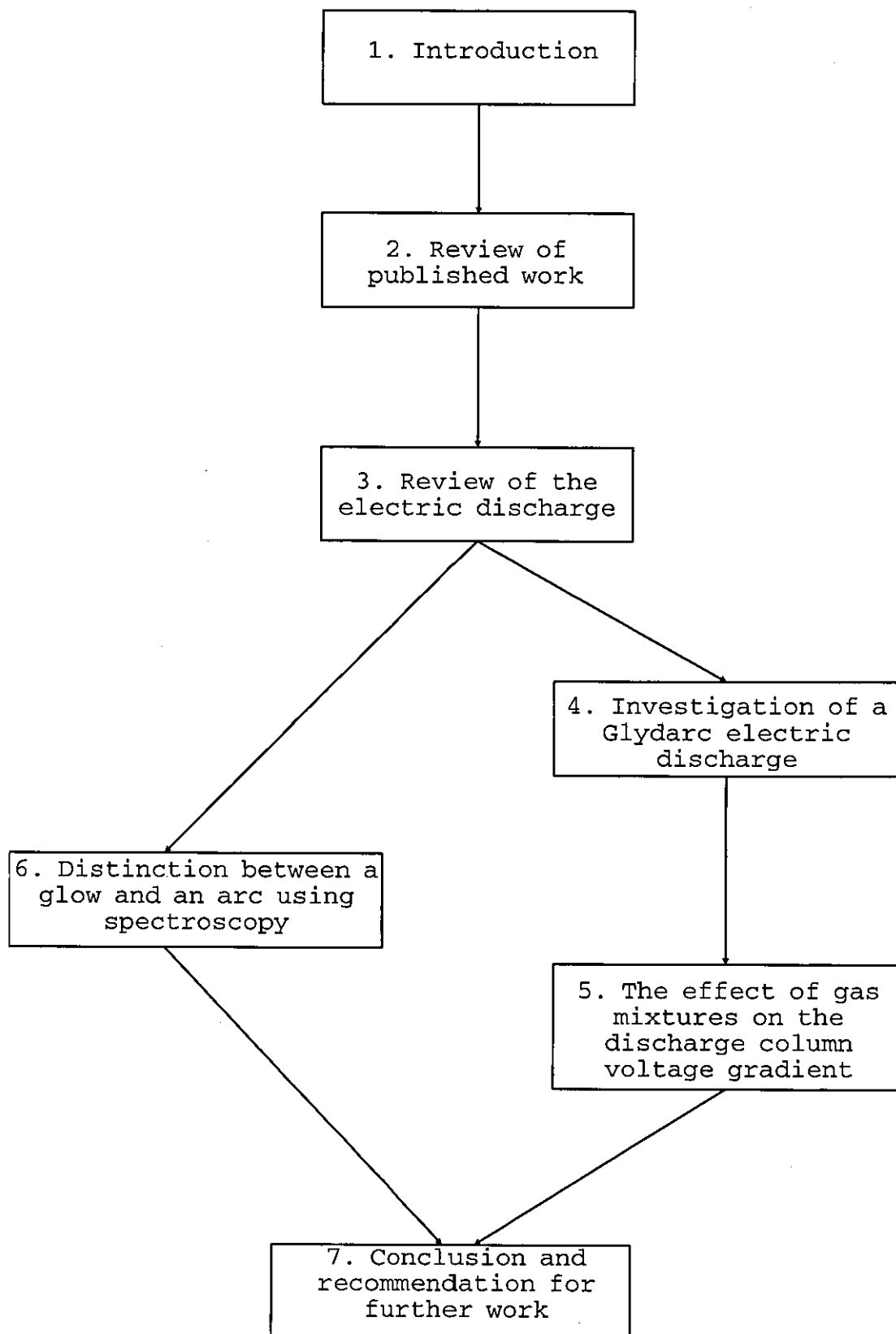


Fig. 1.1 The structure of the thesis

## **Chapter Two**

**Review of published work on the interaction between electric discharges and gases on the voltage gradient, spectroscopy, and Glydarc electric discharge**



## **§2.1 Introduction**

Electrical discharges with gases have a long and distinguished history (Beynon, 1972). The characteristic of the discharge voltage and the discharge current is dependent upon the role of the gas and gas flows, material and geometry of the electrode, the pressure of gases. However much of the physical behaviour of these interactions has not been understood, due to the underlying complex processes.

The employment of the electric discharges as a tool to destroy the harmful gases in the environment management has stimulated research into interaction between the electric discharges and the gas flows and the suitable discharge devices at atmospheric pressure with high power input. A key factor in the chemical reaction using the electric discharge is to keep the discharge as the glow discharge.

The literature covered by the electric discharges and the diagnostics of the discharge mode is vast. This review will emphasise those having a substantial element of gas or gas mixtures with the electric discharge and those using the emission spectral lines to diagnose the electric discharge. In particular, the research on the interaction of the electric discharges with gases, the voltage gradient on the discharge positive column and the discharge mode diagnosed using the spectral lines, and the Glydarc electric discharge device are given.

## **§2.2 Interaction between electric discharges and gases**

### **(1) Subsonic gas flows**

It is necessary to maintain a stable glow discharge. However, when the gas pressure or the discharge current is

increased, the glow discharge may become unstable and collapse into arc like filaments or streamers (Francis, 1956). Such an instability of the glow discharge is accompanied with a substantial decrease in the electron energy, well below the energy level of 1 eV, leading to little use for chemical reactions. The postulation (i.e. the instability of the electric discharge is due to thermal effects) forms the basic assumption in combining the electric discharge and the gas flow together in various discharge regions.

This assumption implies that local uneven heating decreases the gas density that increases in return the electron temperature, electron density, and electrical conductivity. Therefore the local current density increases and so does the Ohmic heating which causes the temperature of the gas to go up further and as a result instability occurs (Ecker et al, 1964). The mechanism in molecular gases is rather similar but more complicated (Nighan et al, 1964).

It is also expected to get a high power glow electric discharge when it is required. Unfortunately the aim cannot be achieved simply increasing the discharge voltage and the discharge current (Hill, 1971). One way to overcome such limits is to combine the electric discharge with various flow configurations of the active medium of gases. Then the gas flows can be utilised in disposing the waste heat by convecting it out of the discharge.

If the discharge is operated in a still gas, the interaction will occur between the still gas and the discharge. It is thus concluded that the convective and diffusion processes play a major role in the production of electrons and ions. The distribution of electrons and ions in the discharge region varies gradually from the inner to outer regimes.

Wassertroma et al (1978) studied the interaction between subsonic gas flows ( $\text{CO}_2\text{-N}_2\text{-He}$ ) and the glow discharge. The characteristic of the discharge voltage and the discharge current showed that the discharge voltage was increased to 8.5 kV at mass flow rate of 0.9 g/s from 4 kV at mass flow rate of 0.22 g/s whereby the discharge current was around 40 mA and the maximum pressure at inlet was 6,650 Pa. The reason behind the increase of the discharge voltage however was not explained.

It was shown that with the introduction of cooled rapidly flowing gas through the discharge column, the output radiation power was raised (Detusch et al, 1969; DeMaria, 1973; Harry et al, 1987). In addition to its role in removing heat, it was recognised that a uniform flow across the channel could improve the stability characteristic of the discharge (Eckbreth et al, 1972).

## **(2) Supersonic gas flows**

Investigations were carried out into the characteristics of the discharge voltage and the current influenced by supersonic gas flow and highly swirled and turbulent flow. It was shown that turbulent gas had a strong influence on the characteristics of electric discharges mainly due to

(1) the ambipolar diffusion,

(2) the increase of the effective heat conductivity of the discharge gas (Gentle et al, 1964; Schwartz et al, 1975).

These experiments showed that the stability criterion was not obvious as the traditional gas discharge expressed its stability decided by the slope of the discharge voltage

and the discharge current curve. (i.e. when the gas discharge becomes unstable it constricts and degenerates into bright filaments accompanied by a sharp increase in the current while the voltage decreases). Moreover it also showed that the stability of the gas discharge could be further enhanced if shock waves were intentionally introduced in the supersonic flow (Wasserstrom et al, 1978). The phenomenon is complicated and not fully understood.

It is very hard to deal with all the regions in the discharge at the same time due to the complexity of the discharge involved. Therefore research work was concentrated on the positive column of the discharge because the positive column is most widely used, being an important part in industrial applications. Brunet et al (1985) modelled a positive column of a cylindrical glow discharge with a flowing gas of  $N_2$ . The modelling was confined to the two-dimensional, weakly ionised and collision dominated gas discharge. Good agreement was obtained compared to the experimental results for electric discharges at low pressure in gas flows with low Reynolds numbers under the laminar gas profile.

Rubtsov et al (1988) researched the interaction between electric arc and turbulent gas flow in which studies were performed for an arc with a turbulent draught of Ar in a cylindrical channel. The study showed that the arc temperature changes more markedly in the initial segment, where the role of turbulent heat transport and reabsorption of radiation increases. Electrical conductivity in the turbulent flow was calculated taking account of temperature pulsation with ideal gas. The calculated values of the electrical conductivity coefficient in the turbulent flow were lower than those in the laminar. It explained partly the higher discharge voltage in the experiment.

Evans et al (1989) investigated the formation of streamers in a fast gas flow using a high speed cine camera at the flow rate of 0.022 kg/s at 5,000 Pa, corresponding to an average gas velocity of 340 m/s. Although the formation of streamers took place in electronegative gases at lower currents, they occurred at the same value of power. The voltage gradient in electronegative gases was higher due to the reduction of the electron density in the column. This confirmed the obtained results which had shown that the formation of streamers was due to thermal instabilities caused by non-uniform cooling by convection.

A model was developed in order to investigate the problem of ionising a high speed neutral gas with turbulent flow (Karditsas, 1990). The theoretical calculation, applicable for the high speed neutral gas flow through the turbulent coefficient and the conduction loss term, was based on the electron energy and particle balance equations. The results showed that the curves of the discharge voltage and the discharge current were affected by the magnitude of the turbulent diffusion coefficient, and the discharge parameters were affected by the high speed flow through the turbulent diffusion coefficient and conduction loss term. However this modelling study requires further experimental validation.

Galeev et al (1990) investigated a glow discharge in a supersonic gas stream. The experiment was focussed upon the influence on the properties of the discharge mode and the flow rate of the plasma forming gas, the geometry of the discharge chamber, the material of the electrodes and their thermal states. According to Galeev et al (1990), the most effective electrodes were those metals with high thermal conductivity and low voltage drop, providing helpful guidelines in choosing the electrode for the plasma processing.

Yahya (1990) also studied the relationship between the discharge column and the gas flow. His results claimed that the discharge column tended to follow the gas flow streamlines and contacted the downstream electrode. When the gas velocity was increased, the contact point was carried further along the direction of the gas flow. The discharge column touched the downstream electrode by crossing streamlines. This was a very interesting phenomena. However, Yahya did not provide a comprehensive knowledge on how the influence of the fast gas flow profiles and electric discharge acted on the crossing point at the downstream electrode.

The interaction of the gas flow with the electric discharge was also attempted in an arc plasma reactor. Huang et al (1991) studied the fluid dynamics numerically using general conservation equations and auxiliary relations. The two recirculation zones existed with low injection rate for a hollow cathode geometry. When the plasma gas flow rate was increased, the downstream recirculation zone was swept away leaving only an upstream recirculation zone.

### **§2.3 Voltage gradient in electric discharges**

The characteristic of the discharge voltage and the discharge current is paid much attention in all kinds of electric discharges. The voltage gradient in electric discharges can be derived from the V-I characteristic. Fig. 2.1 shows the general curve of the voltage gradient (Harry, 1993a).

The voltage gradient of the discharge column in arcs containing metal vapour of sodium (Na) and potassium (K) was measured using the technique of photographs by Hörmann (1935). The test was carried out using a free burning

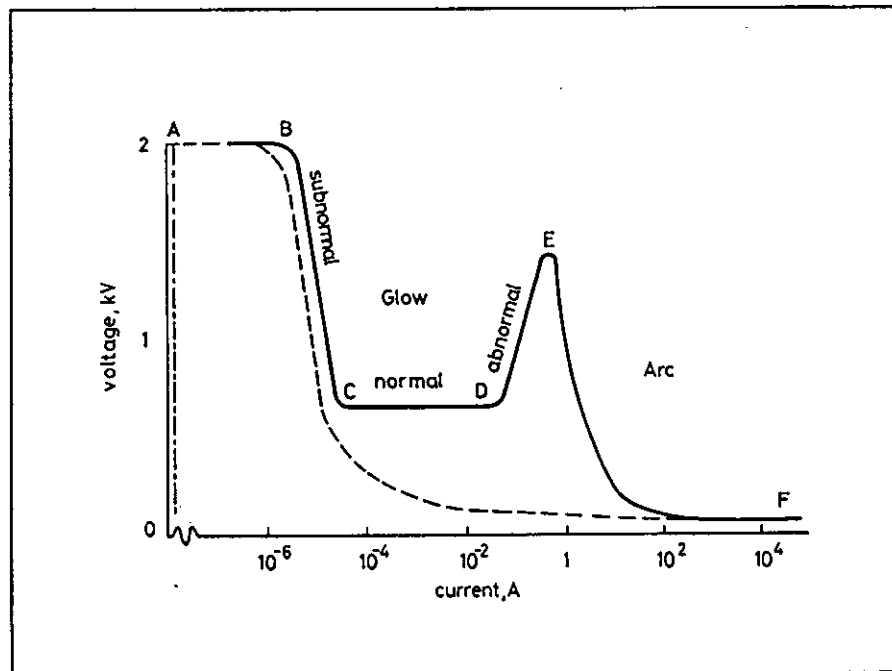


Fig. 2.1 The characteristic of the discharge voltage and the discharge current (Harry, 1993)  
(the broken line shows the variation of voltage gradient in the discharge column)

carbon arc with the discharge current of 10 A. He reported that the voltage gradients were 0.9 V/mm and 0.7 V/mm respectively.

Eberhagen (1955) measured the voltage gradient in the metal vapour of strontium (Sr) with an air-stabilized arc. The voltage gradient varied from 1.05 V/mm to 1.1 V/mm depending upon the concentration of Sr.

Somers and Smit (1956) measured the voltage gradient in an arc in  $N_2$  at one atmospheric pressure or higher. Maecker (1956) determined the voltage gradient in the carbon arc in air was 2 V/mm - 4 V/mm with currents ranging 4 - 12 A.

King (1961) investigated the voltage gradient of the free burning arc in air or  $N_2$ . His study covered the discharge current ranging from  $10^4$  A to  $10^4$  A. Fig. 2.2 showed the voltage gradient from his tests. The higher voltage gradient with  $N_2$  from the discharge current 10 A to 100 A was explained due to the formation of NO in air as the gas temperature increased.

King (1964) also did research on the voltage gradient of an arc column under forced convection in air or  $N_2$ . Fig. 2.3 shows the voltage gradient. The air flows varied with axial gas flow, inward radial gas flow to stabilised gas flow with up to sonic velocity. The higher voltage gradient was partly due to the forced convection. His research also showed that the diameter of the discharge column was reduced with forced air flow compared with the free burning arc.

De Galan (1965) determined the voltage gradient in 10 A DC arc with mixtures of carbon, salts (KCl, KF, LiF) and  $Al_2O_3$ . The voltage gradients varied from 1 V/mm to 1.6 V/mm.



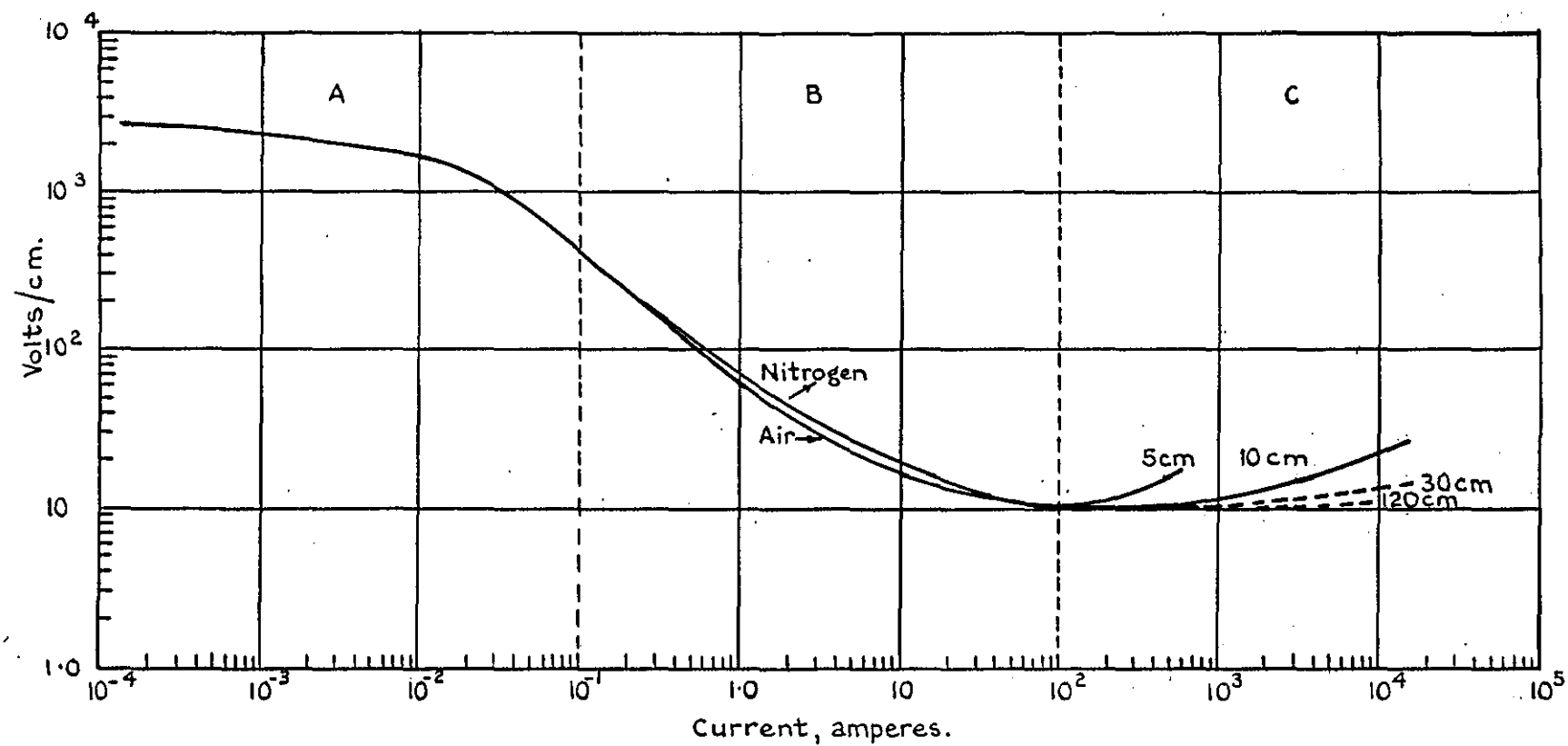


Fig. 2.2 Dependence of the voltage gradient and the discharge current of an arc in air and  $N_2$  (King, 1961)

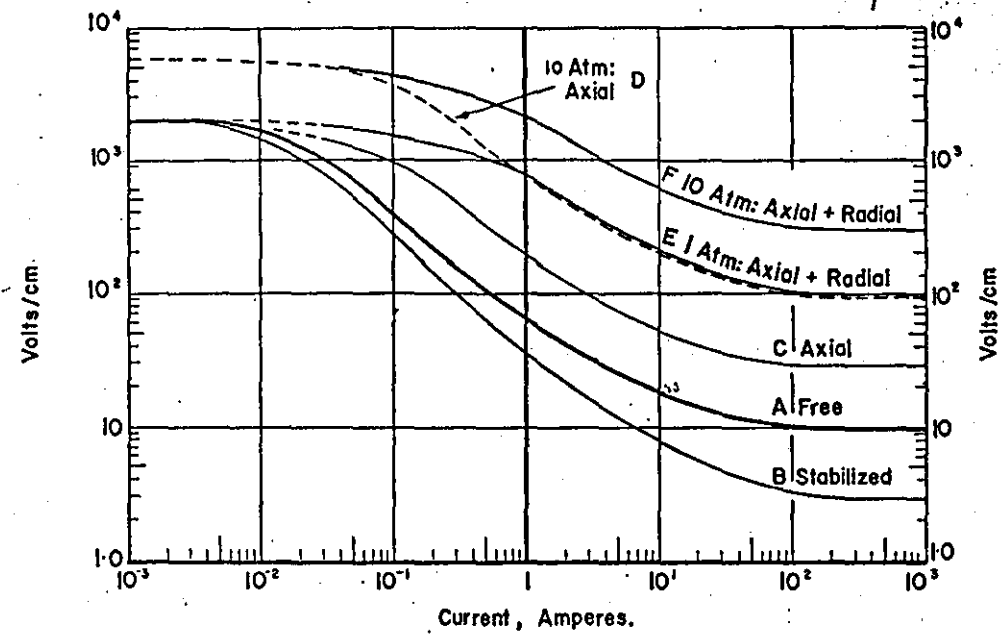


Fig. 2.3 The voltage gradient as a function of current in different configuration of gas flows  
(King, 1964)

The voltage gradient was increased using mixture of  $H_2$  and Ar (Griffing, 1971). The increase of the voltage gradient was considered due to the high thermal conductivity of  $H_2$ . Table 2.1 summaries the voltage gradient measured in the arc discharge.

## **§2.4 Measurement of the voltage gradient**

The measurement of the voltage gradient could be carried out using different methods as follows:

(1) deducing it from the difference of the discharge voltage between two points or the discharge voltage against the discharge length.

Fig. 2.4 shows one arrangement used in a glow discharge. The probes used commonly were Langmuir probes (Francis, 1965). Using the discharge voltage against the discharge length is the most conventional method in which the discharge voltage was measured when the discharge length was varied, keeping the discharge current constant. It was employed most both in a glow discharge and an arc discharge. King (1961, 1964) also used this method to measure the voltage gradient in air and  $N_2$ .

(2) by the deflection of an electron beam shot transversely across the discharge.

Aston (1923), Thomson (1933), Stein (1953), Little et al (1952), and Chaundy (1954) used this method to measure the voltage gradient. The voltage gradient was proportional to the deflection of the electron beam but was also affected by the edge effects. The method was applied to strong voltage gradient region such as 3 V/mm in a glow discharge.

Table 2.1 Discharge column voltage gradient in arc discharges

Value (V/mm)	Medium	Current/Pressure (A/1.013x10 <sup>5</sup> pa)	Source
0.9	Na	10	Hörmann (1935)
0.7	K	10	Hörmann (1935)
1.05	Sr	20	Eberhagen (1955)
2 - 4	N <sub>2</sub>	4-12	Somers et al (1956)
2x10 <sup>2</sup> - 1.0	N <sub>2</sub> or air	10 <sup>-4</sup> - 10 <sup>4</sup>	King (1961)
0.2	N <sub>2</sub>	100 (stabilized)	King (1964)
3.0	N <sub>2</sub>	100 (axial gas)	King (1964)
1.06	KCl+C	10	De Galan (1965)
1.05	KF+C	10	
1.21	LiF+C	10	
1.50	Al <sub>2</sub> O <sub>3</sub> +C	10	

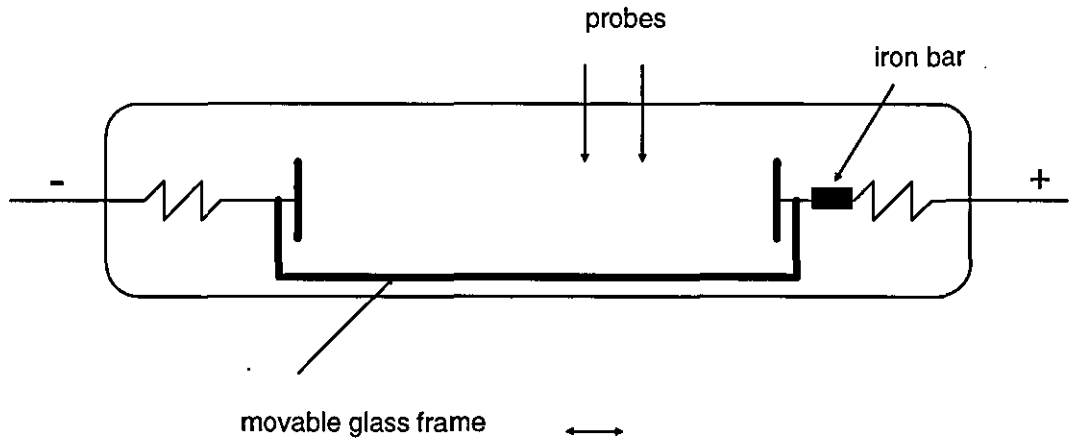


Fig. 2.4 Schematic diagram of measuring the voltage gradient (Francis, 1965)

(3) deducing it from the Stark effect.

The measurement is based on splitting of atomic energy levels and its effects on the spectral lines acted by the voltage gradient. The Stark effect was easily observed with existence of  $H_2$  with high voltage gradient. Stenbing (1931) measured the voltage gradient in the dark space region. Barbeau *et al.* (1991) reported that the measurement of the voltage gradient in the cathode dark region was shown in Fig. 2.5. The minimum requirement using the Stark effect was 120 V/mm with an advanced spectral analyser.

## **§2.5 Measurement of emission lines using spectroscopy**

Diagnostic of electric discharges using spectroscopy has been investigated extensively because it can provide information concerning the spatial and temporal variations of species concentration, electron density and temperature of electric discharge gas and electrons, and the voltage gradient.

Much information using spectroscopy on electric discharges is available. The measurement of the temperature of electric discharges has been summarised by Finkelnburg et al (1956), and Griem (1964), von Engel (1965). Lapworth (1974) reported the measurement of the temperature of the discharge using the absolute intensity of a spectral line. Chien and Benenson (1980) determined the temperature of an arc discharge using the relative line intensity technique. de Galan (1966) calculated the electron density and the electron temperature using the Saha equation with spectral lines. Bochkova et al (1965) gave detailed information using the spectral lines to determine the concentrations of gas mixtures. Knight et al (1984) investigated the arc discharge intensity using the emission line.

### **§2.5.1 Common spectral emission lines used for the electric discharge diagnosis**

The spectral emission lines used for electric discharge diagnosis depend upon their intensity, width and transition probability. Roberts (1972), Smith et al. (1978), Housby et al. (1978) and Ikeda et al. (1982) showed the lines used for diagnosis for circuit breakers and furnace type arcs. Bengtson (1963), Wiese et al. (1966, 1969), Kock and Richter (1968), Corliss (1970) reported the spectral lines used for diagnosis of  $\text{SF}_6$  as an arc quenching gas.

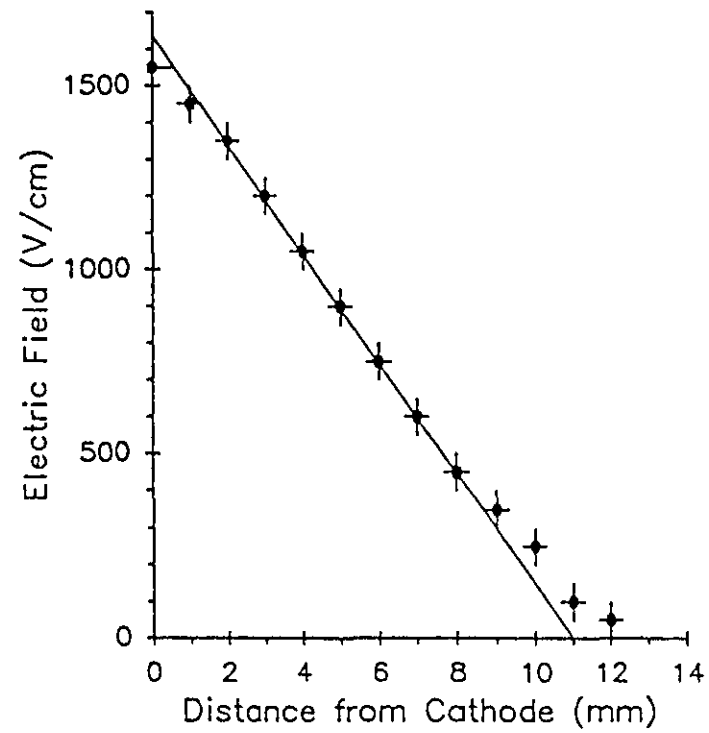


Fig. 2.5 The voltage gradient in a glow discharge ( $p=80$  Pa, discharge current=6 mA) (Barbeau, et al. 1991)

Table 2.2. Emission lines from a glow discharge with argon						
	Wavelength(nm)	Assignment (eV)		Intensity		
		upper	lower			
Ar II	294.3	21.35	17.14	m		
Ar II	297.9	21.43	17.27	w		
Ar II	349.1	21.49	17.94	m		
Ar II	354.6	23.26	19.76	m		
Ar II	356.0	23.16	19.68	s		
Ar II	357.7	23.01	19.55	m		
Ar II	358.2	23.07	19.61	w		
Ar II	358.9	22.95	19.49	m		
Ar II	372.9	19.97	16.64	w		
Ar II	376.4	22.79	19.49	m		
Ar II	385.1	19.97	16.75	w		
Ar II	396.9	23.17	19.97	w		
Ar II	394.4	19.55	16.41	w		
Ar II	404.3	21.49	18.43	w		
Ar II	407.2	21.50	18.45	s		
Ar II	410.4	22.51	19.49	s		
Ar II	413.2	21.43	18.43	m		
Ar II	415.9	14.53	11.55	s		
Ar I	419.1	14.51	11.55	w		
Ar I	419.8	14.58	11.62	s		
Ar I	420.1	14.50	11.55	s		
Ar I	426.0	14.74	11.83	w		
Ar I	426.6	14.53	11.62	w		
Ar II	427.8	21.35	18.45	vs		
Ar I	430.0	14.51	11.62	w		
Ar II	433.1	19.61	16.75	w		
Ar II	433.2	19.31	16.44	w		
Ar II	434.8	19.49	16.64	s		
Ar II	437.1	21.49	18.66	m		
Ar II	438.0	19.64	16.81	w		
Ar II	440.0	19.26	16.44	w		
Ar II	442.6	19.55	16.75	m		
Ar II	443.0	19.61	16.81	w		
Ar II	448.2	21.50	18.73	w		
Ar II	454.5	19.87	17.14	s		
Ar II	458.0	19.97	17.27	m		
Ar II	459.0	21.13	18.43	m		
Ar II	461.0	21.14	18.45	vs		
Ar II	465.8	19.80	17.14	s		
Ar II	472.7	19.76	17.14	m		
Ar II	473.6	19.26	16.64	w		
Ar II	476.5	19.87	17.27	vs		
Ar II	480.6	19.22	16.64	m		
Ar II	488.0	19.68	17.14	m		
Ar II	496.5	19.76	17.27	w		
Key: vs: very strong; s: strong; m: medium; w: weak						



Table 2.3 Emission lines used in the discharges

Species	Wavelength (nm)	Source
FI	623.94	Bengston (1963)
FII	402.50	
FII	410.34	Wiese et al (1966)
SI	469.51	
SII	532.1	
SII	545.38	
SIII	383.2	Wiese et al (1966)
CuI	510.55	
CuI	515.3	Corliss (1970)
CuI	529.25	Kock et al (1968)
CuI	570.02	
CuI	578.2	Corliss (1970)
HeI	667.81	
N <sub>2</sub>	337.13	
N <sub>2</sub> <sup>+</sup>	391.44	Behringer et al (1994)
ArI	425.9	
ArI	696.54	
ArI	706.72	
ArI	738.40	Thornton (1993)
Ar	811.5	Bochkova (1965)

Wagatsuma et al. (1985) reported the spectral emission lines from the low pressure glow discharge with Ar, N<sub>2</sub> and neon at pressure 400 Pa - 1.3x10<sup>3</sup> Pa (Table 2.2). Thornton (1993) gave the spectral line (696.5 nm) used for the temperature of the arc discharge with Ar at atmospheric pressure. Table 2.3 shows the spectral lines used for diagnosis of the circuit breaker and arc furnaces and glow and arc discharges.

## **§2.6 The gases used for the electric welding**

The gas mixtures were explored for the welding processes extensively. The need for the gas mixtures was developed to meet the new welding processes. The choice of gases was based on the trial and error but recently this can be done theoretically according to applications (Norrish, 1974). This can be seen for the options of shielding gases. CO<sub>2</sub> is most used for the arc process but varies according the applications. The main function of shielding gases is to provide a suitable medium for the stable operation of the self-contained arc and to provide a protection from the contamination of the atmosphere. Furthermore the gases are used to control the weld bead geometry and the mechanical properties.

The mixtures of gases for the welding processes are intensively diverse. The gases chosen are usually Ar, He, CO<sub>2</sub>, O<sub>2</sub>, H<sub>2</sub>. The mixtures of gases can be grouped according to the welding processes.

### **§2.6.1 Gas mixtures for gas metal arc welding (GMAW) processes**

Pure Ar is not suitable for GMAW welding processes because the arc is unstable and the resultant weld bead is

unacceptable. The GMAW processes used for the carbon steels use mixtures of Ar, CO<sub>2</sub> and O<sub>2</sub> or CO<sub>2</sub> only. The content of O<sub>2</sub> may vary between 1% to 8% while the content of CO<sub>2</sub> is between 1% to 25% according to the application.

The addition of O<sub>2</sub> (2% to 3%) and CO<sub>2</sub> (12% to 15%) to Ar can improve the arc stability and increase the operating tolerances of the voltage settings and wire speed settings. The experimental tests indicated that the metal dip transfer was improved (Norrish, 1974). It was reported that the mixtures of Ar with 5% of CO<sub>2</sub> gave a porous appearance in multiple-pass welding (Stenbaka et al, 1987).

Mixtures of Ar and He are common for the GMAW welding processes of stainless steel. The high content of He (60% to 80%) is very helpful for dip transfer because the discharge voltage is increased. As a result the fusion process is also improved especially at low currents. The low content of He (20% to 40%) is also developed for spray and pulsed transfer welding. This mixture gives excellent bead profiles while keeping the smooth spray transfer (Kennedy, 1970). The use of He, however, increases the cost of the production because He is more expensive than Ar.

Bricknell et al (1985) carried out a test using mixtures of Ar and chlorine, Ar and Freon as a shielding gas. The results showed that the stability of the discharge was improved. However the industrial exploration was restricted by environmental concerns although the certain mixture of Ar and Freon is non-toxic. This mixture may be used for totally automated applications in totally enclosed controlled-environment chambers.

### **§2.6.2 Gases for gas tungsten arc welding (GTAW) and the plasma welding**

Ar is widely used for the GTAW although mixtures of Ar with up to 5% H<sub>2</sub> are often used to increase speed, and improve profile. These gases however do not apply to ferritic steels which are susceptible to hydrogen-induced cold cracking.

He or mixtures of He and Ar are used for materials with high thermal conductivity such as copper because it gives the necessary increase of heat input. This results from the higher discharge voltage at the same discharge length and the discharge current compared with that using pure Ar.

The plasma gas and the shielding gas are required for plasma welding. The most suitable plasma gas up to date is Ar in applications. Ar is also used for the shielding gas although addition of up to 8% of H<sub>2</sub> may be selected to increase arc constriction, fusion characteristics and travel speeds based on the higher discharge voltage with H<sub>2</sub>.

### **§2.7 Research on the Glydarc electric discharge**

A Glydarc electric discharge is characterised by its inherent simple geometry and construction, and large range working pressure up to atmospheric pressure and above.

The Glydarc electric discharge uses two electrodes that diverge. The electrodes are made from either sheet metals such as copper, stainless steel or copper tubes which are water cooled. Fig. 2.6 shows the basic configuration of a Glydarc electric discharge.



Fig. 2.6 The basic configuration of a Glydarc electric discharge

The discharge voltage and the discharge current of a Glydarc electric discharge depend on the discharge gap between electrodes, gas and its pressure like other electric discharges. The discharge current in a Glydarc electric discharge can vary from a few hundred milliamperes to tens amperes.

The arc starts from the shortest gap at the bottom of the electrodes. The arc goes upwards following the curvature of the electrodes. The discharge length increases. The length varies from time to time. The arc extinguishes at the top of the electrodes or at some point where the maximum discharge length was reached. Its length of the discharge column is restricted by the limitation of the power supply. The arc completes one cycle. The discharge repeats the same process again starting from the shortest gap between the electrodes.

The repeating frequency of a Glydarc electric discharge is influenced by the discharge current, the discharge gap and the velocity of flowing air. The repeating frequency was 0.35 Hz without flowing air with the discharge current of 2 A and 2 mm gap between the electrodes at atmospheric pressure for example.

The earliest report on using a Glydarc type electric discharge was in 1904 (Laroche et al., 1991). The research and the pilot applications of the Glydarc electric discharge have been carried out again for the past ten years. There are more than 100 journal and conference papers published up to date. Lesueur et al. (1988) used it to destroy harmful gases. In their work the Glydarc electric discharge was used to heat the harmful gases in order to convert them into non-harmful gases.

The Glydarc electric discharge has also been used for dissociation of volatile organic compounds, dissociation of

$\text{SO}_x$  and  $\text{NO}_x$ , and hydrogen sulphide ( $\text{H}_2\text{S}$ ). The Glydarc discharge experiment with high concentrated mixtures of  $\text{H}_2\text{S}$  and  $\text{CO}_2$  was carried out using a three-electrode, three phase AC power supply. It was claimed that 92% of hydrogen sulphide was completely dissociated after two successive treatments. It was also reported that 32% of the input power was used for the chemical process. However, how this efficiency was measured was not clearly shown. The Glydarc electric discharge was considered as a non-thermal glow discharge because this high efficiency of dissociation took place (Czernichowski, 1991).

Czernichowski et al (1991) reported that a semi-industrial pilot arrangement of the Glydarc discharge had been used to destroy xylene ( $\text{C}_8\text{H}_{10}$ ) vapour. The Glydarc electrodes were contained in the tube which has an inner diameter of 85 mm and operated at atmospheric pressure. Less than 0.1 kW of electrical energy was used to treat 1  $\text{m}^3$  of gas mixture from 200 ppm at the input to 50 ppm at the outlet.

Lesueur et al (1993) reported that the Glydarc discharge was used for partial dissociation of hydrogen sulphide ( $\text{H}_2\text{S}$ ). The results showed that nearly 80% of hydrogen sulphide with the concentration of 2,000 ppm was converted after a single stage of treatment.

Meguernes et al (1993) attempted a comparison of the oxidisation of methane by  $\text{CO}_2$  in an electric arc and in the Glydarc discharge. The mixtures of methane and  $\text{CO}_2$  were passed through the arc column of the Glydarc electrodes at 6.5  $\ell/\text{min}$ . methane and 4  $\ell/\text{min}$ . Ar respectively. The Glydarc electric discharge was assumed to be a glow discharge. The results showed that a complete dissociation of methane using the electric arc was in good agreement with the theoretical calculation for thermodynamic equilibrium at 2,000 K. The Glydarc discharge test showed

that the dissociation of methane was incomplete but with a higher chemical efficiency up to 40%.

Czernichowski et al (1993) reported the removal of  $\text{SO}_x$  from flue gases was tested using the Glydarc discharge with 70% of  $\text{SO}_2$  conversion into elemental sulphur and water at one-step laboratory scale set-up.

Fridman et al (1993) developed a model for the Glydarc electric discharge using equations of dissipation power of the discharge. The calculation showed that 80% of the input energy was employed in a non-thermal process. However the calculated results were still to be verified from the experimental results.

Harry et al (1993) reduced the breakdown voltage of a Glydarc electric discharge in air by using an auxiliary electrode, which was inserted into the bottom gap of the main electrodes of the Glydarc electric discharge. The test showed that the breakdown voltage could be reduced by 50% with the use of the auxiliary electrode. As a consequence the open circuit voltage of the main high voltage transformer could be the same as the discharge voltage of the Glydarc electric discharge.

Cormier et al (1995) developed a new model for a Glydarc electric discharge using an energy balance. The calculation of the electron temperature however was not sufficient in choosing the parameters such as the probability ( $Q_{ie}n_e$ ) of ionisation collided with electrons and the gas ionisation potentials  $E^*$  in air. He concluded that the electron temperature was in the range of 10,000 K while the temperature of the gas varied from 6,000 K to 7,000 K. This result was promising for the verification of the glow discharge in the Glydarc discharge. However, no justification of the experimental data was supported.



Table 2.4 summarises research of the Glydarc electric discharge. Czernichowski (1994) also provided an excellent summary of general Glydarc electric discharge applicable to the various chemicals.

## **§2.8 Summary**

The interaction between the electric discharge and gases has been reviewed for gas flows ranging from subsonic to supersonic flows. The characteristic of the discharge voltage and the discharge current was dependent upon the gas flows.

The voltage gradient and its measurement in the electric discharge were described. The voltage gradient in the discharge column of arcs was in the order of 1 V/mm when the discharge current was more than 1 A.

The gas and gas mixtures used for welding and plasma processes were also described. The different gases used in the electric welding were to protect electrodes and improve the welding properties.

The use of the spectral emission lines as a diagnosis for the electric discharge was presented. Table 2. 2 shows emitted lines from the glow discharge at low pressure with Ar and Table 2. 3 summarise the common spectral lines used in the discharges.

The Glydarc electric discharge has been described and its applications are grouped based on the dissociation of harmful gases and the modelling of the physical processes.

Table 2.4 The main research on the Glydarc electric discharge

Topic	References
Dissociation of H <sub>2</sub> S into sulphur and hydrogen	Czernichowski (1993)
Light hydrogens changed into synthesis gas (CO + H <sub>2</sub> )	Lesueur et al (1994)
SO <sub>2</sub> into sulphur	Czernichowski et al (1995)
N <sub>2</sub> O into nitric acid	Fridman et al (1995)
CFCs into H <sub>2</sub> , CO, etc.	Czernichowski et al (1994a)
NO <sub>x</sub> into N <sub>2</sub>	Czernichowski et al (1991)
CO <sub>2</sub> into CO	Czernichowski et al (1994b)
Heavy hydrocarbons into lighter ones	Meguernes et al (1994)
Volatile organic compounds treatment	Czernichowski et al (1991)
Flue gases treatment	Labbe et al (1993)

## **Chapter Three**

### **Review of the electric discharge**

### §3.1 Gases

A gas in the normal state allows a very small current of electricity to pass through it (about  $10^{-19}$  A), therefore the gas can be used as a perfect insulator. However under certain conditions when the electric field is established between two electrodes the gas can become an almost perfect conductor. The transition from insulating state to conducting state is called an electric discharge.

The nature of the electric discharge can be extremely varied and can involve applied discharge voltage over large amount of range (e.g. from a few tens of volts in welding processes to a few MV in lightning flashes over paths of kilometres). The gas pressure, the different kinds of gases also contribute the properties of the discharges. The atomic, molecular, electronic, ionic and photon collision processes in the gas and at electrodes, which can be involved in the various mechanisms of the electric discharge, are themselves of fundamental interest to the use of the electric discharge. All these properties of the electric discharge are important in the operation of all machines related to the discharge.

The working mediums of the electric discharge can be gases or metal vapours. The characteristics of gases such as potentials of ionisation, excitation and dissociation will determine the property of the discharge. The degree of ionisation for instance is difficult to be measured if not impossible. Therefore the calculation based on the known physical laws becomes necessary to get approximations to these parameters.

Electric discharges involve the use of mixed gases in which might be mixtures of stable molecules and neutral atoms; excited molecules, positively charged ions and negatively charged electrons. These complexes of mixtures

are treated as a perfect mixture of gases for approximation.

### §3.1.1 Kinetic theory of gases

An ideal gas is one in which the atoms do not affect each other's motion. The perfect gas equation is written as

$$pV=RT$$

or

$$p=nkT \quad (3.1)$$

where  $V$  is the volume of the gas,  $R$  is the universal gas constant,  $n$  is the number density of gas atoms and  $k$  is the Boltzmann's constant.

The gas pressure  $p$  can be expressed as

$$p= \frac{1}{3} mn \langle u^2 \rangle \quad (3.2)$$

where  $m$  is the mass of a gas atom and  $\langle u^2 \rangle$  is the mean square velocity. Equation 3.2 suggests that atom of small mass has higher velocities on the average than atoms of large mass at the same temperature. Therefore an electron accelerated through a relatively low potential difference can have a larger velocity than a gas atom. The probability of ionisation for a collision should be higher between an electron and a gas atom than that between two gas atoms.

### §3.1.2 Excitation, ionisation and dissociation

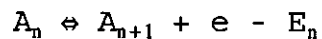
#### Excitation

The atom always lies in the ground state at normal conditions because the total energy of its electron has its smallest energy value  $E_0$ . If the atom is raised to a higher energy value  $E_n$  by external force such as the voltage gradient, thus the atom will then be in an excited state.

#### Ionisation

Ionisation refers to the process in which one or more electrons can be removed from an atom. This process also needs the external energy. Ionisation can be self-sustained or non-self-sustained once it is initiated. However an external source of ionisation is required to maintain the ionisation of non-self-sustained process.

The ionisation process can happen at the first level or multiple levels depending upon the energy received. The general physicochemical ionisation processes can be expressed as follows



$$n = 1, 2, \dots, m \quad (3.3)$$

where  $A_n$  is the  $n$ th level ionised particle and  $E_n$  is the ionisation energy necessary for ionisation from the  $n$ th to the  $n+1$ th level of ionisation. The ionisation energy is obtained by using spectroscopic data experimentally. Table 3.1 shows the ionisation energy for common gases and material used in the electric discharge.

Table 3.1 Ionisation potentials (eV)

Element	Level of ionisation					
	I	II	III	IV	V	VI
Ar	15.755	27.62	40.90	59.79	75.0	91.3
He	24.580	54.40				
H <sub>2</sub>	13.595					
N <sub>2</sub>	14.54	29.61	47.43	77.45	97.86	551.92
O <sub>2</sub>	13.614	35.146	54.934	77.394	113.873	138.08
W	7.94					

## Dissociation

Diatomic molecules such as  $H_2$ ,  $N_2$  or  $O_2$  absorb energy firstly by rotation and secondly by vibration at high temperature. When the vibrational energy reaches a sufficiently high level, the valence bonds holding the two atoms together is broken down. The atoms will be in a monatomic state. Subsequently the dissociation occurs.  $O_2$  starts to dissociate at about 3,000 K, whereas  $N_2$  starts to dissociate at about 4,500 K at atmospheric pressure (Cambel, 1963). Table 3.2 shows the dissociation energies for common gases used in the electric discharge.

Both dissociation and ionisation depend on pressure and temperature. Therefore a gas may be ionised at a higher temperature if the pressure is increased.

The energy levels for ionisation are higher than that for dissociation, perusing Table 3.1 and Table 3.2. Thus ionisation becomes significant when the gas is substantially monatomic. The case for ionisation and the dissociation can be treated separately.

**Table 3.2 Dissociation Energies**

Molecule	Dissociation energy (eV)
$H_2$	4.477
$N_2$	9.76
$O_2$	5.08
OH	4.37



### §3.1.3 Degree of ionisation

The  $i$ th degree of ionisation is defined as:

$$\alpha_i = \frac{n_i}{n_H} \quad (3.4)$$

$$\alpha_0 = 1 - \sum_{i=1}^m \alpha_i \quad (3.5)$$

where  $n_i$  is the number density of  $i$ th ions and  $n_H$  the number density of heavy particles that are inclusive of neutral atoms and ions but exclusive of electrons.

The degree of ionisation for the ionised reaction of equation 3.3 can be determined from the equilibrium constant  $K_{i+1}$  according to the law of massive action (Zemansky, 1957). The degree of ionisation is given as follows:

$$\begin{aligned} K_{i+1} &= \left( \frac{2\pi m_e}{h^2} \right)^{\frac{3}{2}} \frac{(kT)^{\frac{5}{2}}}{p} \frac{2Z_{i+1}}{Z_i} e^{-\frac{E_i}{kT}} \\ &= \frac{\alpha_{i+1} \sum i \alpha_i}{\alpha_i (1 + \sum i \alpha_i)} \end{aligned} \quad (3.6)$$

$$i = 0, 1, 2, \dots m$$

The degree of ionisation is influenced by temperature and pressure. Fig. 3.1 shows the effect of the temperature

and the pressure on the ionisation of degree of Ar at atmospheric pressure (Cambel, 1963).

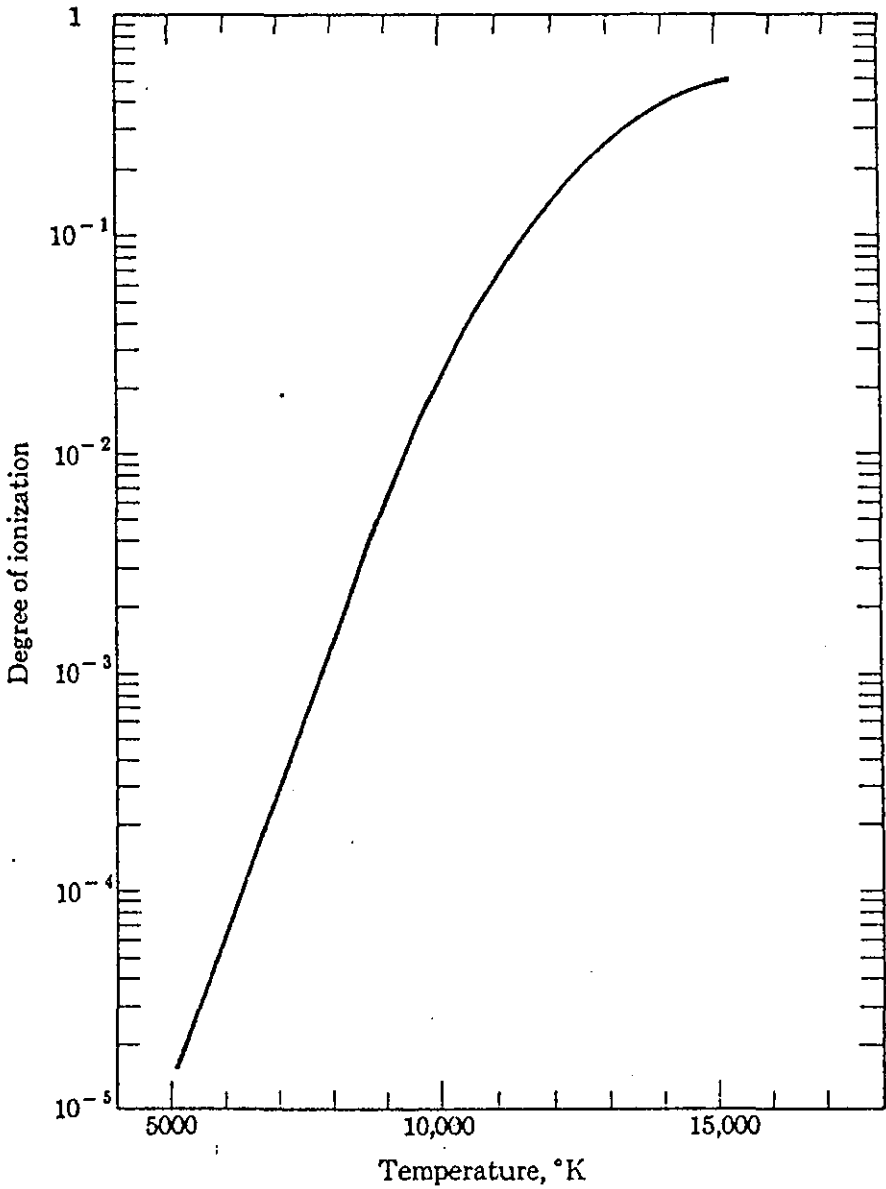


Fig. 3.1 Degree of ionisation of Ar (one atmospheric pressure) (Cambel, 1963)

#### §3.1.4 Thermal conductivity

Thermal conductivity  $\kappa$  is commonly defined as the rate at which heat crosses unit area perpendicular to the direction of the temperature gradient. The dimensions of the thermal conductivity is  $\text{J}(\text{msK})^{-1}$

The electrons and ions will not greatly alter the thermal conductivity if the plasma is only slightly ionised. However the charged particles will have a marked influence on the thermal conductivity when the degree of ionisation is high.

The thermal conductivities of Ar, He and the mixtures of Ar and He are shown in Fig. 3.2 (Cambel, 1963).

The thermal conductivity of gases depends on the followings (Boumans, 1965):

- (a) The normal classical conductivity due to the motions of atoms, molecules, ions and electrons.
- (b) The conductivity due to thermal diffusion and the transport of energy of reaction, such as energy of dissociation and ionisation.

Atoms of dissociated gases diffuse outwards from the centre of the plasma to the boundaries and may recombine in the cooling region. This process of diffusion contributes to energy consumption and affects the thermal conductivity.

The dominant factor in the thermal conductivity is the dissociation process. Dissociation increases with increase of temperature.

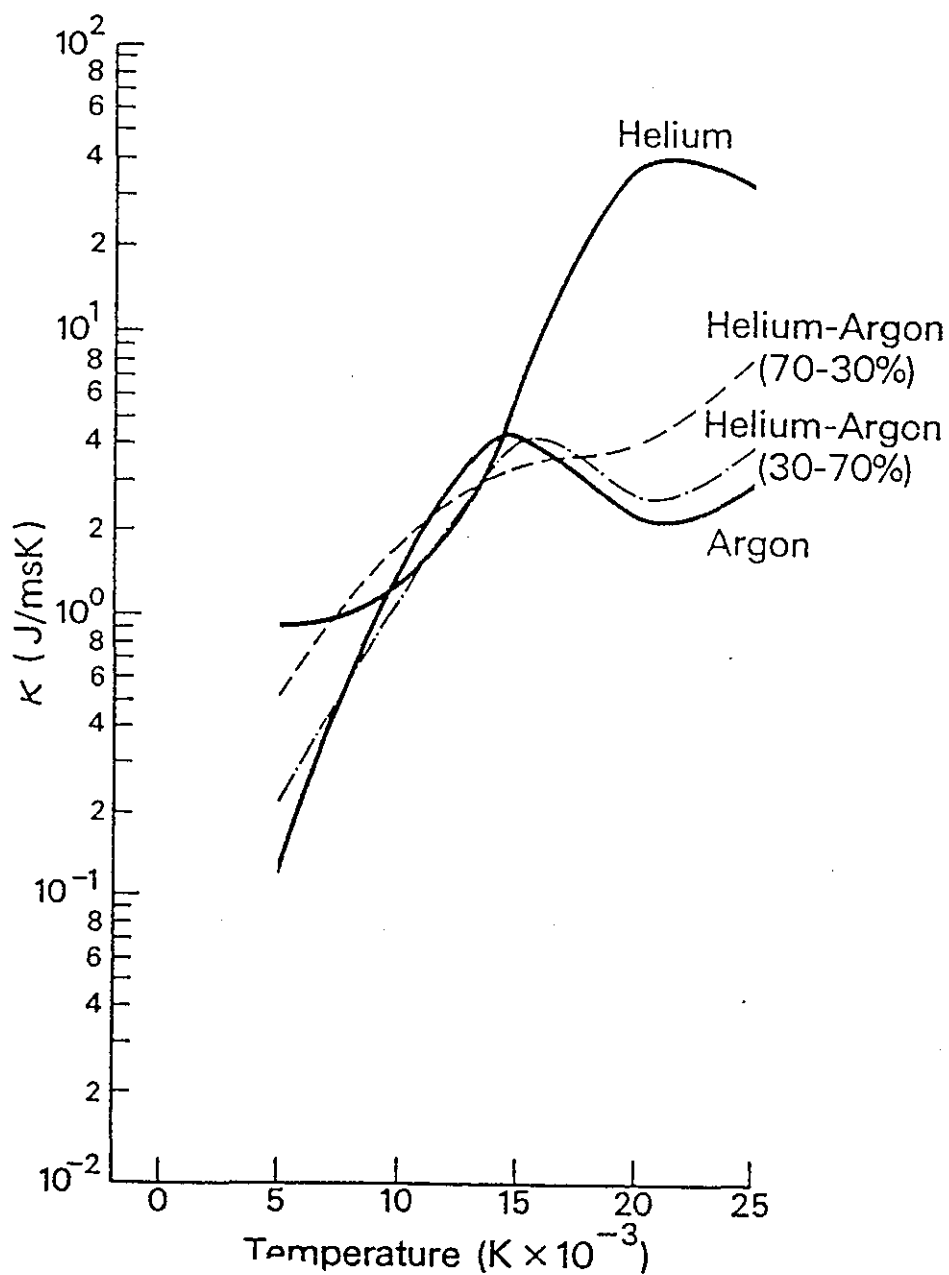


Fig. 3.2a. Thermal conductivity of Ar and He and their mixtures at one atmospheric pressure (Mondain-Monval, 1973)

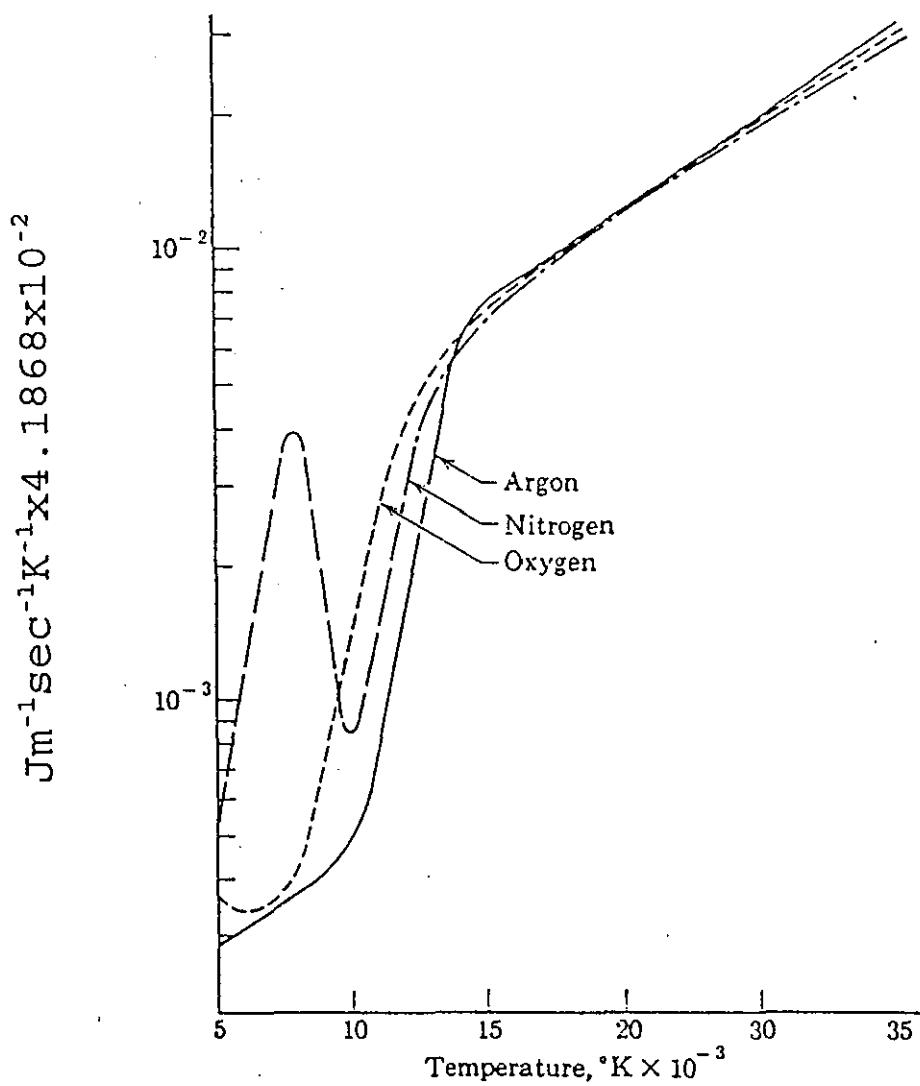


Fig. 3.2b. Thermal conductivity of Ar, N<sub>2</sub> and O<sub>2</sub> at one atomspheric pressure (Cambel, 1963)

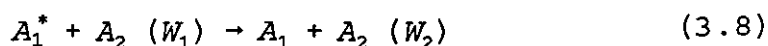
### §3.1.5 Inelastic collisions of the first kind and the second kind

If the kinetic energy of an electron is not much higher than the ionisation potential of an atom when the electron collides with the atom, the ionisation process is



Further ionisation by collisions between the electron and atoms cannot happen since two slow electrons are produced unless these electrons are accelerated and have larger energy than the ionisation potential again by the external electric field. It is defined as the collision of the first kind, which is the Townsend primary process.

If a neutral atom  $A_2$  with kinetic energy  $W_1$  collides with an excited atom  $A_1^*$ , the process is



where  $W_2$  is the raised energy of atom  $A_2$  after collision. This is the collision of the second kind. Atom  $A_2$  can be ionised if the excitation energy of  $A_1$  is larger than the ionisation potential of  $A_2$ . If  $A_1$  is a metastable atom this collision may happen many times, which is called the Penning effect. It is important as an ionising agent in inert gas mixtures (Beynon, 1972).

### **§3.2 Glow discharge**

The general appearance of the glow discharge is shown in Fig. 3.3 with gas pressure at a few hundred Pa. It can be seen that when the gas pressure has reached 1,330 Pa the positive column, the Faraday dark space and the negative glow can only be observed. The colour of the positive column depends on the particular gas used. The positive column fills most of the discharge length. The negative glow is the most luminous part of the discharge. Its colour again depends on the particular gas used, but it is usually different from that of the positive column for example the positive column is dark red and the negative glow is dark blue if Ar is filled. At high pressure the Faraday dark space and the negative glow are pressed to the cathode surface.

The characteristics of the discharge voltage and the discharge current for electric discharges is shown in Fig. 3.4. At current is around 100 mA the glow discharge may occur with a voltage drop at the cathode of approximately 300 V.

#### **§3.2.1 The glow discharge column, the anode and the cathode**

The properties of the positive column are independent of the length of the column unless it is too short. The positive column, also called plasma column suggested originally by Langmuir, has equal concentrations of positive and negative charges or ions. The plasma column as a whole is electrical neutral, but there will be highly conducting when a certain amount voltage is applied to it. The positive column contains the mixtures of electrons, positive ions and unionised atoms. There is a tendency for a negative space charge to be set up at the anode end of the plasma column because electrons move much faster than

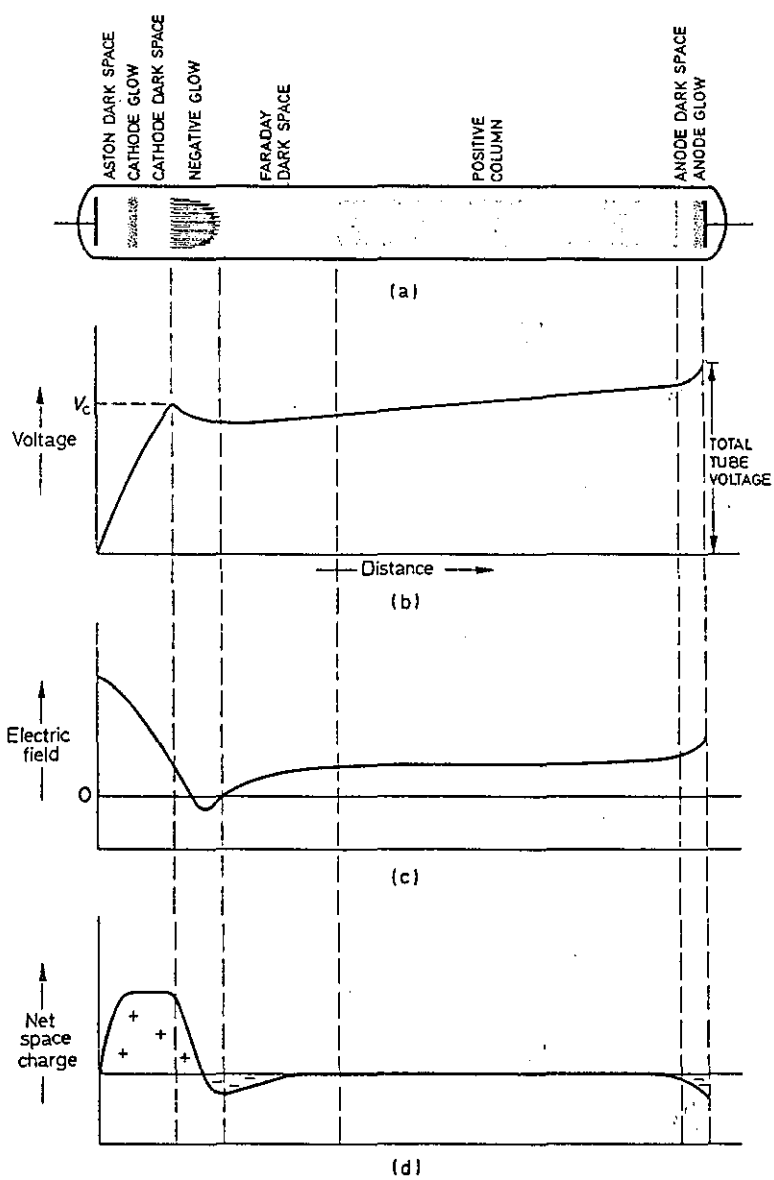


Fig. 3.3 The general appearance of the glow discharge at a few hundred Pa (Beynon, 1972)



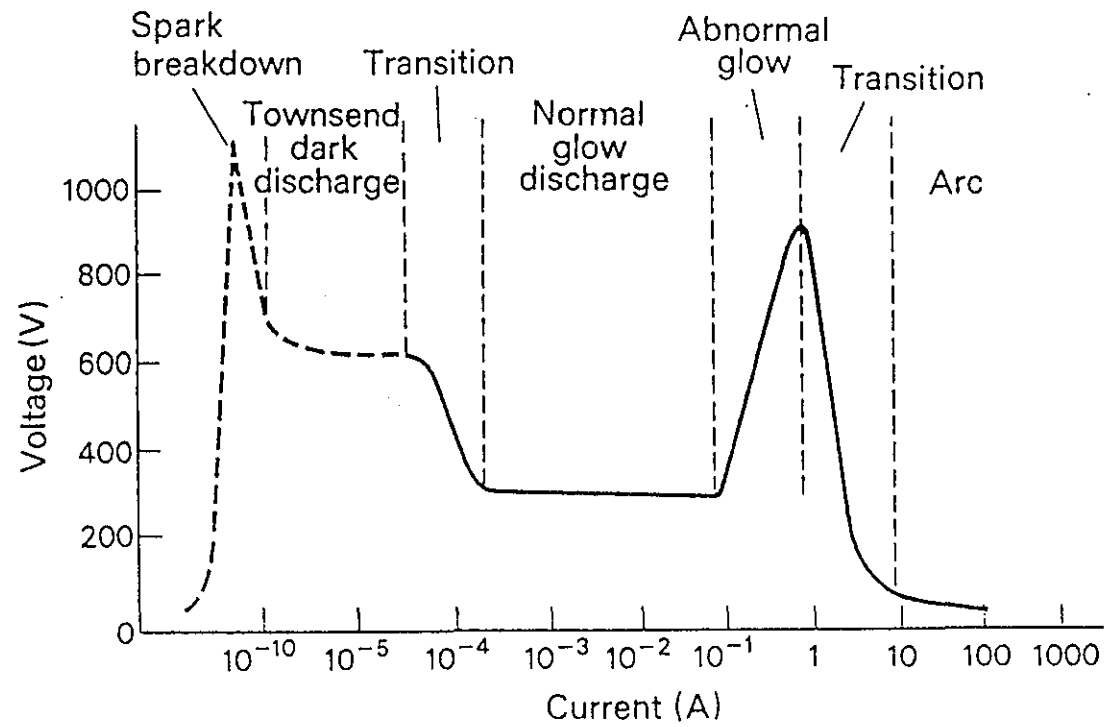


Fig. 3.4 The voltage-current characteristic of an electric discharge at about 100 Pa (Guile, 1986)

the positive ions. The positive column, however, is fed continuously with positive ions repelled from the anode zone and the space charge is neutralised.

The discharge current through the gas is transferred to the external circuit by the electrons hitting the anode. The anode repels positive ions and negative space charge is summed up in front of it. Therefore the electric field is formed and much larger than that in the positive column. The voltage across the space charge region is called the anode fall  $V_a$ . The similar progresses also occur around the cathode. The voltage drop across the cathode is known as the cathode fall  $V_c$ . Usually the cathode fall is of about 300 volts (ranging 10 volts to 500 volts) and the anode fall is of about 20 to 30 volts. However it is difficult in determining the anode fall voltage of a glow discharge. It is commonly accepted that the anode fall is of the order of the ionisation potential of the gas and to increase at low pressure.

### §3.2.2 The mobilities of particles

When electrons and positive ions have drift velocities  $v_e$  and  $v_i$  respectively in an electric field strength  $E$  then the mobilities of electrons and positive ions are defined as

$$\mu_e = \frac{v_e}{E}$$

$$\mu^+ = \frac{v_i}{E} \quad (3.9)$$

The mobilities of electrons and positive ions are expressed in the unit of m/s per V/m or  $\text{m}^2\text{V}^{-1}\text{s}^{-1}$ . The mobility of electrons is much larger than that of ions, being strictly dependent on electric field strength and the number of electrons. For example the typical value of the mobility of electrons  $\mu_e$  is  $10^9 - 10^{11} \text{ m}^2/\text{Vs}$  but the mobility of ions  $\mu^+$  is  $4.4 \times 10^6 - 7.9 \times 10^7 \text{ m}^2/\text{Vs}$  (von Engel, 1983). The mobility of electrons can also be given by the relation as follows according to the kinetic theory of gases

$$\mu_e = \frac{ce\lambda_e}{m_e \sqrt{\frac{3kT}{m_e}}} \quad (3.10)$$

where  $\lambda_e$  is the mean free path of electrons. It should be noted that the constant  $c$  is an uncertainty factor of unit order of magnitude ( $0.75 < c < 1.38$ ). Its numerical is determined by the method of averaging.

The calculation of the mobility of electrons leads to calculation of the mean free path of electrons. There exists a relationship between the mean free path of electrons  $\lambda_e$  and the mean free path of atoms  $\lambda$ , which is the mean distance that an atom travels between collisions.  $\lambda_e$  is larger than  $\lambda$  because an electron is smaller than an atom.

$$\lambda_e = 4\sqrt{2}\lambda \quad (3.11)$$

$$\lambda = \frac{1}{\sqrt{2}\pi nd^2} \quad (3.12)$$

where  $n$  is the number density of atoms and  $d$  is the diameter of an atom.

It is difficult to determine the mobility of electrons  $\mu_e$  because of the lack of information of the mean free path of different gases at atmospheric pressure.

### **§3.2.3 The density of the discharge current**

It is not an easy task to determine the density of the discharge current. Thus the estimates of current density rely on indirect observations. It is believed that the densities should lie in the followings after improvement of these observations over years (Table 3.3)

## **§3.3 Arc discharge**

An arc discharge is referred to as a discharge of electricity between electrodes in a gas or in vapour from electrodes. It is characterised by the fact that a voltage drop at the cathode is in the order of the excitation potential of the electrode vapour (about 10 volts) and the discharge current can be varied from a few amperes to almost unlimited values (Fig. 3.4).

### **§3.3.1 The arc cathode, the anode and the discharge column**

The voltage in the arc discharge varies along the axis in a similar way to the glow discharge in that most of the voltage appears across the cathode zone, less across the anode. The cathode zone and the anode zone occur over very short distances from electrode surfaces. Thus the gradients of the discharge voltage in these fall regions can be extremely high. The cathode fall is usually about 10 to 20

Table 3.3 The density of the discharge current

Glow discharge cathode: proportional to the square of gas pressure. In air at atmospheric pressure about  $10^6$  to  $10^7$  A/m<sup>2</sup>.

Anode current density:  $10^6$  to  $10^9$  A/m<sup>2</sup>

Discharge column:

noble-gas low pressure (A/m <sup>2</sup> )	metal-doped low pressure (A/m <sup>2</sup> )	metal-seeded high pressure (MHD) (A/m <sup>2</sup> )	Metal-doped high pressure (excimer laser) (A/m <sup>2</sup> )
$10^2$ - $10^3$	$10^2$ - $10^3$	$10^4$ - $10^6$	$10^6$ - $10^7$

volts, whereas the anode fall of metallic anodes might vary between 1 volt to 10 volts with relatively high current. There is not a great deal of reliable data on the anode fall voltage. Along the positive column there is a weak gradient of the discharge voltage, which is less than that in the glow discharge.

It is difficult to measure the density of the discharge current because the cathode spot to which the arc is anchored is very small. Observations over years suggested that the density of the current may be expressed as follows:

The cathode current densities:

non-thermal arc cathode: about  $10^{10}$  up to  $4 \times 10^{12}$  A/m<sup>2</sup>.

thermionic arc cathode:  $10^6$  to  $10^8$  A/m<sup>2</sup>

---

The anode current density:  $10^6$  to  $10^9$  A/m<sup>2</sup>

The discharge column:  $10^6$  A/m<sup>2</sup>

### §3.3.2 The condition for stabilising electric discharge

A characteristic of the discharge voltage and the discharge current is presented in Fig. 3.4, which shows the negative dynamic impedance. The stabilising resistance is required to limit the discharge current. The stabilising condition for the electric discharge can be written as

$$\frac{\partial v}{\partial i} + \frac{\partial v_d}{\partial i_d} \geq 0 \quad (3.13)$$

where  $\partial v_d / \partial i_d$  is the dynamic resistance of the discharge,

and  $\partial v/\partial i$  is the stabilising impedance, which is presented by the load line on the generalised discharge voltage and discharge current characteristics. The stability of the electric discharges was exhaustively treated first by Kaufman in 1900 and later by Dälenbach. The detail can be found in handbooks (Mierdel, 1929).

### §3.3.3 Excitation of spectra

A wavelength of light emitted by an excited atom is determined by the Plank's law

$$f = \frac{(E_N - E_M)}{h} \quad (3.14)$$

---

where  $f$  is the frequency of the light,  $h$  is Plank's constant equal to  $6.6 \times 10^{-34}$  Js,  $E_N$  is the excited energy at Nth level,  $E_M$  is the excited energy at Mth level.

Spectral lines of element with low ionisation potential show longer wavelengths. Similarly the spectral lines of element with high ionisation potentials show shorter wavelengths. Because the second ionisation potential of all elements is higher than the first, excitation energies of singly charged ions can also reach a higher value than that of atoms, but emission is limited to 9.5 eV - 10 eV. In general emission lines from ions will have shorter wavelengths.

Under normal conditions, the return of an atom from a metastable to a ground level may occur in one of the two ways:

(i) an atom, colliding with an electron, is raised to an excited state, from which it can pass to the ground state, the transition being accompanied by radiation;

(ii) the excited atom transfers its energy to another atom by collision of the second kind and is reduced to the ground state without emission of radiation.

The transition from high levels to low levels produces a group of high intensity lines which can be observed in both emission and absorption spectra. Molecular spectra can be produced by diatomic and polyatomic molecules.

The excitation of an atom requires an energy greater than or equal to the excitation energy of a given level. The energy required can be transferred by

---

(a) transition of the kinetic energy of electrons, ions or atoms colliding with the atom;

(b) collision of the second kind;

(c) absorption of light quanta.

However not all collisions can produce excitation. This is because there is a definite probability of energy transfer on collision.

Spectral lines are produced not only by single ionisation atoms, but also by those which are multiply ionised. The energy required to produce spectra from multiply ionised atoms is high.

Emission processes are closely related to the life of excited atoms. The probability of secondary processes increases with the lifetime of an excited atom.



The life of a metastable state depends strongly on the electron concentration. The presence of the number of metastable atoms determines the conditions under which a self-sustained discharge can occur.

The excitation and the ionisation processes in the electric discharges finally result in a fixed concentration of excited atoms and ions. This will determine the wavelength and the intensities of the spectral lines.

### **§3.4 Summary**

The equation of perfect gas, the excitation and the ionisation and the degree of ionisation for gases used in the electric discharges were explained. The basic characteristic of the electric glow discharge and the arc discharge were reviewed and the general characteristics of the discharge voltage and the current was presented as well. The normal stable working condition for electric discharges was given. The excitation of spectral lines was described.

## **Chapter Four**

---

### **Investigation of a Glydarc electric discharge**

#### §4.1 Introduction

Destruction of harmful waste and toxic material has been attempted in various ways such as incineration, landfill and sea disposal. The use of landfill is decreasing in favour of incineration due to lack of available sites for landfill and concerns about damage to the environment in the long term. One of the disadvantages of incineration is its limited use for chemical waste because no selection of chemical for recycling use of material can be made.

Electric glow discharges might offer an alternative approach to reduce harmful gases because the chemical reactions can be selected according to the application. Nanosecond pulse corona, dielectric barrier discharge and RF, AC and DC source of power can be used to produce the electric glow discharges.

---

The use of electric glow discharges for the destruction of harmful waste and toxic material in environmental control has received much attention in recent years and some research pilot schemes have been conducted, such as the destruction of volatile organic compounds (VOCs) in France (Harry, 1993). The extension of the practical use of electric glow discharges depends on further improvements in efficiency of transfer of the electric power to the chemical process, optimal system design of the electrodes and power supply and good understanding of the chemical and physical processes involved.

Glow electric discharges have been studied extensively over the past decades for chemical reactions with gases such as nitrogen and carbon monoxide etc. (McTaggart, 1967, Yamamoto, 1996). A common use of a glow discharge is often seen in ozone generators in water plants and fluorescent

lamps. Another example is that a glow discharge can dissociate  $\text{CO}_2$  into CO and atomic oxygen under electron bombardment in the discharge region at pressure of about 133 Pa - 1,330 Pa (McTaggart, 1967).

Although the Glydarc electric discharge used for chemical reactions has been studied extensively since it was reported in 1904, the fundamental characteristic of a Glydarc electric discharge such as the relationship between the discharge voltage and the discharge current is not well understood. The relationship between the air flow rate and the discharge voltage and the discharge current of a Glydarc electric discharge is not available. From the engineering design point of view, it is important to know these relationships because these are crucial in designing an optimum system of a Glydarc electric discharge used with injected gases for industrial applications.

---

This study investigated a Glydarc electric discharge and focussed on the interaction between the electric discharge and subsonic air flows, and the characteristic of the discharge voltage and the discharge current. The theory of measurement for the discharge voltage was based on the basic laws applied to the non-linear electrical circuit (Shepherd, et al 1979). The simulation of optimal electrodes was carried out using a computer gas dynamic program.

#### **§4.2 Experimental arrangement of a Glydarc electric discharge and power supplies**

The electrodes used in the test were made of stainless steel sheet which prevents oxidation from the injected gases. The electrodes are 200 mm high and maximum 51 mm wide and 1.5 mm thick (Fig. 4.1).

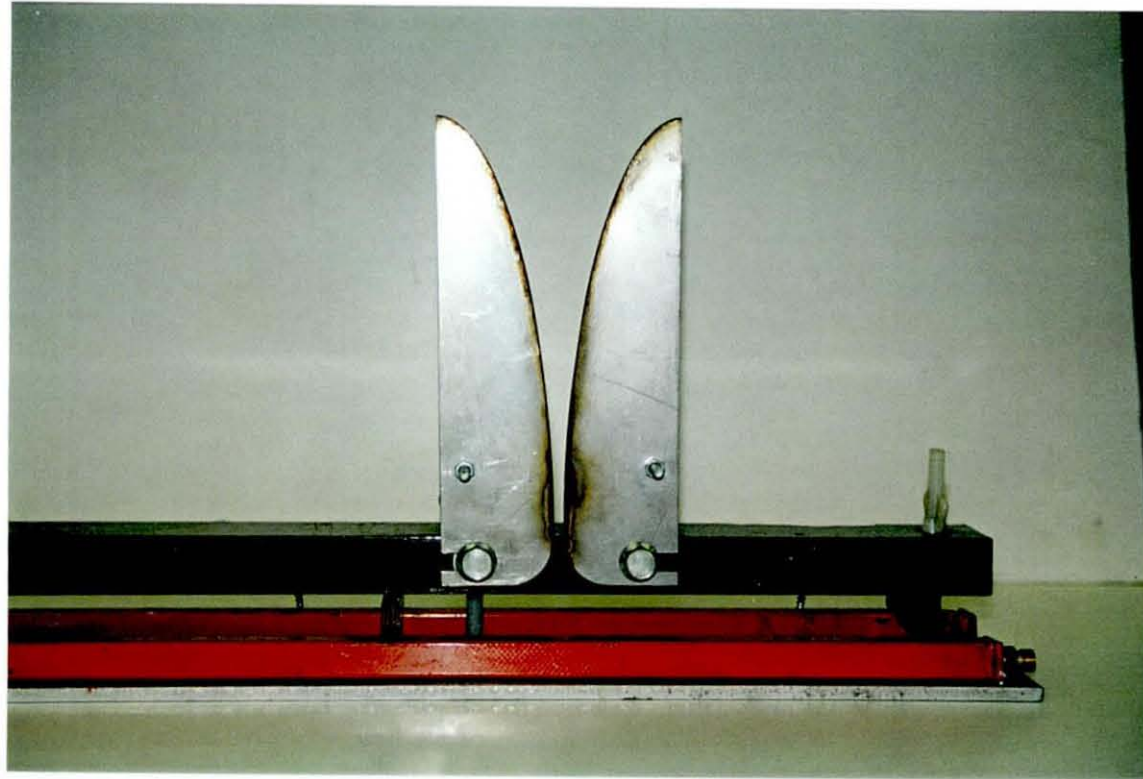


Fig. 4.1 Glydarc electrodes

A high voltage probe with the ratio of 1,000 : 1 was connected to a digital multimeter to measure the discharge voltage.

The discharge current was measured with a conventional moving coil ammeter using a shunt with a scaling of 75 mV/3A. The discharge current waveform was also measured by an oscilloscope.

Fig. 4.2 shows the electrical circuit. The high voltage transformer has two groups of secondary coils which can be connected in parallel to provide higher discharge current or in series to provide higher open circuit voltage. The high voltage transformer can provide a maximum open circuit voltage of 9 kV and a maximum current of 3 A. The DC voltage and the DC current were rectified from an AC power supply with a rectifier assembly (140BV150H, International Rectifier). The discharge voltage was regulated manually by a three-phase autotransformer.

The gas system is shown in Fig. 4.3 schematically. An oil-free diaphragm gas compressor pump (Compton, Dawson McDonald & Dawson Ltd.) was used in the test. This pump has a 120 l gas reservoir at a maximum pressure of  $8 \times 10^5$  Pa. The gas in the gas reservoir was released through the gas duct and then the electric discharge region to atmosphere. A gas volume flow meter (10 l - 100 l/min.) and a gas pressure meter (1,000 Pa -  $8.12 \times 10^5$  Pa) were employed to measure the gas flow and the pressure near the entrance of the duct. The gas velocity at the outlet of the duct can be calculated because the diameter of the outlet hole is 2 mm.

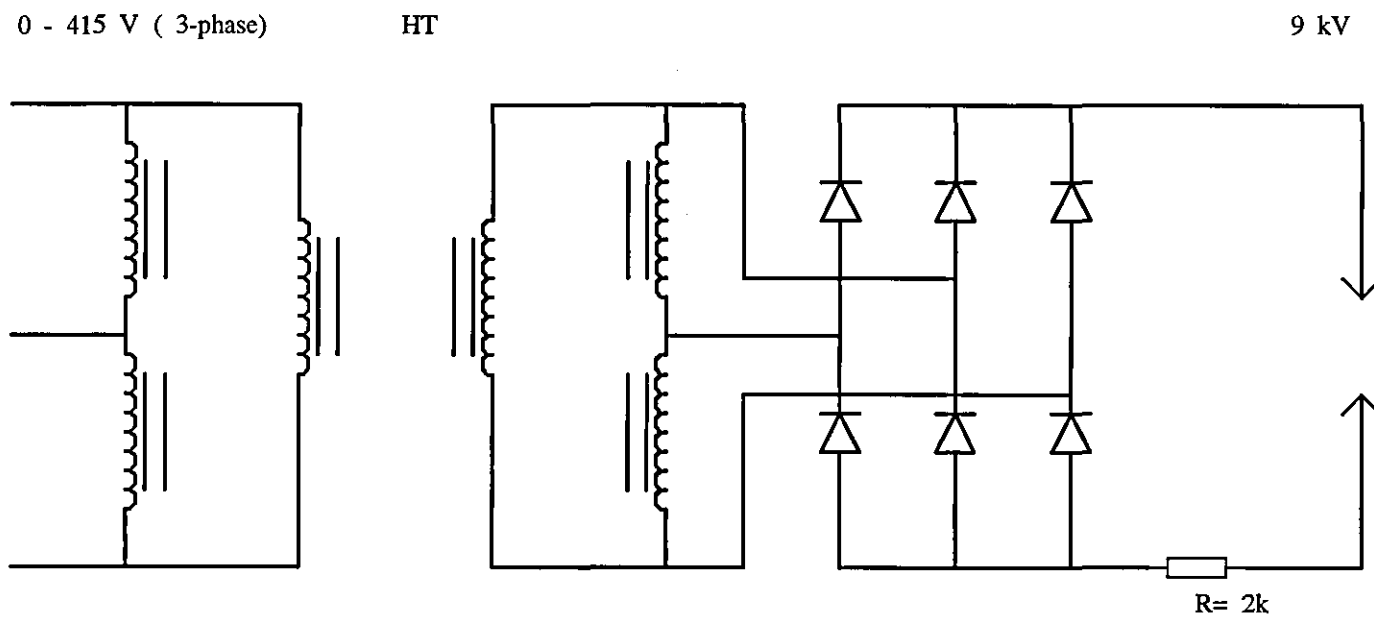


Fig. 4.2 A schematic circuit of the Glydarc electric discharge

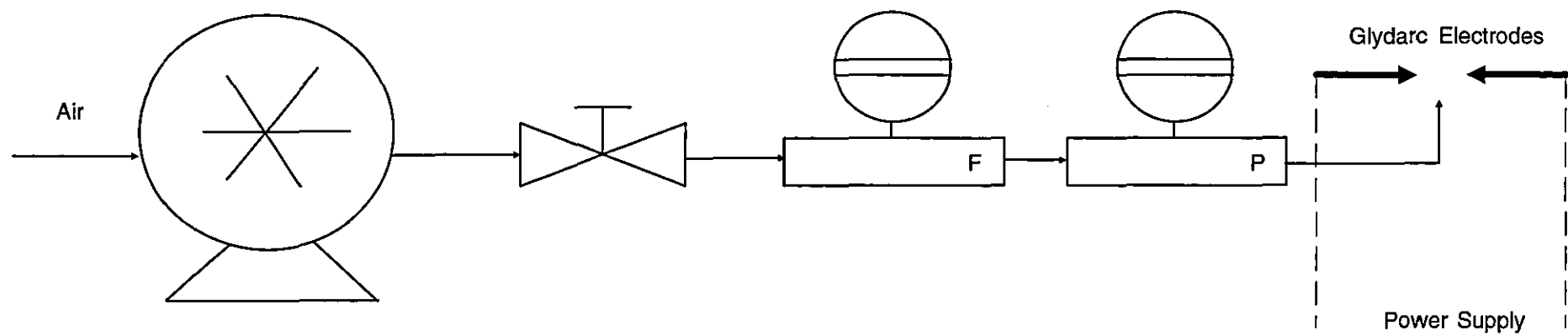


Fig. 4.3 The schematic diagram of the experimental arrangement



### **§4.3 Characteristics of the discharge voltage and the discharge current in a Glydarc electric discharge**

The characteristic of the Glydarc electric discharge was measured using both the DC power supply and the AC power supply with and without inductor used in the circuit. The open air was used in the test.

#### **§4.3.1 A Glydarc electric discharge with an AC power supply with stabilising resistor only**

A series of tests was carried out on a Glydarc electric discharge in both still air and subsonic air flows. The characteristic of a Glydarc electric discharge is shown in Fig. 4.4. The stabilising resistor was 1.8 k $\Omega$ . The shortest distance between electrodes was fixed at 1 mm. The flow rate of air was varied up to 100  $\ell$ /min.

Fig. 4.4 shows that the discharge voltage increased with increase of the discharge current. The discharge voltage also increased at the same discharge current when flowing air was injected. The gradient of the discharge voltage and the discharge current was positive and linear. As a result the dynamic resistance was constant (i.e.  $\Delta V/\Delta I = \text{constant}$ ).

Fig. 4.5 shows the waveforms of the discharge voltage and the discharge current of the Glydarc electric discharge measured with a digital storage oscilloscope. Both the discharge voltage and the discharge current were non-sinusoidal. The discharge current was discontinuous with the discontinuous angle  $\varphi$  measured from current zero.

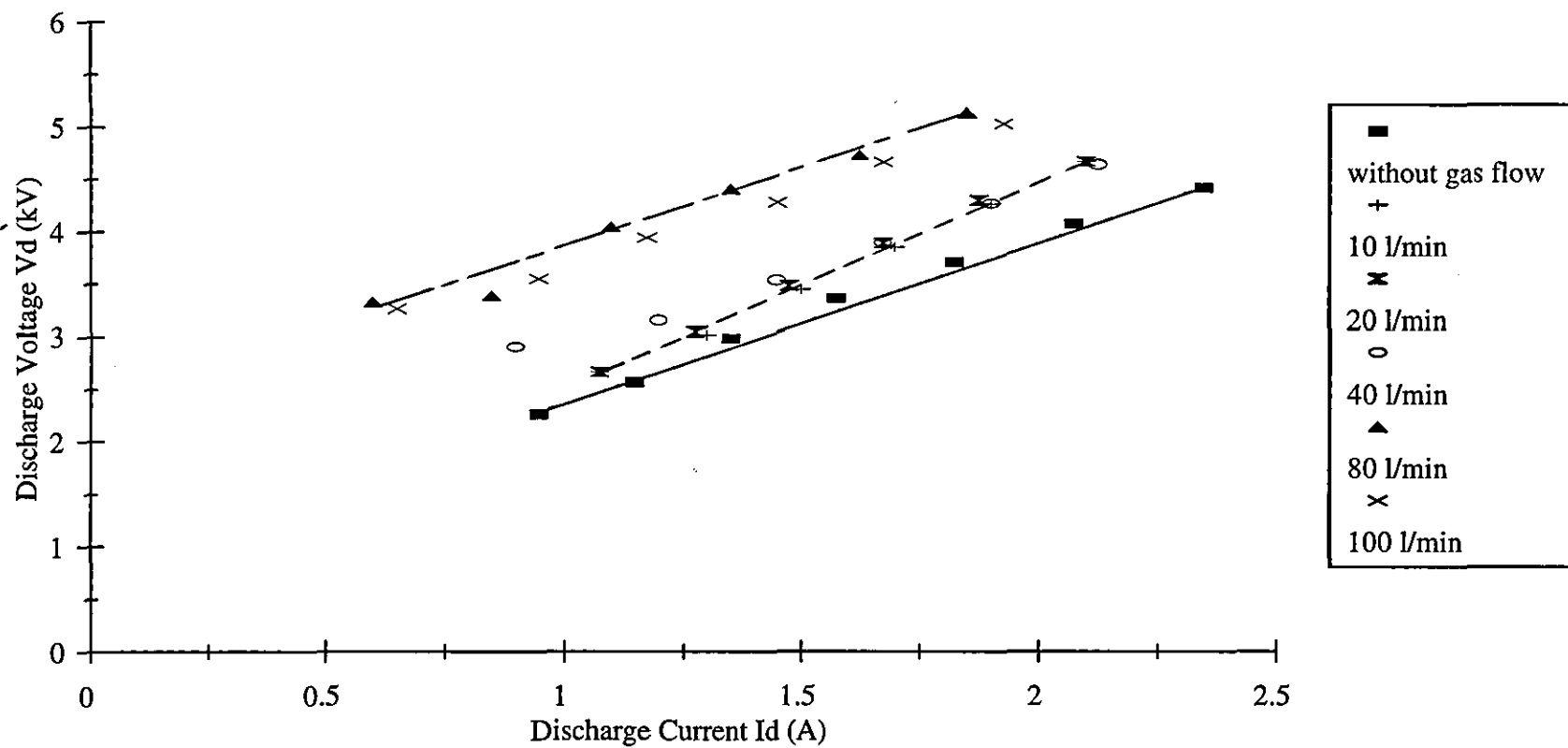


Fig. 4.4 Variation of discharge voltage and current using AC

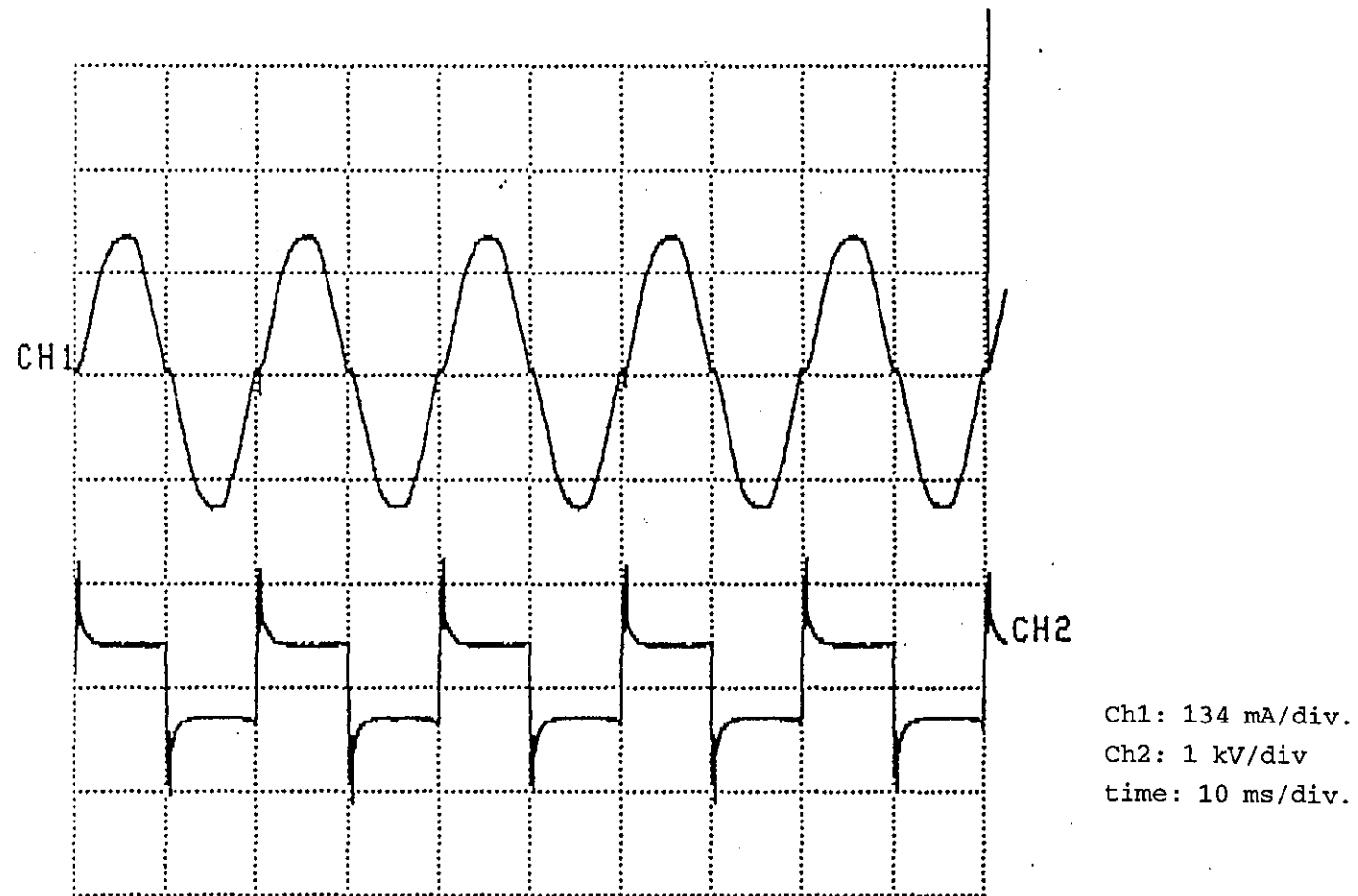


Fig. 4.5 Waveform of the discharge voltage and current

#### **§4.3.2 A Glydarc electric discharge with an AC power supply with an inductor**

A wide range of inductors was used varying from 0.5 H to 10 H in order to reduce the angle of discontinuity of the discharge current. The characteristics of the discharge voltage and the discharge current are shown in Fig. 4.6. It was observed that the electric discharge was more stable than that without an inductor. The discharge voltage was decreased with increase of inductance at the same velocity of air flow compared with that without an inductor. As a result the discharge current was less with increase of inductance than before.

#### **§4.3.3 A Glydarc electric discharge with a DC power supply**

The characteristic of the Glydarc electric discharge using a DC power supply is shown in Fig. 4.7. The stabilising resistor was 2 k $\Omega$ . The tendency of the discharge voltage and the discharge current was similar to that using the AC power supply. The discharge voltage and the discharge current fluctuated with time (the peak voltage and the peak current could be as high as 4 kV and 2 A respectively).

The discharge voltage was increased with increase of the discharge current. The discharge voltage also increased when the subsonic air was injected. Fig. 4.7 shows that the increase of the discharge voltage at air flow rates of 80  $\ell/\text{min}$  and 100  $\ell/\text{min}$  was not significant. The gradient of the discharge voltage and the discharge current was positive and linear. Therefore the dynamic resistance was constant.

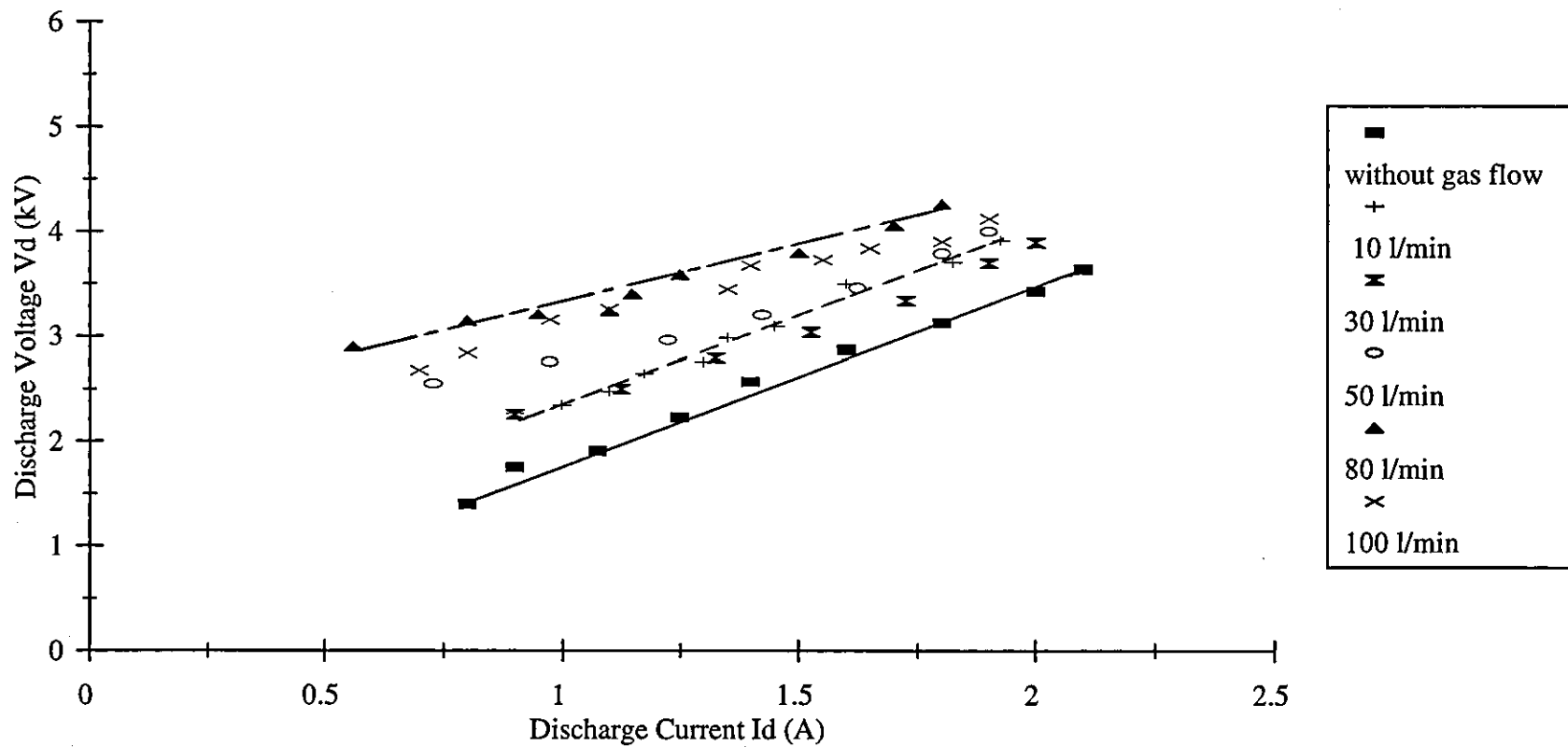


Fig. 4.6 Variation of the discharge current and voltage using AC with a series inductance of 2 H

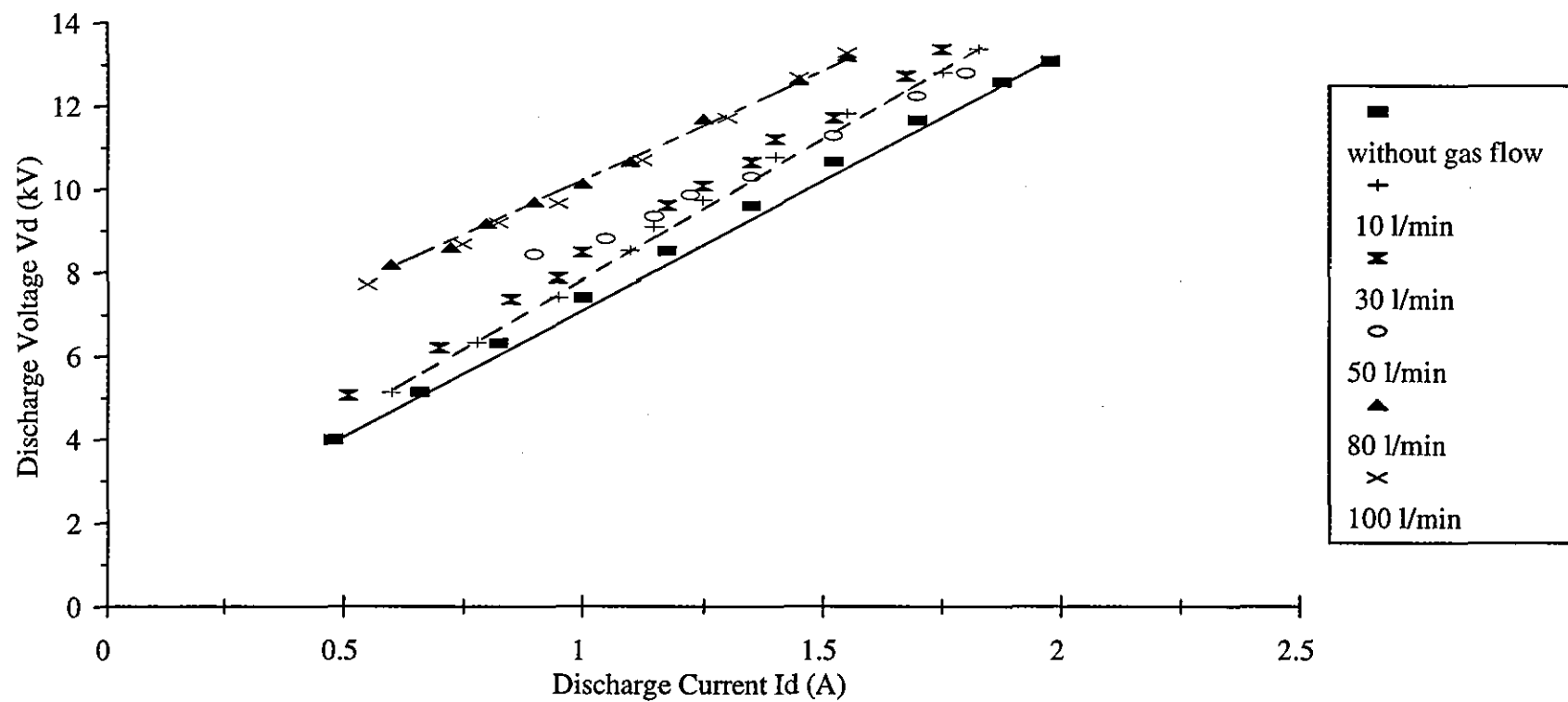


Fig. 4.7 Variation of discharge voltage and current using DC

#### §4.4 Discussion

The characteristics of the Glydarc electric discharge using AC and DC power supplies showed that the discharge voltage increased with increase in the discharge current. This contrasts with the conventional characteristic of the electric discharge (i.e. the discharge voltage decreases when the discharge current is increased). This positive slope of the characteristic was mainly due to the air flow and the varying length of the discharge column (Cormier et al, 1995).

The objective of using air flows in the glow discharge was to convect heat out of the discharge region to keep the glow discharge from changing to an arc discharge and increasing the discharge current. In case of a Glydarc electric discharge it is to inject gases which are provided to be treated. The flowing air convected heat from the discharge region and decreased the temperature of the discharge column, as a result the electrical conductivity of the discharge column decreased and increased the discharge voltage. The increase of the discharge voltage between the high flow rates 80 l/min and 100 l/min was not significant partly because the cooling effect of the air flow might reach its maximum effect and the discharge length did not increase further.

The variation of the maximum discharge current with air flow at high velocity was smaller than that with air flow at low velocity. This difference was due to the limited voltage of the high voltage power supply.

The discharge length could vary over a large range even when the discharge root was in the same position. The discharge length between the electrodes of the Glydarc electric discharge increased with the discharge moving upwards, and the discharge voltage increased as well.

If the effect of increase in voltage caused by the changing length of the discharge column was subtracted from the total voltage, the discharge voltage should level out or be negative. Otherwise the multiple Glydarc electric discharges could occur with common stabilising resistors. A test was carried out to determine whether the positive V-I characteristic existed. The experiment showed that when the two parallel Glydarc electric discharges with common stabilising resistors were tested, the Glydarc electric discharge showed that only one was stable (Cormier, et al 1995).

The discharge current was not continuous, and affected the accurate reading of the instruments (Harry, 1965). The angle  $\phi$  of discontinuity of the discharge current depended on the size of the gap between the electrodes. For instance if the gap between the electrodes was fixed at  $l$  mm and the power supply was sinusoidal with maximum magnitude  $V_{\max}$ .

$$f(l) = V_b = V_{\max} \sin \phi \quad (4.1)$$

$$\phi = \sin^{-1} \frac{V_b}{V_{\max}} \quad (4.2)$$

where  $V_b$  was the breakdown voltage of the discharge.

Equation 4.2 shows that the angle  $\phi$  of discontinuity of the discharge current can be reduced by increasing the magnitude of  $V_{\max}$ . Alternatively an inductor can be employed in an AC discharge circuit to reduce the angle of discontinuity of the discharge current. An inductor with ranging inductance of 0.5 H to 10 H was available. Value of



inductance of 2 H and 5 H were chosen and as a consequence The discharge current was more smooth than before, because the impedance of the inductor was equal to 0.628 k $\Omega$  and 1.57 k $\Omega$  respectively. These choices of the inductor were taken into account the smooth discharge with less reduction of the maximum discharge current.

#### **§4.5. Computer simulation of the gas profile of a Glydarc electric discharge**

The Glydarc electrode was simulated using the FLUENT programme (version 4.2) to investigate the gas profiles.

The general approach to modelling turbulent flows using time-averaged equations involved augmenting the transport properties to account for the effects of the turbulent eddy flow. This involved replacing the fluid viscosity ( $\mu$ ) with an effective turbulent viscosity ( $\mu_t$ ) which was a function of the flow.  $\mu_t$  was calculated by considering the kinetic energy of the turbulence ( $\kappa$ ) to its rate of dissipation ( $\epsilon$ ). This was the  $\kappa$ - $\epsilon$  model of turbulence. The  $\kappa$ - $\epsilon$  model in FLUENT was originally designed for non-ionised gases it is used here to investigate the gas flow around the Glydarc electrodes.

The configuration of the Glydarc electric discharge was axi-symmetrical and the thickness of the electrodes was 1.5 mm thick, 200 mm high and 51 mm wide, thus two-dimensional symmetric calculation was needed for sufficient calculation. The grid used for calculation was evenly spaced. The computational cells were 100x46. The velocity of inlet gas was divided into two groups. The velocity of gas used in zone 1 was 0.1 m/s and the other in zone 2 was 5 m/s. The air at the input point was assumed uniform with the turbulent effect considered in the discharge region by using the general  $\kappa$ - $\epsilon$  model in the

program. The parameters used in the simulation are shown in Table 4.1.

The model in the simulation assumed that the Glydarc discharge was enclosed in an adiabatic cylindrical vessel and hence heat from the discharge was removed by convection of air flow rather than by conduction.

**Table 4.1. Coefficients used in the simulation in FLUENT**

---

domain size:	430mm x 280mm
gas:	air
density:	1.2 kg/m <sup>3</sup>
turbulent intensity:	10
turbulent schmidt number:	0.7
temperature:	293 K
viscosity:	10 <sup>-5</sup> kg/m s
thermal conductivity:	0.0241 W/mK
molecular weight:	28
specific heat of fluid:	1004 J/kgK
binary diffusion rate:	2.88x10 <sup>-5</sup> m <sup>2</sup> /s
pressure:	1.0133x10 <sup>5</sup> Pa

---

#### **§4.5.1 Optimum shape of the Glydarc electrodes**

A series of simulations was carried out for different ranges of electrodes. The first simulation of gas profiles for the Glydarc electrodes was based on the existing electrodes. The gas profile is shown in Fig. 4.8. It was shown that the velocity profiles decreased along the axis. The gas velocity did not change quickly with increase of distance from the electrodes.

Fig. 4.8 suggested that the shape of the electrodes should be less divergent (one third longer) than it was to increase the interaction volume between the gas and the discharge.

The simulation using FLUENT is limited because it was not practical to modify the program for combination of the electric discharge parameters such as heat produced with gas flows. This is due to the complexity and licence of the program. As a result the information from the simulation is limited to gas profiles.

#### **§4.6 Measurement of the discharge voltage in an AC Glydarc electric discharge**

It was shown that the direct measurement of the discharge voltage in a Glydarc with an AC power supply was unstable because of the high peak transient voltage in the discharge circuit and therefore the sum of the low and the high readings were averaged.

Fig. 4.9 shows that the measurement of the discharge voltage in the Glydarc electric discharge with stabilising resistor only. Fig. 4.10 shows that the discharge voltage with the combination of the resistor and the inductor.

The internal resistance of the power supply was different for AC or DC output. The difference was due to the resistance of the rectified assembly in the DC power supply. The average internal resistance of the power supply was 2.52 k $\Omega$  and 1.87 k $\Omega$  in the DC and AC power supplies respectively. The resistance per winding in the secondary coil of the high voltage transformer is 0.440 k $\Omega$ .

The discharge voltage and the discharge current were not sinusoidal. The error in measurement resulted because

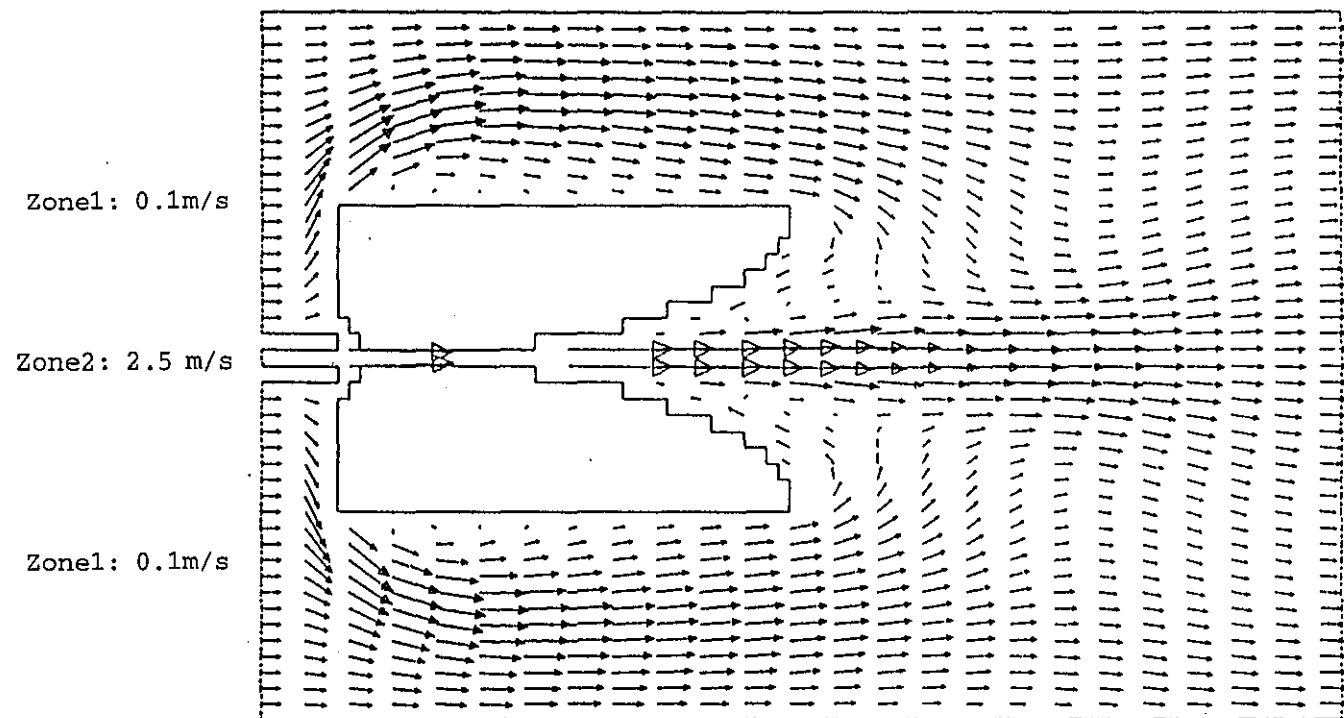


Fig. 4.8 The gas profile in a Glydarc discharge

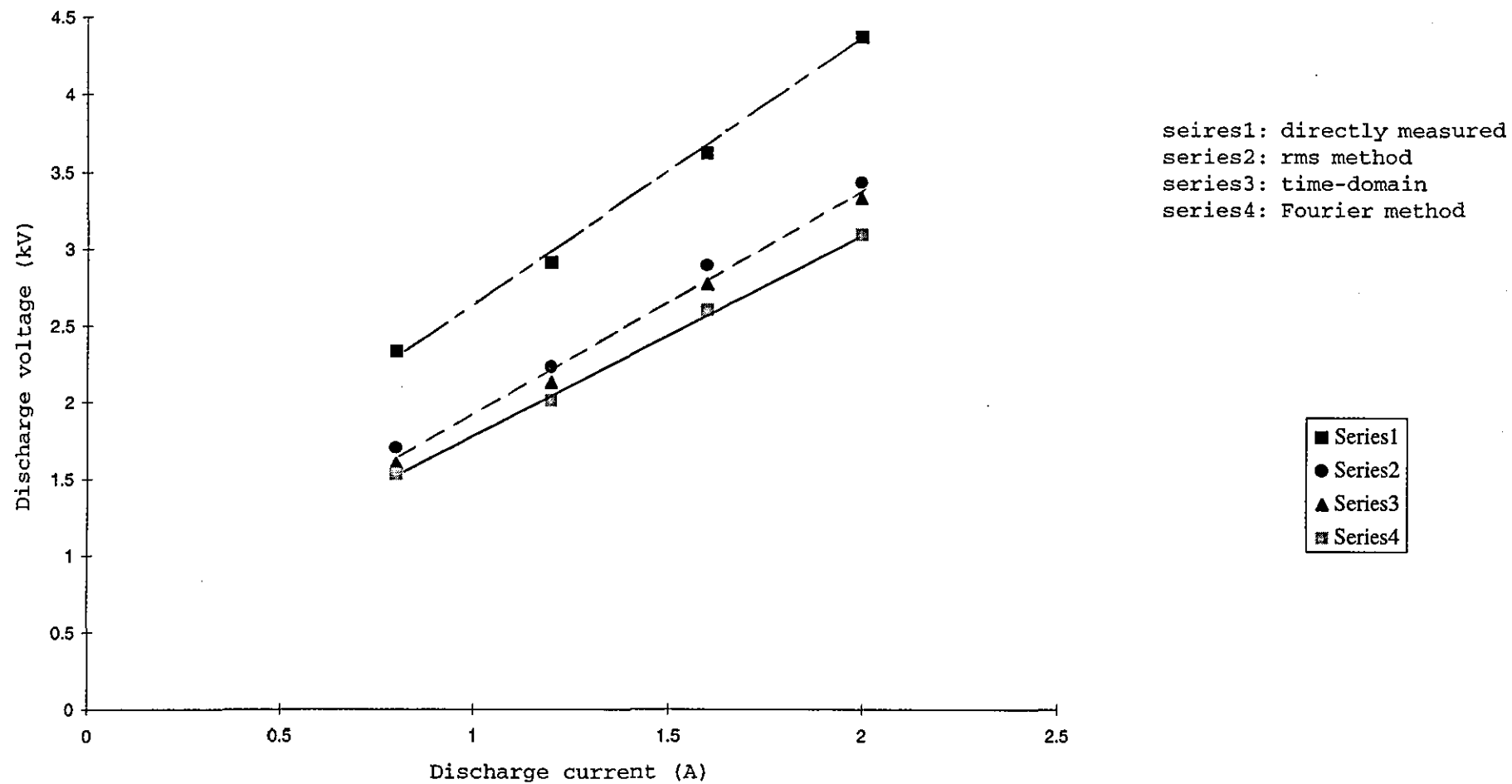


Fig. 4.9 Dependence of the discharge voltage and current measured with a stabilising resistor ( $R=2\text{ K}$ )

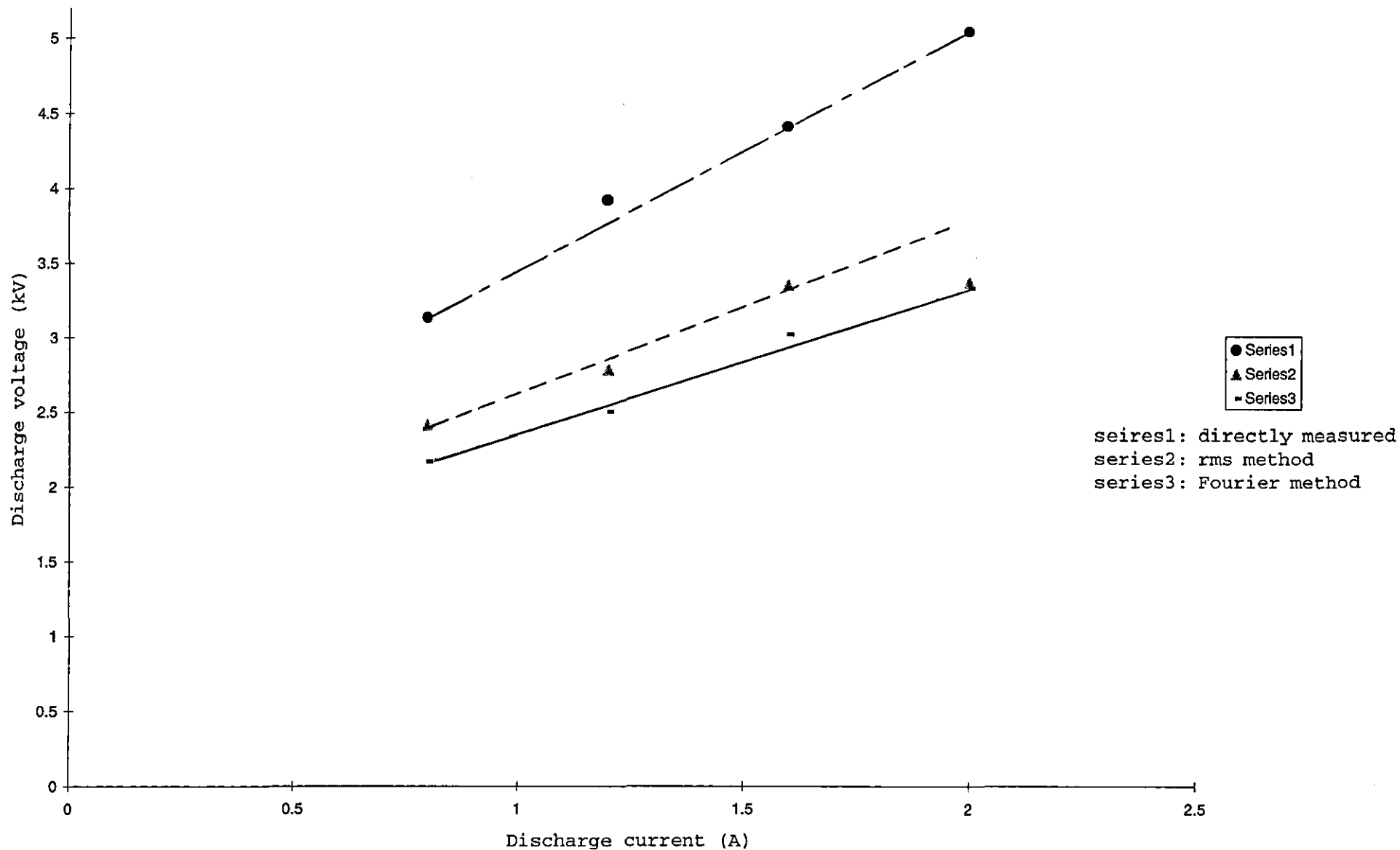


Fig. 4.10 Dependence of the discharge voltage and current measured with a R-L ( $R=1\text{ k}$  and  $L=2\text{ H}$ ) in series

conventional meters are designed for measurement on 50 Hz sinusoidal waveform. A rectified moving coil meter was used since its variation of measurement error with the duration of arc extinction could be calculated (Harry, 1965).

$$\epsilon = 1 - \cos \varphi \quad (4.3)$$

The maximum discontinuity degree measured was  $16^\circ$ , therefore the maximum error was 4%.

#### §4.7 Simulation of the discharge voltage and the discharge current for a Glydarc electric discharge

The PSPICE simulation programme was used to simulate the discharge circuits (see Appendix A). The electric discharge used in the simulation (Fig. 4.11) was described

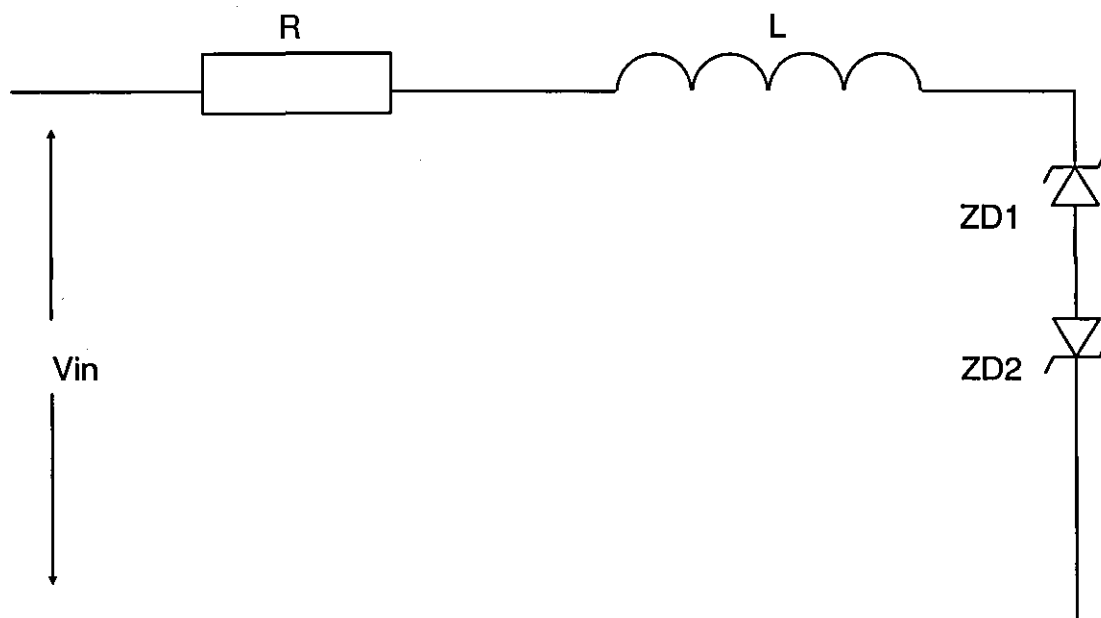


Fig. 4.11 Schematic circuit of the discharge for simulation using PSPICE

by two series back to back zener diodes which were equivalent to the function of the discharges over a small current range.

The simulation was carried out with a series of resistors from 100  $\Omega$  to 4 k $\Omega$  and a series of inductors from 0.5 H to 10 H. Fig. 4.12 and Fig. 4.13 show the discharge voltage and the discharge current with a resistor and with a resistor and inductor in series respectively.

The simulation showed that the combination of 1 k $\Omega$  resistor and 1 H inductor was best, based on the small voltage drop across the resistor and the angle of discontinuity of the discharge current.

#### **§4.8 Summary of the results**

The results show that the Glydarc electric discharge does not have a real positive dynamic V-I characteristic. The increase of the discharge voltage in the Glydarc electric discharge was mainly due to the effect of increase in length of the discharge column and the cooling effect of the flowing air.

The computer simulation using the FLUENT program indicates that the Glydarc electrode should be less divergent (one third longer than the original). The less divergent electrodes could have more interactive volume with flowing gases. This would be useful in the destruction of the harmful gases.

The indirect measurement of the discharge voltage enabled meaningful results to be obtained for the discharge voltage where the discharge current was not continuous. The indirect measurement also avoided the need for a high input impedance meter.



The PSPICE simulation showed that a combination of 1 k $\Omega$  and 1 H was best for stabilising the Glydarc electric discharge because of the small voltage drop across the components and the continuity of the discharge current.

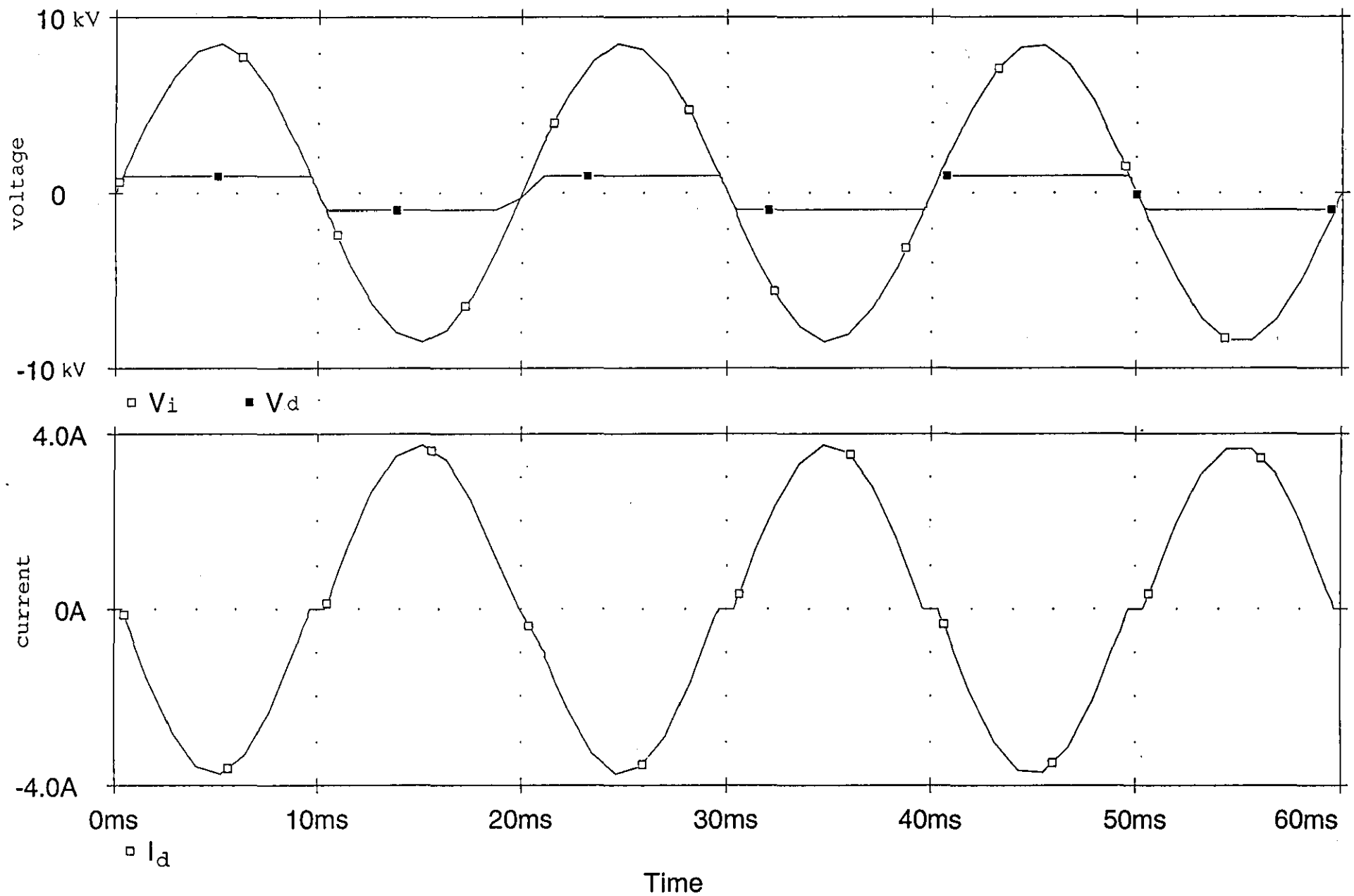


Fig. 4.12 Waveforms of the discharge voltage and current with a resistor ( $R=2k$ ) in PSPICE

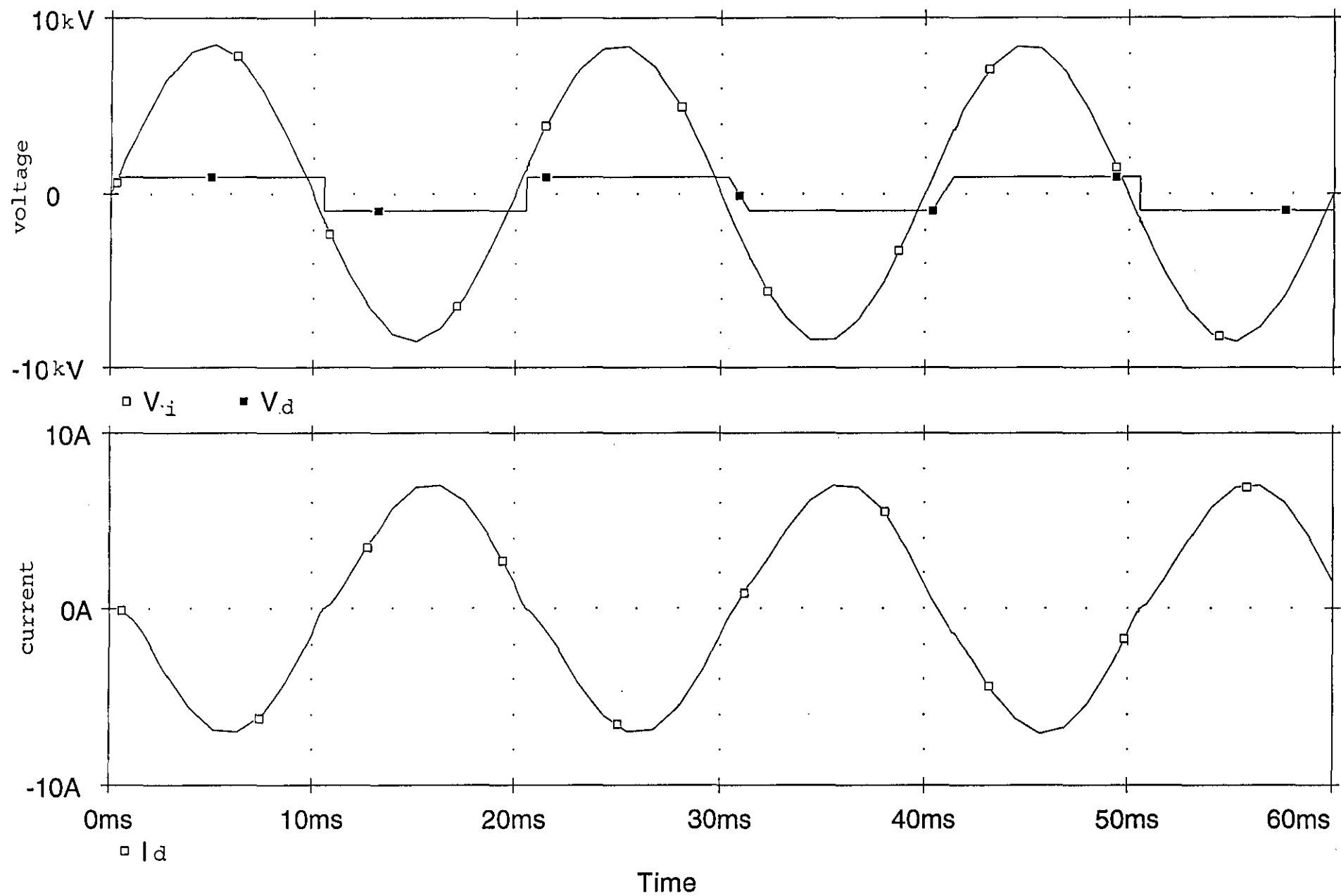


Fig. 4.13 Waveforms of the discharge voltage and current with a R-L ( $R=1k$ ,  $L=1H$ ) in PSPICE

## **Chapter Five**

**Gas mixtures and their effect on increasing the discharge column voltage gradient in a plasma torch**

## §5.1. Introduction

Ar is a gas often used in plasma processing because of the ease of ignition of the electric discharge and protection of electrodes from the surrounding medium. The cost of using Ar is low compared with using other inert gases.

The disadvantage of using Ar, however, is that the discharge column voltage gradient is lower than that using other gases such as  $H_2$  or He. The discharge column voltage gradient using Ar is usually in the order of 0.1 V/mm. As a consequence, the low gradient of the discharge voltage requires much high current for the high power input. For example if 100 kW input power is required the discharge current needed is over 1,000 A when the discharge length is 1 m long.

A higher discharge voltage is preferred where high power is required. This reduces the current required and also reduces the capital cost of equipment and increases the lifetime of electrodes.

Ar is still used in many plasma processes although Ar has been replaced by other gases or gas mixtures such as air in plasma cutting because it is more cost-effective. The use of other gas or mixtures of gases are limited because the effect of different gases on the discharge column voltage gradient has not yet been fully understood and no quantitative information is available. Furthermore there is a reluctance to use gas mixtures in plasma processes, partly because Ar already serves the present needs, whilst industrial users have little experience with mixtures of gases.

The present study investigates mixtures of gases used in plasma processes. The objective was to increase the

discharge column voltage gradient and therefore increase the power input for a given current. The hypothesis here is that the discharge column voltage gradient can be changed by the addition of a small quantity of other gases such as  $N_2$  or sulphur hexafluoride ( $SF_6$ ). The mechanism of the increase of the discharge column voltage gradient is that the electron density and the electron mobility are altered by the addition of a small amount of appropriate gas (<10% in volume) in the mixtures based on Ar.

The theoretical approach used is based on the Saha equation, on the assumption that local thermal equilibrium exists in the plasma column of a plasma torch. Mixtures based on Ar with addition of  $N_2$ ,  $O_2$  and  $SF_6$  are tested in a plasma torch.

The influences of other parameters such as temperature of the discharge gas, ionisation potentials, thermal conductivities of gases are discussed.

## **§5.2. The mobilities of electrons and positive ions**

The mobilities of electrons and positive ions influence the discharge column voltage gradient. The influence depends most on electrons because the electrons move much faster than positive ions. The theoretical calculation of the discharge column voltage gradient is related to the mobility of the electrons. However the mobility of electrons  $\mu_e$  is difficult to calculate because of the lack of information of the mean free path of electrons in different gases at atmospheric pressure.

The mobility of electrons is defined from the kinetic theory of gases, and mean free path of electrons and mean free path of atoms are given (Chapter 3)

$$\mu_e = \frac{ce\lambda_e}{m_e \sqrt{\frac{3kT}{m_e}}} \quad (5.1)$$

$$\lambda_e = 4\sqrt{2}\lambda \quad (5.2)$$

$$\lambda = \frac{1}{\sqrt{2}\pi nd^2} \quad (5.3)$$

The mean free path of an atom varies inversely with the number density of particles. The perfect gas equation shows that the pressure varies directly with the number density of particles. Therefore

$$\lambda \propto 1/p \quad (5.4)$$

$$\lambda p = \text{constant} \quad (5.5)$$

The mobility and the pressure of electrons are linked by equation 5.2 and the product of the mobility and the pressure however is almost constant, decreases with increasing the gas pressure (Beynon, 1972; von Engel, 1983). This relation will be used to choose the values of the mobility in high pressures because the mobilities at low pressures are available from the work of Brown (1966). As a word of caution, it should be noted that the calculation of the mean free path of electrons has an error at atmospheric pressure ( $1.013 \times 10^5$  Pa) because equations 5.2 and 5.3 are based on the low pressure (<100 Pa) and low value of the discharge column voltage gradient (0.1 V/mm).

However the calculation of the electron mean free path by using these equations will enable to understand the magnitude roughly.

### §5.3. Electric field strength in a plasma torch

The electric field strength in the positive column of the discharge is

$$E = \frac{J}{\sigma} \quad (5.6)$$

The electrical conductivity and the electric field strength can be written as

$$\sigma = en_e(\mu_e + \mu^+) \approx en_e\mu_e \quad (5.7)$$

$$E = \frac{J}{en_e\mu_e} \quad (5.8)$$

The discharge column voltage gradient can be considered only for the longitudinal effect because of its negligible effect of the radial direction value. Equation 5.8 shows that either reducing the number density of electrons  $n_e$  or the mobility of electrons  $\mu_e$  in the electric discharge will increase the value of electric field strength in the discharge column if the electric current density is kept constant. In arcs electrical conductivity may be more dominated by electron-ion Coulomb collisions than by electron-neutral collisions. The number density of electrons can vary in the order of 3 - 5 magnitude while the mobility of electrons may only vary in the order of 2



magnitude or less (von Engel, 1982, Virens et al, 1983).

#### **§5.4 Tailoring the electric discharge gases for a plasma torch**

Several factors effect the voltage gradient in the discharge column. These can be divided into two main groups:

(1) Thermal;

(2) Electronic and molecular.

Here the thermal factors are taken to be those what are governed by the design of the plasma device (nozzle dimension, gas flow rate etc.). Electronic and molecular processes are those what are associated with the inelastic collision properties of gases which may be modified by varying the gas mixtures.

The electronic processes are here considered as

(a) excitation;

(b) dissociation;

(c) ionisation;

(d) the electrochemical nature of the gas (electropositive or electronegative);

(e) and the gas transport properties.

The discharge voltage in the plasma arc is also influenced by the gas transport properties and especially the thermal conductivity, and gas flow rates. The effect on the discharge voltage caused by the different physical processes may be modelled by series resistances, which are

equivalent to the effects of excitation and ionisation of atoms ( $R_{ei}$ ) and the dissociation of molecules ( $R_{ds}$ ) and heat losses other than by de-ionisation or de-excitation in the column ( $R_h$ ) (Fig. 5.1); (where  $R_e$  is the corresponding resistance of the electrode voltage drops)

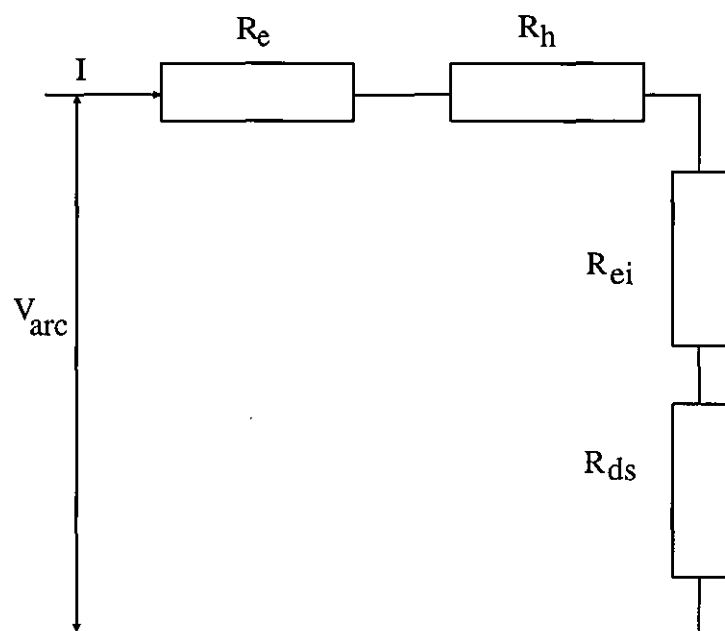


Fig. 5.1 Schematic diagram of the discharge voltage caused by effects of excitation, ionisation ( $R_{ei}$ ) and dissociation ( $R_{ds}$ ), electrodes fall ( $R_e$ ), and the heat loss ( $R_h$ )

#### §5.4.1 Mean free path of electrons

The mean free path of electrons can also be expressed

$$\lambda_e = \frac{1}{n_0 Q_0 + n_i Q_i} \quad (5.9)$$

where  $n_0$  and  $n_i$  are the number densities of neutral particles and ions, and  $Q_0$  and  $Q_i$  the effective cross-section of neutral particles and ions for elastic collisions with electrons respectively.

When gas mixtures are used, the mean free path of electrons is expressed as follows

$$\lambda_e = \frac{1}{\sum n_{k0} Q_{k0} + \sum n_{ki} Q_{ki}} \quad (5.10)$$

$$\frac{1}{\lambda_e} = \frac{1}{\lambda_{1e}} + \frac{1}{\lambda_{2e}} + \dots + \frac{1}{\lambda_{ke}} \quad (5.11)$$

where the subscripts 1, 2, ..., k denote the various gas components. This implies that the mean free path of electrons in gas mixtures is influenced most by the shortest mean free path of the electrons. The resultant mean free path of electrons in gas mixtures can be much shorter when each gas component is of the same magnitude. Large differences among individual free path of the gas components will have less influence on the resultant mean free path of electrons. For example, two gas components have mean free paths of electrons  $\lambda_1$  and  $\lambda_2$ , if  $\lambda_1$  is much smaller than  $\lambda_2$ , then the resultant mean free path  $\lambda$  will be affected by  $\lambda_1$ . If  $\lambda_1$  is much larger than  $\lambda_2$ , the resultant

mean free path  $\lambda$  will be affected by  $\lambda_2$ .

For gas mixtures using two components of different gases the resultant mean free path of electrons can be reduced by half on condition that they have almost the same electron mean free paths. Thus the discharge column voltage gradient is influenced by the mean free path of electrons because of equation 5.1. The equation however is derived from the low pressure and low voltage gradient of the discharge column, it shows that the voltage gradient can be altered by the electron mean free path.

#### **§5.4.2 Electronegativity of gases**

The electronegativity of a gas is a measure of the ability of a molecule to attract electrons to itself. This can be used as a way of increasing the discharge column voltage gradient by limiting the number of the free electrons in a discharge by attaching them to gas molecules. This will lead to the formation of negative ions which are much heavier than the electrons and these negative ions are not accelerated to high velocity, do not significantly contribute to ionising the gas further and do not release electrons.  $\text{SF}_6$ ,  $\text{O}_2$  and the halogens are examples of electronegative gases.

When electric discharges are in operation, there are many electrons and ions in the discharge column ( $<10^{18}/\text{m}^3$ ). The discharge current is mainly carried by free electrons. The higher the number density of electrons the lower the discharge column voltage gradient because of equation 5. 8.

The mobility of electrons can be altered using two component gases. The most effective way to increase the discharge column voltage gradient is the decrease of the number density of the electrons which can vary over a large

range ( $10^{18}/\text{m}^3$  -  $10^{20}/\text{m}^3$ ). An effective way of achieving this is to attract the electrons to the gas molecules forming negative ions. The unattached electrons can be slowed down and be prevented from ionising the gas further.

From the calculation of electron number density (Appendix B) it is apparent that the optimum gas for the increase of the discharge column voltage gradient is not a single gas but rather a combination of gases designed to provide the best effective combination of electron-attachment, electron-slow-down.

The attachment of electrons in the mixtures of gases depends on the cross section of attachment of gases used.  $\text{SF}_6$  and its mixtures with Ar are of great practical potential for special circumstance in industry because the larger cross sections of attachment are found among the electronegative gases. The cross section of attachment  $\sigma_a$  varies with the energy of electrons. It was reported (Christophorou et al, 1983) that the attachment cross sections are larger in the low energy region ( $<2.0$  eV). This suggests that a gas or a buffer gas in the mixtures of gases should reduce the energy of electrons to the region in which electrons can be attached by electronegative gas. One of the gases which can slow down the velocity of electrons is  $\text{N}_2$ . The buffer gas ( $\text{N}_2$ ) scatters the electrons into the region where the electronegative gas ( $\text{SF}_6$ ) captures electrons most efficiently. The mixtures of gases act synergistically. This suggests that a gas mixture should contain a strong electronegative gas, a buffer gas and an inert gas to increase the discharge column voltage gradient and keep the discharge stable.

#### **§5.4.3 Ionisation and excitation potentials**

Electric discharges are influenced by the ionisation

potentials and excitation potentials of the gases used. The excitation values of the gases depend on their electron configurations, ranging from a few electron volts to tens of electron volts, for example, Ar has 13.0 eV - 13.3 eV of excitation potentials.

When mixtures of gases are used there are two cases which should be considered:

(a) the minor gas used has lower ionisation potential than the major gas.

(b) the minor gas has higher ionisation potential than the major gas.

When the minor gas has a lower ionisation potential than the major gas, the electron number density of the mixtures of gases is much influenced by the minor gas. Thus the discharge voltage is lowered. When the minor gas has a higher ionisation potential than the major gas, the electron number density of the gas mixture is influenced by two steps, first the major gas and then the minor gas. Therefore the choice of the minor gas should have a higher ionisation potential than the major gas to increase the discharge column voltage gradient. For example He is better than  $N_2$  in increasing the discharge column voltage gradient because He has a higher ionisation potential (24.580 eV) than  $N_2$  (14.5 eV).

### **§5.5 The Saha equation**

Theoretical calculation of the electron number density was based on the Saha equation. The degree of ionisation for the first ionisation potential of one pure gas can be easily calculated (Cambel, 1963). When multiple ionisation potentials and mixtures of gases are concerned, the

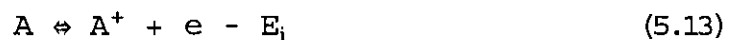
calculation of the Saha equation must be modified. Cambel (1963) gave equations for calculation of degree of ionisation when the first and the second ionisation potential of a pure gas were considered. However the equations for mixtures of gases were not available. The following paragraphs showed the general equations for the calculation of degree of ionisation using the Saha equation, which were the basis of the theoretical calculation for the test.

The degree of ionisation in electric discharges is important because it shows the mode of electric discharges. The degree of ionisation for example in an arc discharge is much higher ( $>10^{-6}$ ) than that in a glow discharge ( $>10^{-10}$ ). The degree of ionisation is difficult to measure directly in many engineering problems for example the arc discharge. Saha (1920) derived an equation of ionisation by using Nernst's theorem which is from classic thermodynamics.

$$\frac{\alpha^2}{1 - \alpha^2} = \frac{cT^{\frac{5}{2}}}{p} e^{-\frac{E_i}{kT}} \quad (5.12)$$

where  $\alpha$  is the degree of ionisation,  $c$  is a constant.

When the case of single ionisation is considered such as for the reaction:



the Saha equation becomes

$$\frac{\alpha^2}{1 - \alpha^2} = \left( \frac{2\pi m_e}{h^2} \right)^{\frac{3}{2}} \frac{(kT)^{\frac{5}{2}}}{p} \frac{2Z_{i+1}}{Z_i} e^{-\frac{E_i}{kT}} \quad (5.14)$$

where  $h$  is Planck's constant and  $Z_i$  is the partition function. The partition function is a statistical mechanical quantity which presents the thermodynamic functions of gases such as energy. It is generally expressed

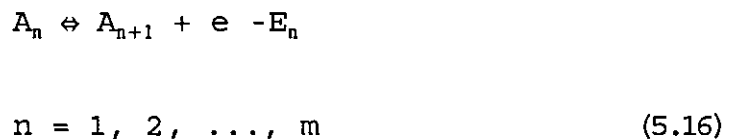
$$Z_i = \sum g_{ij} e^{-\frac{E_{ij}}{kT}} \quad (5.15)$$

where  $g_{ij}$  is a statistic weighted constant (Cambel, 1963). It is an integer which depends on the energy state of an element. This constant  $g_{ij}$  shows the number of states which have the same energy  $E_i$ . The value of  $g_{ij}$  can be referred in the work of Moore (1948).

The Saha equation shows that for any particular gas, the degree of ionisation can be expressed in terms of two variables only, the pressure and the temperature. It should be noted that the Saha equation is applicable to homogeneous systems in thermal equilibrium. Equilibrium conditions are near ideal at higher temperatures and higher densities of electrons such as plasma generated in plasma torches (Cambel, 1963).

#### **§5.5.1 Degree of ionisation for gases**

The general ionisation process is defined as follows (Chapter 3)





where  $A_n$  is the  $n$ th level ionised particle and  $E_n$  is the ionisation energy necessary for ionisation from the  $n$ th to the  $n+1$ th level of ionisation. The  $i$ th degree of ionisation is defined as:

$$\alpha_i = \frac{n_i}{n_H} \quad (5.17)$$

$$\alpha_0 = 1 - \sum_{i=1}^m \alpha_i \quad (5.18)$$

The degree of ionisation for the ionised reaction of equation 5.16 is given as follows:

$$\begin{aligned} K_{i+1} &= \left( \frac{2\pi m_e}{h^2} \right)^{\frac{3}{2}} \frac{(kT)^{\frac{5}{2}}}{p} \frac{2Z_{i+1}}{Z_i} e^{-\frac{E_i}{kT}} \\ &= \frac{\alpha_{i+1} \sum i \alpha_i}{\alpha_i (1 + \sum i \alpha_i)} \end{aligned} \quad (5.19)$$

$$i = 0, 1, 2, \dots, m$$

### §5.5.2 Number density of electrons in the mixtures of gases

The number densities of electrons in a single ionised gas and in single and double ionised gas are seen Appendix C. For the mixture of two gases, the number density of the heavy particles can be expressed by the sum of that of each gas, namely,

$$n_H = n_{H1} + n_{H2} \quad (5.20)$$

where  $n_{H1}$  is the sum of the number density of the heavy particles of the first gas; and  $n_{H2}$  the sum of the number density of the heavy particles of the second gas.

The degree of ionisation for different gas is defined as

$$\alpha_{i,1} = \frac{n_{i,1}}{n_{H1}} \quad (5.21)$$

$$\alpha_{i,2} = \frac{n_{i,2}}{n_{H2}} \quad (5.22)$$

where  $\alpha_{i,1}$  is the  $i$ th degree of ionisation of the first gas; and  $\alpha_{i,2}$  the  $i$ th degree of ionisation of the second gas.

The number density of electrons is equal to the sum of that of each gas, assuming the first gas is ionised to the level  $q$  and the second gas is ionised to the level  $r$ .

$$n_e = \sum_{j=1}^q j n_{j,1} + \sum_{m=1}^r m n_{m,2} \quad (5.23)$$

$$\alpha_e = \frac{n_e}{n_H} = \frac{\sum_{j=1}^q j \alpha_{j,1} + \delta \sum_{m=1}^r m \alpha_{m,2}}{1 + \delta} \quad (5.24)$$

$$\delta = \frac{n_{H2}}{n_{H1}} = \frac{V_{H2}}{V_{H1}} \quad (5.25)$$

where  $v_{H2}$ ,  $v_{H1}$  are volumes of the second and the first gas respectively. The degree of ionisation is given follows:

$$K_{i+1} = \frac{\alpha_{i+1,t}}{\alpha_{i,t}} \frac{\alpha_e}{1 + \alpha_e}$$

$$= \left( \frac{2\pi m_e}{h^2} \right)^{\frac{3}{2}} \frac{(kT)^{\frac{5}{2}}}{p} \frac{2Z_{i+1,t}}{Z_{i,t}} e^{-\frac{E_{i+1,t}}{kT}} \quad (5.26)$$

$$i = 0, 1, \dots, m; \quad t = 1, 2$$

$$\alpha_{0,1} = 1 - \sum_{j=1}^q \alpha_{j,1}$$

$$\alpha_{0,2} = 1 - \sum_{m=1}^r \alpha_{m,2} \quad (5.27)$$

where  $Z_{i,1}$  and  $Z_{i,2}$  are partition functions of the first gas and the second gas respectively.  $E_{i,1}$  and  $E_{i,2}$  ionisation energy level of the first and the second gas.

From equations (Appendix C), the number density of electrons in the mixture of two gases is also written as follows

$$n_e = \frac{\alpha_e}{1 + \alpha_e} \frac{p}{kT} \quad (5.28)$$

### §5.5.3 Equations for the mixture of Ar and O<sub>2</sub>

For the case of the mixture of 90% Ar and 10% O<sub>2</sub> with

a single and double ionisation at atmospheric pressure, the equations are as follows assuming the first gas is Ar and the second gas is O<sub>2</sub>:

$$\frac{\alpha_{1,1}}{\alpha_{0,1}} \frac{\alpha_e}{1 + \alpha_e} = \left( \frac{2\pi m_e}{h^2} \right)^{\frac{3}{2}} \frac{(kT)^{\frac{5}{2}}}{p} \frac{2Z_{1,1}}{Z_{0,1}} e^{-\frac{E_{1,1}}{kT}} \quad (5.29)$$

$$\frac{\alpha_{2,1}}{\alpha_{1,1}} \frac{\alpha_e}{1 + \alpha_e} = \left( \frac{2\pi m_e}{h^2} \right)^{\frac{3}{2}} \frac{(kT)^{\frac{5}{2}}}{p} \frac{2Z_{2,1}}{Z_{1,1}} e^{-\frac{E_{2,1}}{kT}} \quad (5.30)$$

$$\frac{\alpha_{1,2}}{\alpha_{0,2}} \frac{\alpha_e}{1 + \alpha_e} = \left( \frac{2\pi m_e}{h^2} \right)^{\frac{3}{2}} \frac{(kT)^{\frac{5}{2}}}{p} \frac{2Z_{1,2}}{Z_{0,2}} e^{-\frac{E_{1,2}}{kT}} \quad (5.31)$$

$$\frac{\alpha_{2,2}}{\alpha_{1,2}} \frac{\alpha_e}{1 + \alpha_e} = \left( \frac{2\pi m_e}{h^2} \right)^{\frac{3}{2}} \frac{(kT)^{\frac{5}{2}}}{p} \frac{2Z_{2,2}}{Z_{1,2}} e^{-\frac{E_{2,2}}{kT}} \quad (5.32)$$

$$\alpha_{0,1} = 1 - \alpha_{1,1} - \alpha_{2,1} \quad (5.33)$$

$$\alpha_{0,2} = 1 - \alpha_{1,2} - \alpha_{2,2} \quad (5.34)$$

$$\delta = 10\%/90\% = 1/9 \quad (5.35)$$

$$\alpha_e = \frac{\alpha_{1,1} + 2\alpha_{2,1} + \delta(\alpha_{1,2} + 2\alpha_{2,2})}{1 + \delta} \quad (5.36)$$

$$Z_{i,1} = \sum_{j=1}^{\infty} g_{ij} e^{-\frac{E_{j,1}}{kT}} \quad (5.37)$$

$$Z_{i,2} = \sum_{j=1}^{\infty} g_{ij} e^{-\frac{E_{j,2}}{kT}} \quad (5.38)$$

## §5.6 Numerical procedures

Equations 5.29 to 5.38 in section §5.5.3 are formed as a system of non-linear equations and solved using the program C05NBF from the NAG Fortran computing library to obtain the degrees of ionisation. The program was mainly based on the correction at each step of calculation by using the Newton gradient direction. The methods of calculation in the program are iterative, an initial value must be supplied as near the solutions as possible. These initial values are crucial because the convergence of the calculation depends on the first derivatives of functions. The difficult estimate of initial values for the calculation was at temperature ranging from 13,000 K - 14,000 K since rapid change of functions with temperature occurred. Once all the degrees of ionisation were obtained the number density of electrons was calculated from equation 5.28. The computer calculation occasionally gives minus values for the degree of ionisation, which was because of the very small number of the degree of the ionisation and the iteration error may be satisfied. The results of calculations can be justified when all the variables are positive and less than unity (Appendix B).

## §5.7 Theoretical calculation

The theoretical calculation was carried out using an HP main frame computer. The programme was coded using Fortran 77, linked with the NAG Fortran computing library. It included calculations of the number densities and the electric field strength for pure Ar, N<sub>2</sub>, O<sub>2</sub> and their mixtures.

### §5.7.1 The number density of electrons in different gas mixtures

The number densities of electrons in Ar and in the mixtures of Ar and O<sub>2</sub>; Ar and N<sub>2</sub> are shown in Fig. 5.2 ( $p=1.013 \times 10^5$  Pa). The number density of electrons increases rapidly before it is saturated above about 16,000 K. The number densities in different ratios of Ar and O<sub>2</sub>, Ar and N<sub>2</sub> vary little at the same temperature.

### §5.7.2 The calculation of the electric field strength

The electric field strength in the mixture of Ar and N<sub>2</sub> was calculated from equation 5.8. The mobility of electrons in N<sub>2</sub> is expressed as  $3.8481 \times 10^{11}/p$  (Wu, 1988). The density of the discharge current was  $10^6$  Am<sup>2</sup>. Fig. 5.3 shows the discharge column voltage gradient in the different gas mixtures ( $p=1.013 \times 10^5$  Pa).

The discharge column voltage gradient is saturated when the temperature is greater than 16,000 K because the lower ionisation degree was fully reached. The much higher temperature is required to get further ionisation.

## §5.8 Experimental arrangement

Fig. 5.4 shows the experimental arrangement. The gas mixtures used were Ar + O<sub>2</sub>, Ar + N<sub>2</sub>, Ar + SF<sub>6</sub> and Ar + N<sub>2</sub> + SF<sub>6</sub>. The host gas was Ar which was varied from 80% to 95% in volume.

The plasma torch was made by Plasma Systems (SIP Ltd.). It was operated in the transferred mode in the tests. The plasma torch has a vortex gas flow guide. The orifice is shown in Fig. 5.5. The discharge gaps between

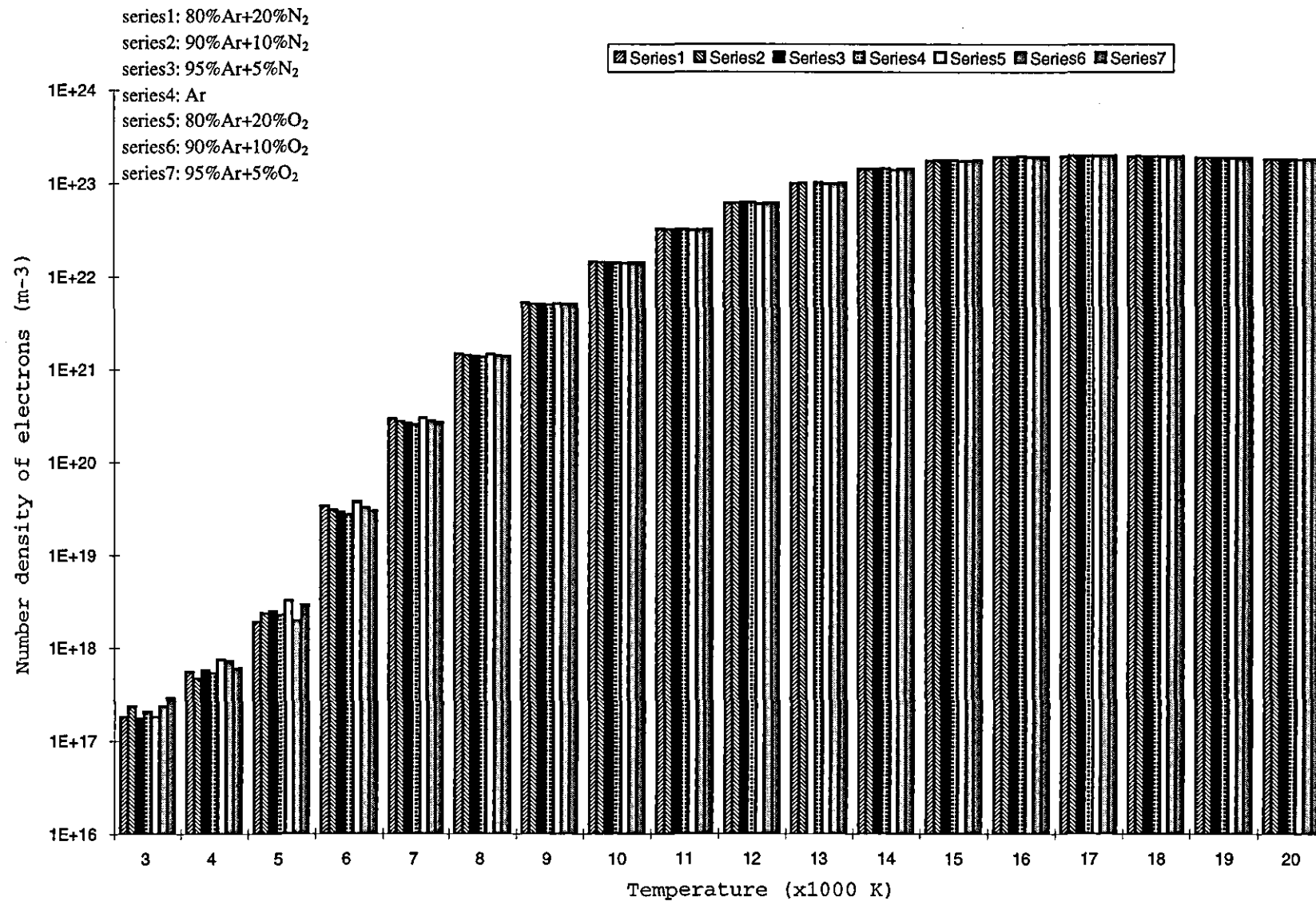


Fig. 5.2 Calculated number density of electrons with temperature in pure argon and mixtures of different gases

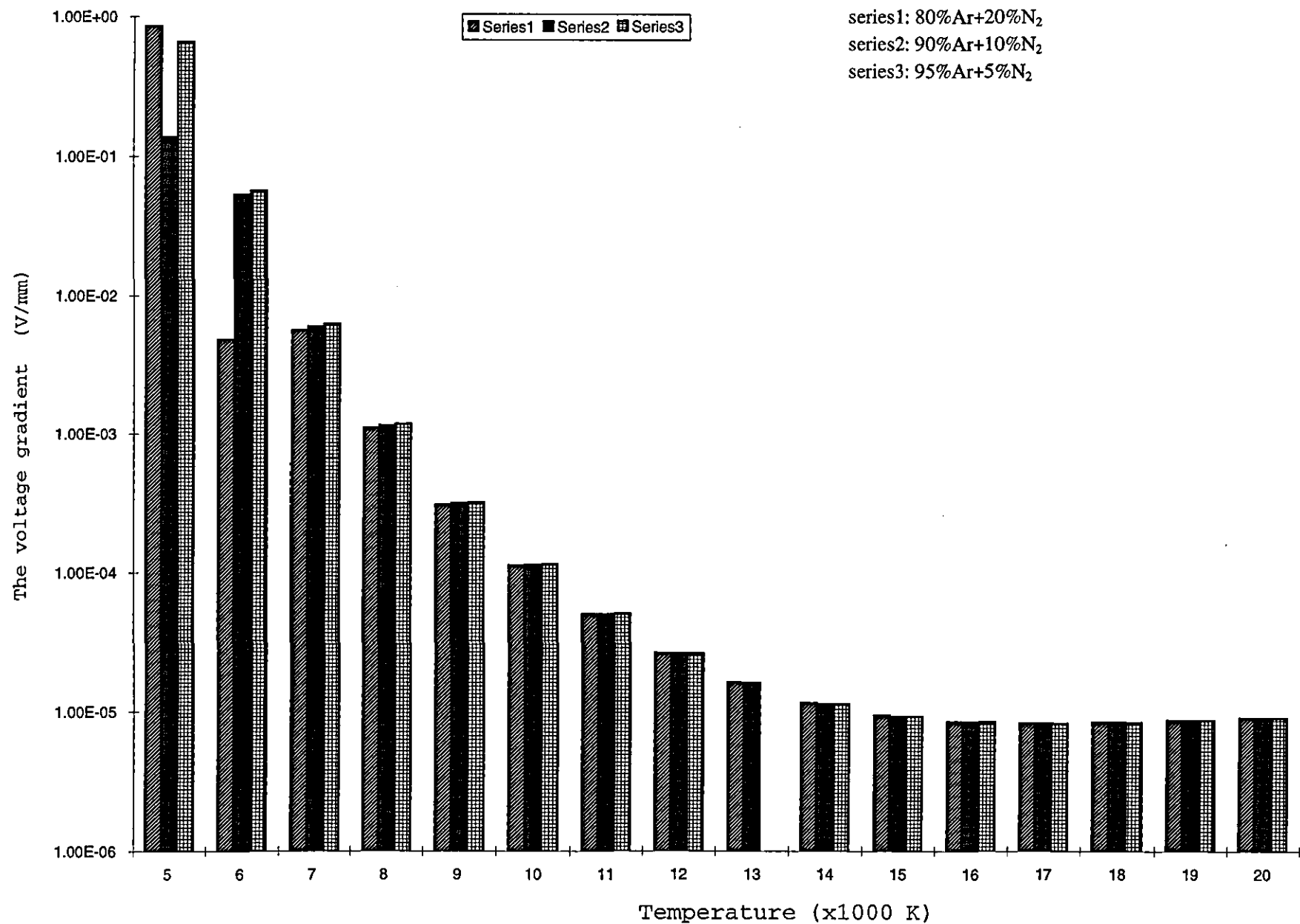


Fig. 5.3 Calculated discharge column voltage gradient in different gas mixtures



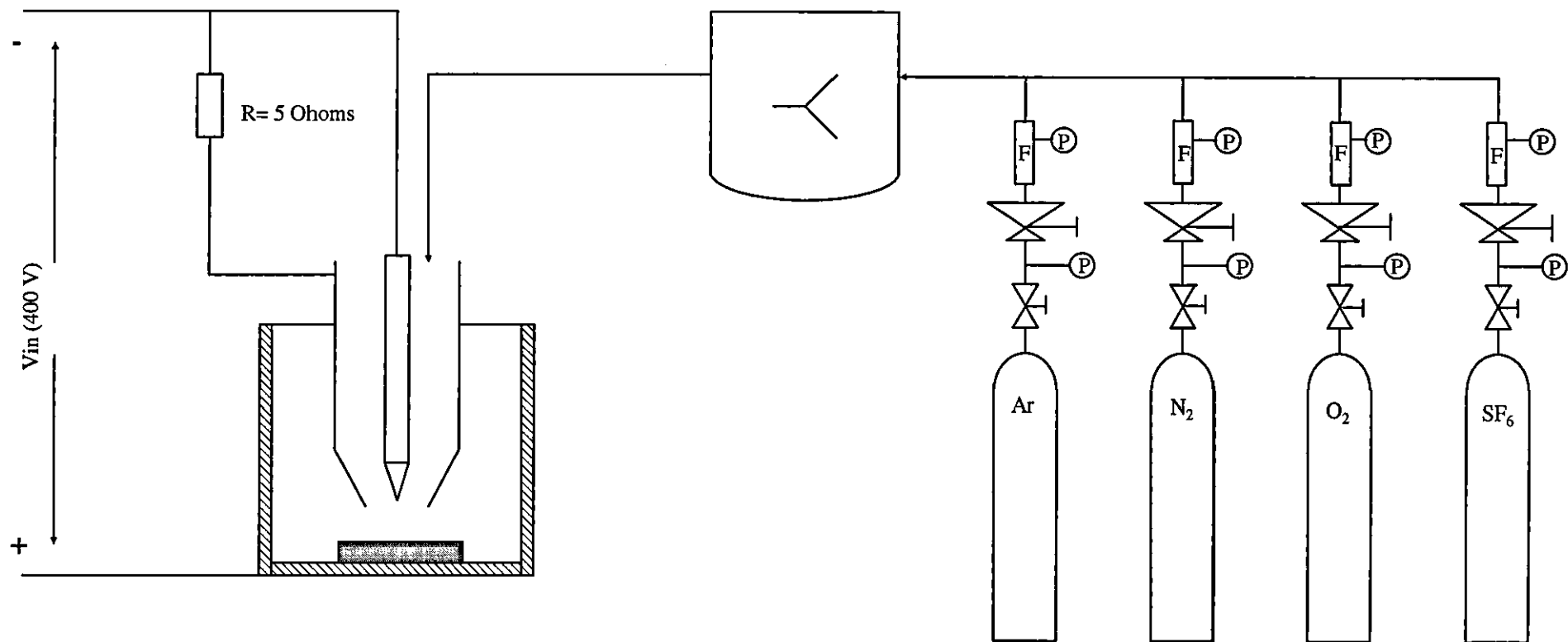


Fig. 5.4 Schematic of the experimental arrangement

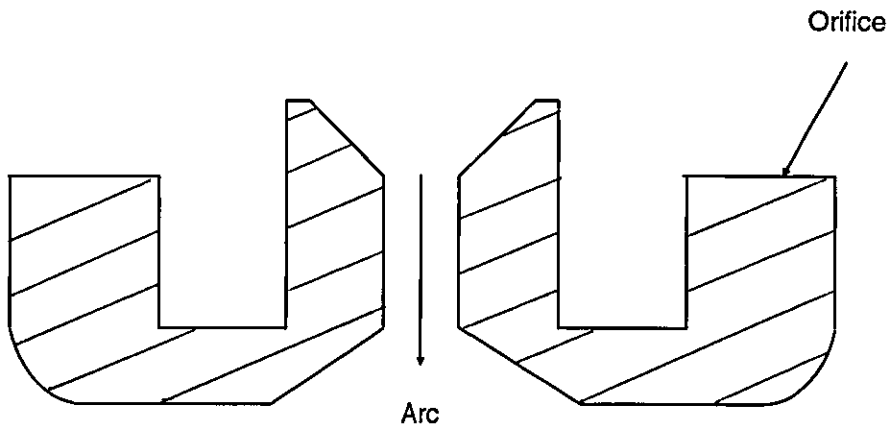


Fig. 5.5 Schematic diagram of the orifice

the cathode and the workpiece (the anode) in the transferred mode were varies from 15 mm to 33 mm.

The discharge chamber was made from a copper cylinder. It was 223 mm high with 110 mm of outer diameter and 107 mm of inner diameter respectively. Fig. 5.6 shows the discharge chamber.

The power supply can provide a maximum open circuit voltage of 400 V and a maximum current of 600 A (TCR4, BOC Ltd.). The plasma torch and the discharge chamber were placed in an inter-locked closure for safe operation.



Fig. 5.6 The air tight chamber

The gases were mixed physically in a gas chamber made from an aluminium cylinder with diameter of 90 mm and height of 190 mm. Different gases were measured by flow meters before they were mixed in the chamber. The arc was initiated by using Ar first and then the mixture of Ar and SF<sub>6</sub>.

The discharge voltage was recorded after the mixture of gases passed through the plasma torch for at least for one minute. The strong smell character of smoking sulphur, which was dissociated from the discharge, could be smelled during the tests!

## **§5.9 Measurements of the discharge column voltage gradient**

The measurement of the discharge column voltage gradient in the different gas mixtures were carried out with and without the gas chamber.

### **§5.9.1 The mixture of Ar and N<sub>2</sub>**

#### **(a) Free burning plasma surrounded by air at atmospheric pressure**

The first series of tests of the mixture of Ar and N<sub>2</sub> were carried out with the plasma column surrounded by air. The discharge length was fixed at 15 mm and 25 mm measured from the bottom of the orifice to the workpiece. Fig. 5.7 shows the relationship between the discharge voltage and the discharge length. The discharge voltage at a separation of  $l_1$  can be expressed as (Fig.5.8)

$$V_{d1} = V_a + V_c + l_1 E \quad (5.39)$$

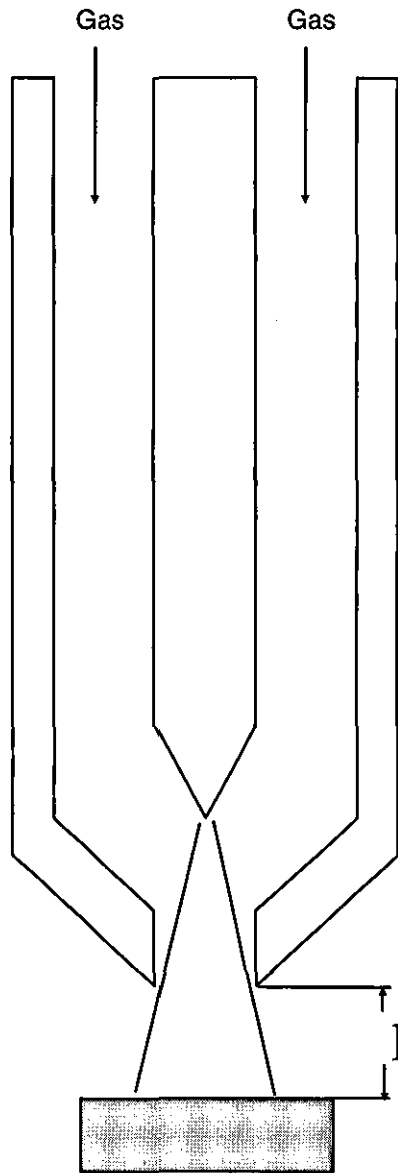


Fig. 5.7 Schematic of measurement of the discharge length

The gradients of the discharge voltage were calculated by  $\Delta V_d / \Delta l$  from the measurements at two different separations, i.e.

$$E = \frac{\Delta v_d}{\Delta l} = \frac{v_{d2} - v_{d1}}{l_2 - l_1} \quad (5.40)$$

Therefore the measurement error in measuring the discharge length can be minimised and the cathode fall and the anode fall are also deducted.

The characteristics of the gradients of the discharge voltage and the current in pure Ar and in the mixture of Ar and N<sub>2</sub> are shown in Fig. 5.9. The gradients of the discharge voltage in pure Ar and in the mixtures of Ar and N<sub>2</sub> are different. The gradients of the discharge voltage in the mixture of Ar and N<sub>2</sub> are lower than that in pure Ar. When more than 20% N<sub>2</sub> was added, the arc ignition was more difficult at low discharge current (<100 A). As the discharge current was increased further(>100 A) striking the arc was as easy as that in pure Ar. The stability of the discharge using pure Ar and the mixture of Ar and N<sub>2</sub> was similar although occasionally an unstable discharge in the mixture of Ar and N<sub>2</sub> was observed for few seconds at low discharge current (<100 A). The maximum discharge current in pure N<sub>2</sub> was 400 A at a discharge length of 25 mm.

The variation of the discharge column voltage gradient with addition of N<sub>2</sub> at different discharge currents is shown in Fig. 5.10. It was found that the discharge column voltage gradient did not increase linearly with addition of N<sub>2</sub>. The variation of the discharge column voltage gradient had no significant difference between addition of 5% N<sub>2</sub> and 20% N<sub>2</sub>. This implies that only small quantity of N<sub>2</sub> was needed (<10%).

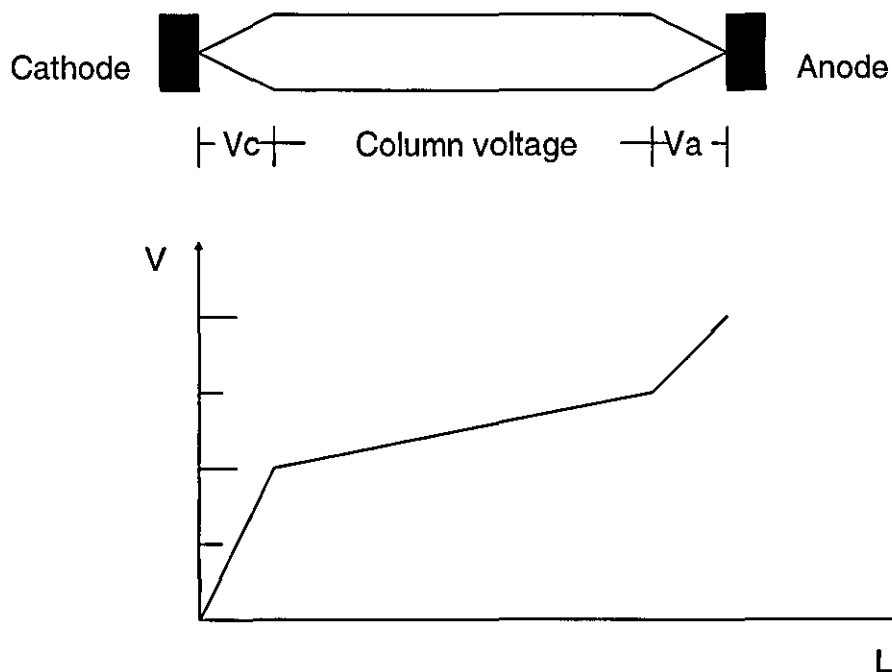


Fig.5.8 Schematic of the cathode, the anode, the column voltages

**(b) Free burning plasma in an air tight chamber**

The air tight chamber was flushed with Ar for at least two minutes to remove the air before the operation of the plasma torch.

Fig. 5.11 shows the discharge column voltage gradient in the mixture of Ar and  $N_2$  with a free burning plasma in an air tight chamber. The discharge column voltage gradient in pure Ar and in all the mixture of Ar and  $N_2$  have no significant difference. The mixture of Ar and  $N_2$  has almost the same values of the discharge column voltage gradient as that with  $N_2$  in air.

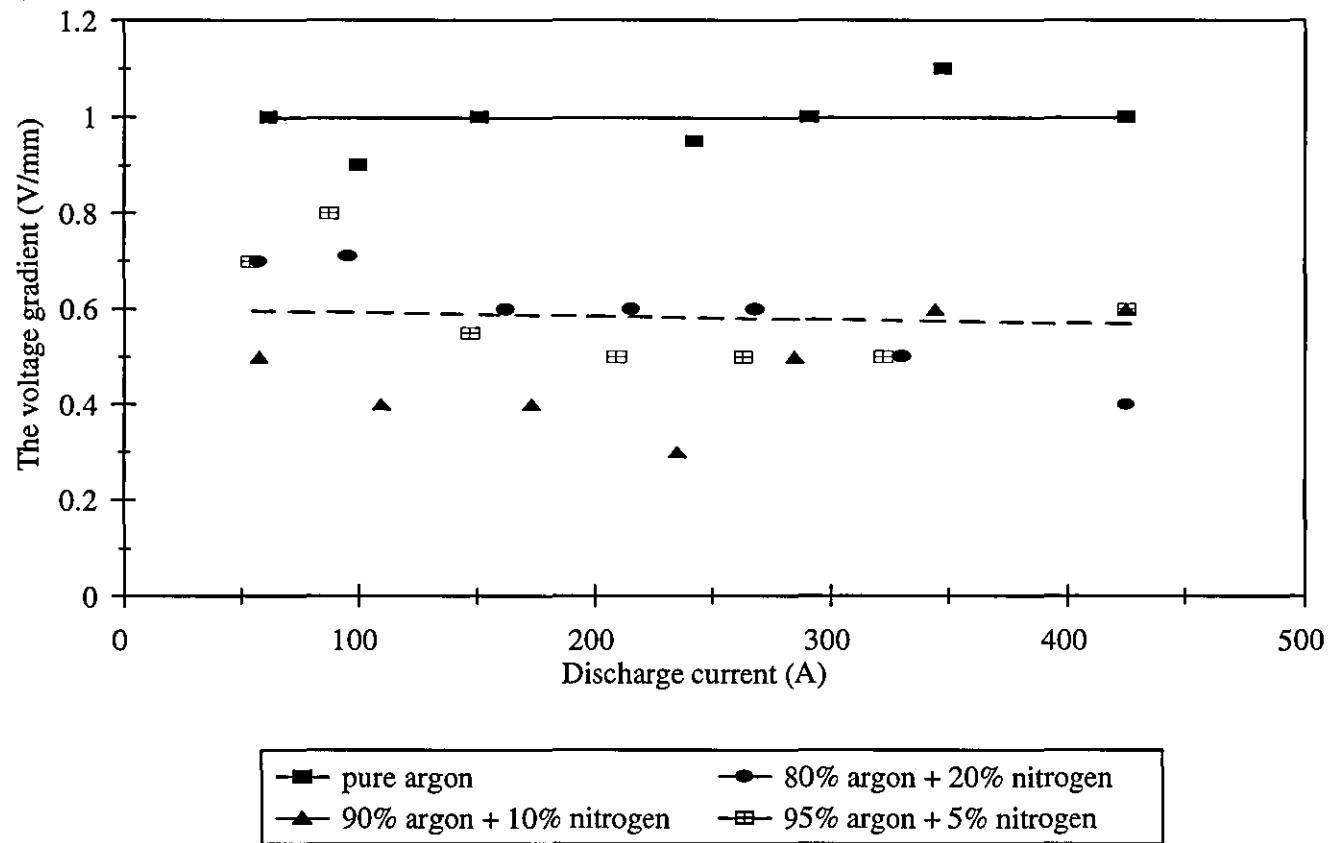


Fig. 5.9 Dependence of the discharge column voltage gradient and the discharge current in different mixtures of Ar and N<sub>2</sub> surrounded by air at atmospheric pressure



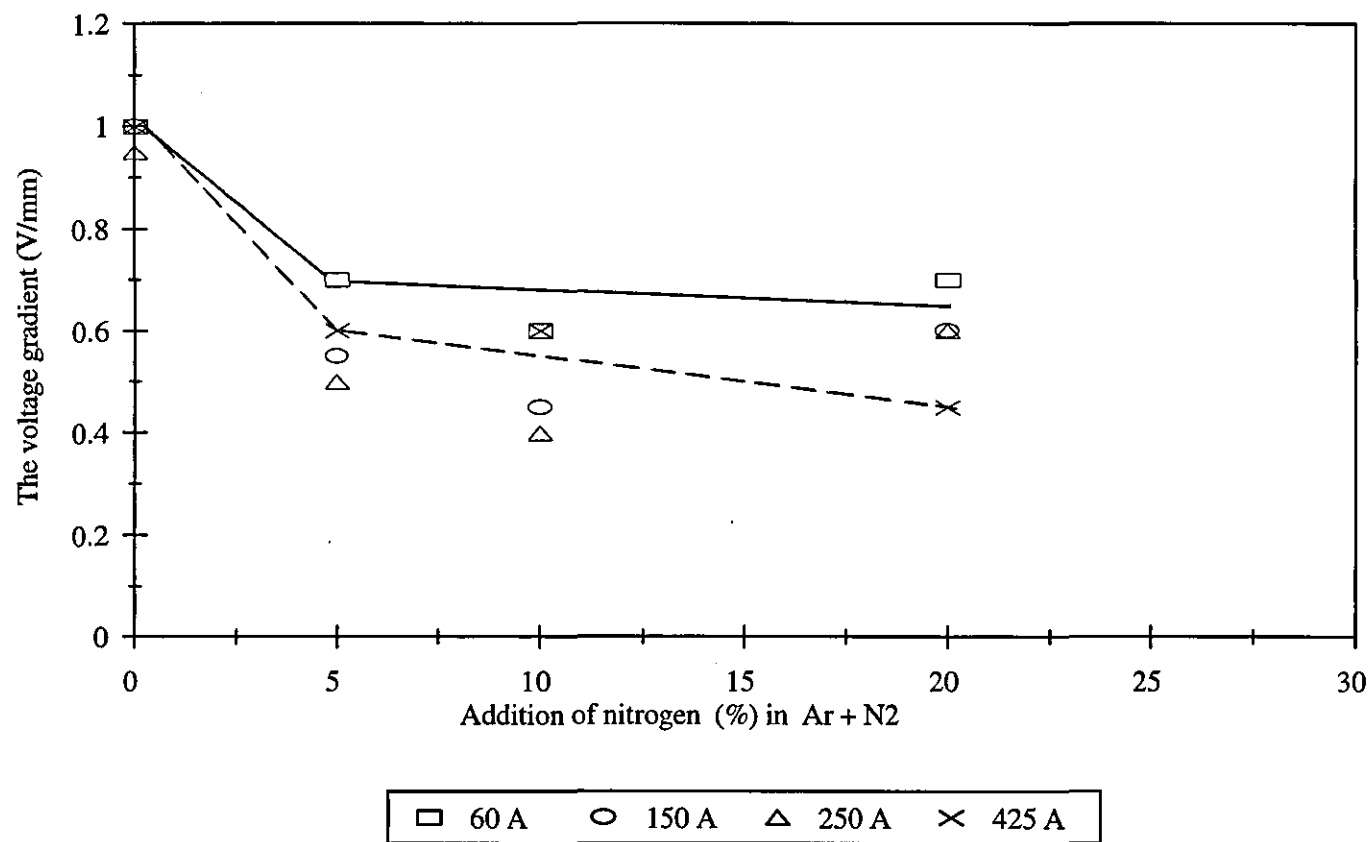


Fig. 5.10 Variation of the discharge column voltage gradient and the addition of  $N_2$  in different mixtures of Ar and  $N_2$  at different currents surrounded by air

Arc ignition at low discharge current ( $<100$  A, discharge length 33 mm) was slightly more difficult compared with high discharge current ( $>150$  A). When more than 20%  $N_2$  was added, several ignitions were required, but once it was started the arc was stable.

The variation of the discharge column voltage gradient with addition of  $N_2$  is shown in Fig. 5.12. The discharge column voltage gradients were almost the same. It also suggested that only a small quantity of  $N_2$  was needed ( $<10\%$ ).

#### **§5.9.2 Free burning plasma in the mixture of Ar and $O_2$ surrounded by air at atmospheric pressure**

A series of tests using the mixture of Ar and  $O_2$  were carried out. The discharge column voltage gradient in pure Ar and in the mixture of Ar and  $O_2$  are shown in Fig. 5.13. They show no significant difference between pure Ar and the mixture of Ar and  $O_2$ . The discharge column voltage gradients had no significant difference with different addition of  $O_2$ . This suggested that there was no advantage using  $O_2$ . The discharge column voltage gradients using the mixture of Ar and  $N_2$ , however, are smaller (30%) than that using the mixture of Ar and  $O_2$  surrounded by air.

During the tests, the arc ignition was more difficult with the mixture of Ar and  $O_2$  than that with the mixture of Ar and  $N_2$ , especially when the discharge current was below 150 A. As the discharge current was increased further ( $>150$  A), the arc ignition became more easy. Once the arc was established, it was stable. The difficulty of arc ignition resulted from oxidation of cathode. When more than 20%  $O_2$  was added, the cathode was seriously damaged and the cathode had to be replaced.

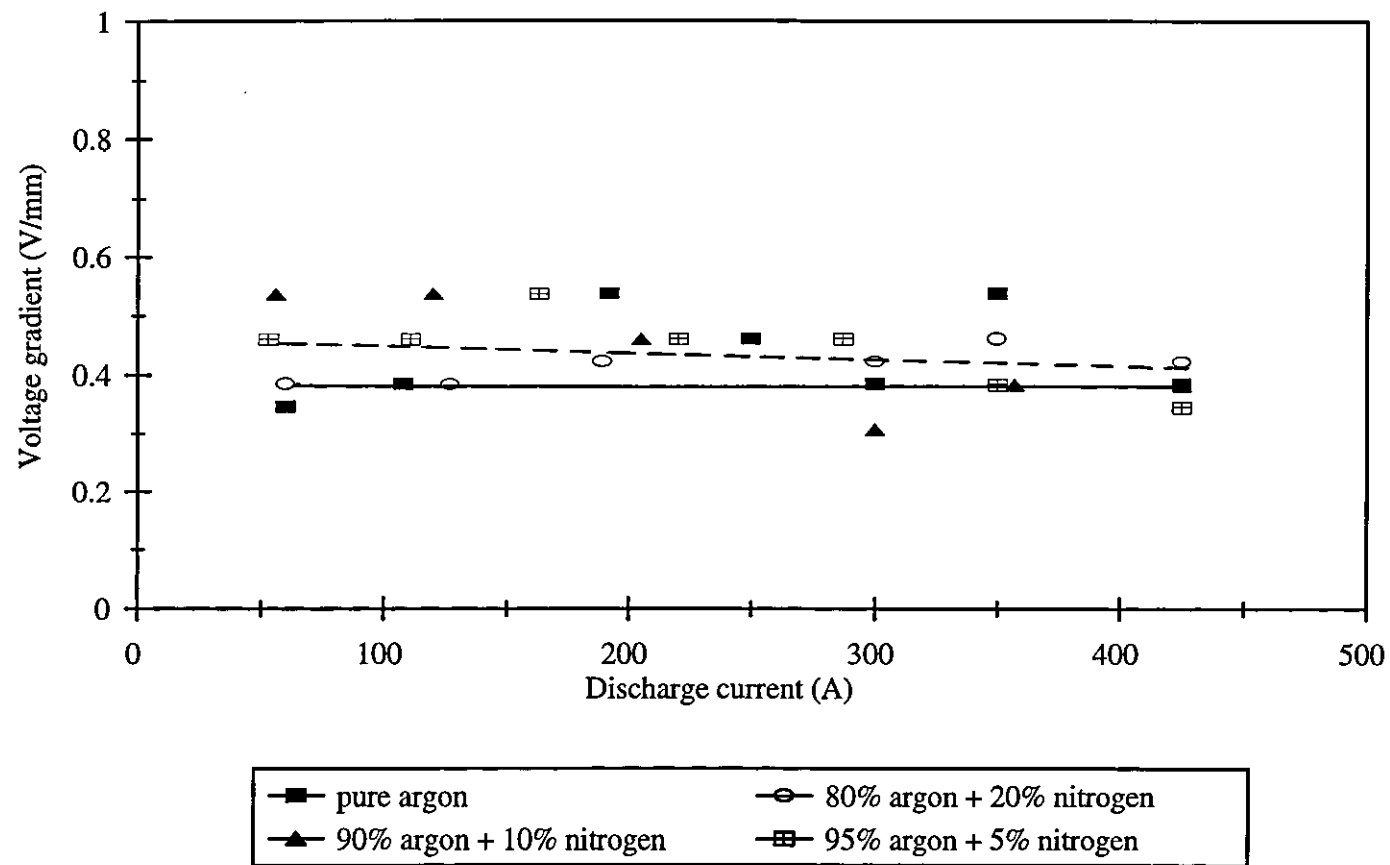


Fig 5.11 Dependence of the discharge column voltage gradient and the discharge current in the mixture of Ar and N<sub>2</sub> in the air tight chamber

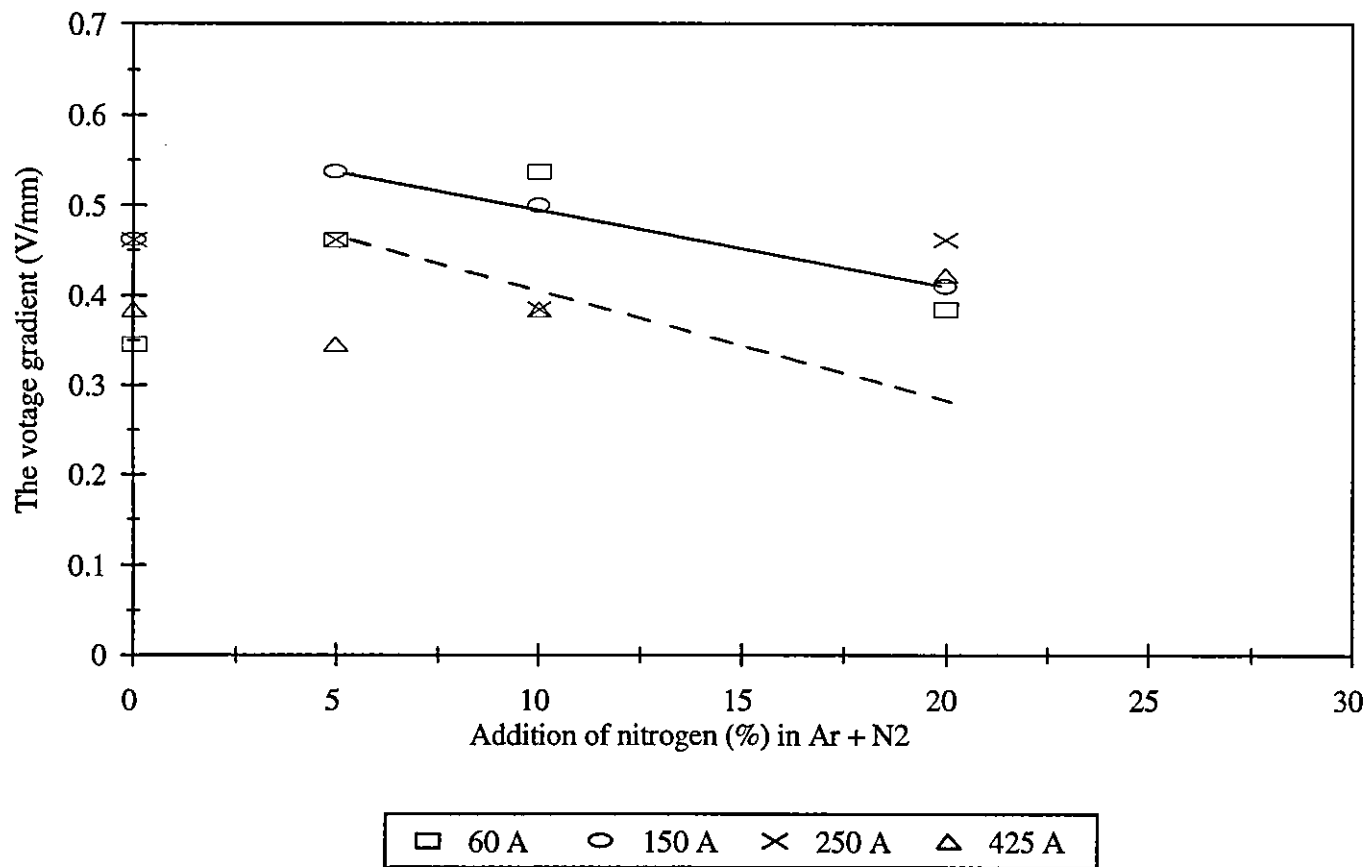


Fig 5.12 Variation of the discharge column voltage gradient with the addition of  $N_2$  in different mixtures of Ar and  $N_2$  at different currents in the air tight chamber

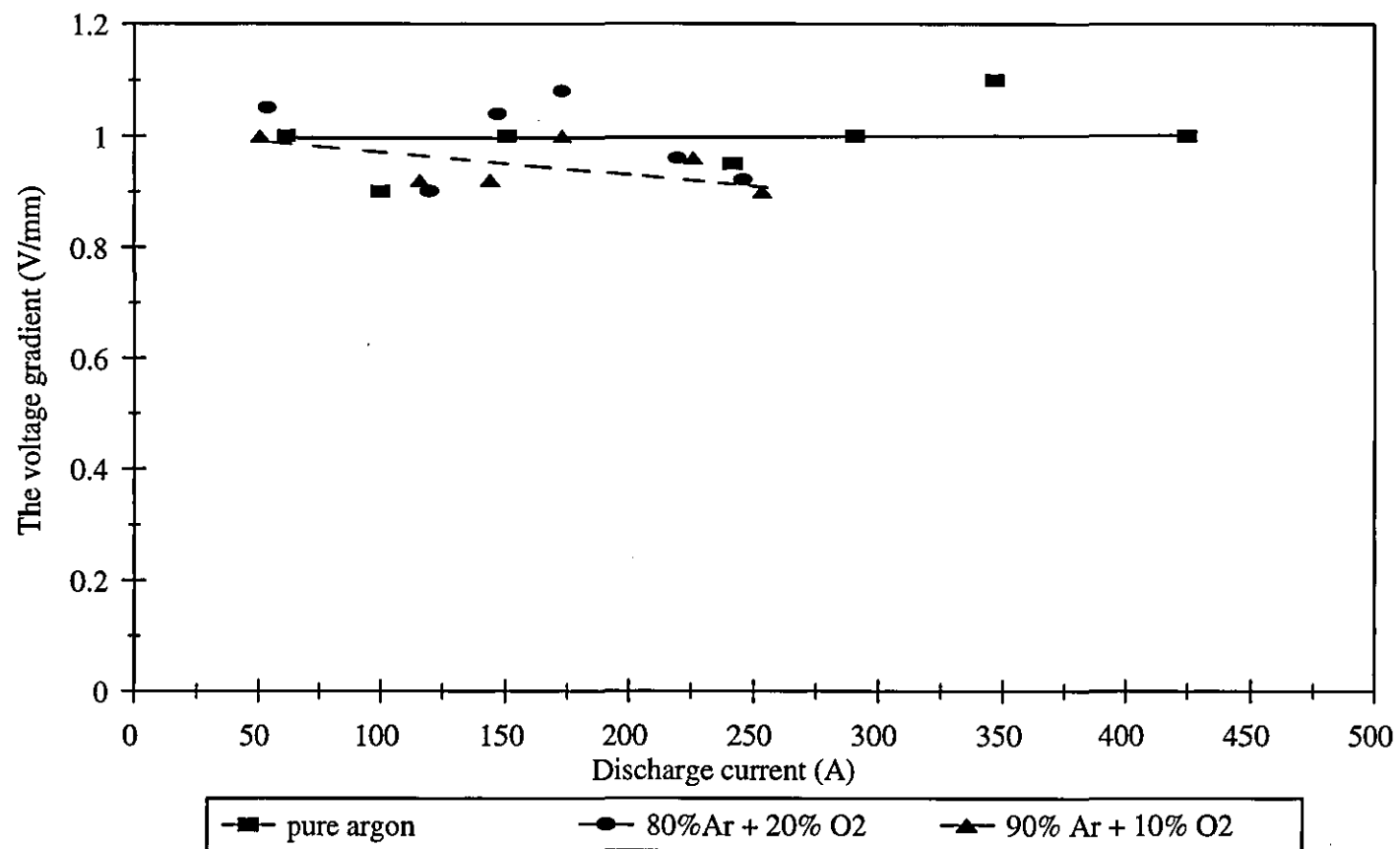


Fig. 5.13 Dependence of the discharge column voltage gradient and the discharge current in the mixture of Ar and O<sub>2</sub> surrounded by air at atmospheric pressure

### §5.9.3 Mixtures of Ar, N<sub>2</sub> and SF<sub>6</sub>

A series of tests were carried out using mixtures of Ar, N<sub>2</sub> and SF<sub>6</sub> because it was believed that the nature of the electronegativity of SF<sub>6</sub> could attract the free electrons from the discharge column. This effect would reduce the density of the electrons in the discharge column and increase the discharge column voltage gradient.

The first test used the mixture of Ar and SF<sub>6</sub> with a volume ratio of 99% Ar and 1% SF<sub>6</sub>. Fig. 5.14 shows the discharge column voltage gradient. The discharge column voltage gradient is only 0.3 V/mm with a discharge current ranging from 60 A to 420 A, which shows no significant difference from the pure Ar test. A second test was carried out using the mixture of Ar and SF<sub>6</sub> with a volume ratio of 95% Ar and 5% SF<sub>6</sub>. Fig. 5.14 shows the discharge column voltage gradient is significantly increased to 0.5 V/mm.

More tests were carried out using 89% Ar, 10% N<sub>2</sub> and 1% SF<sub>6</sub>; and 85% Ar, 10% N<sub>2</sub> and 5% SF<sub>6</sub>. Fig. 5.15 shows the discharge column voltage gradient with the two different mixtures. The discharge column voltage gradients show no significant difference.

Arc ignition was very difficult when SF<sub>6</sub> was added passed through the plasma torch because the breakdown voltage of SF<sub>6</sub> is as high as 8,890 V/mm (Christophorou, 1992).

## §5.10 Discussion

### §5.10.1 Effects of gas mixtures

The cathode and the anode falls are independent of the discharge current. The equivalent resistance  $R_e$  (Fig. 5.1)

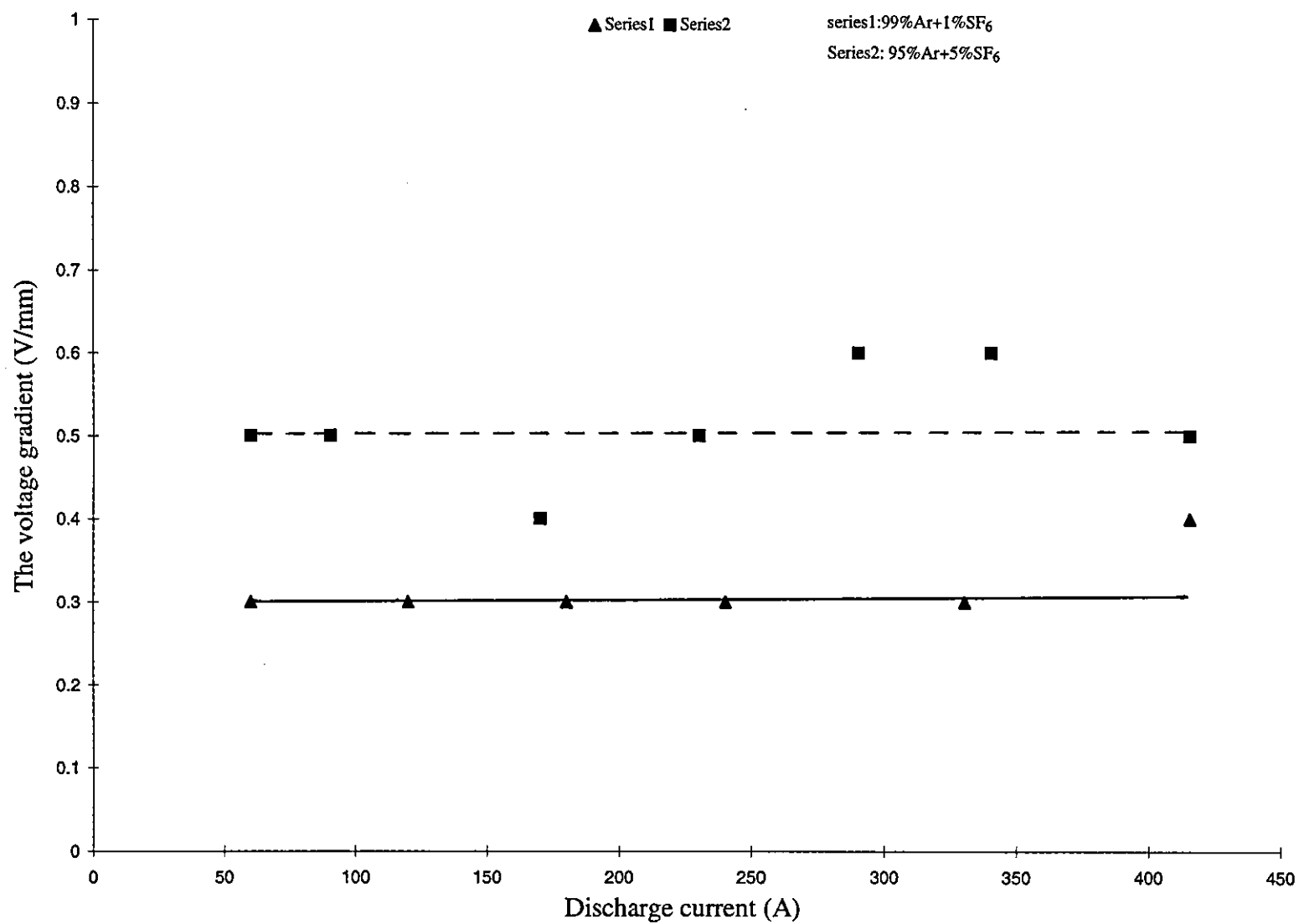


Fig. 5.14 Dependence of the discharge column voltage gradient and the discharge current in different mixtures of Ar and SF<sub>6</sub>

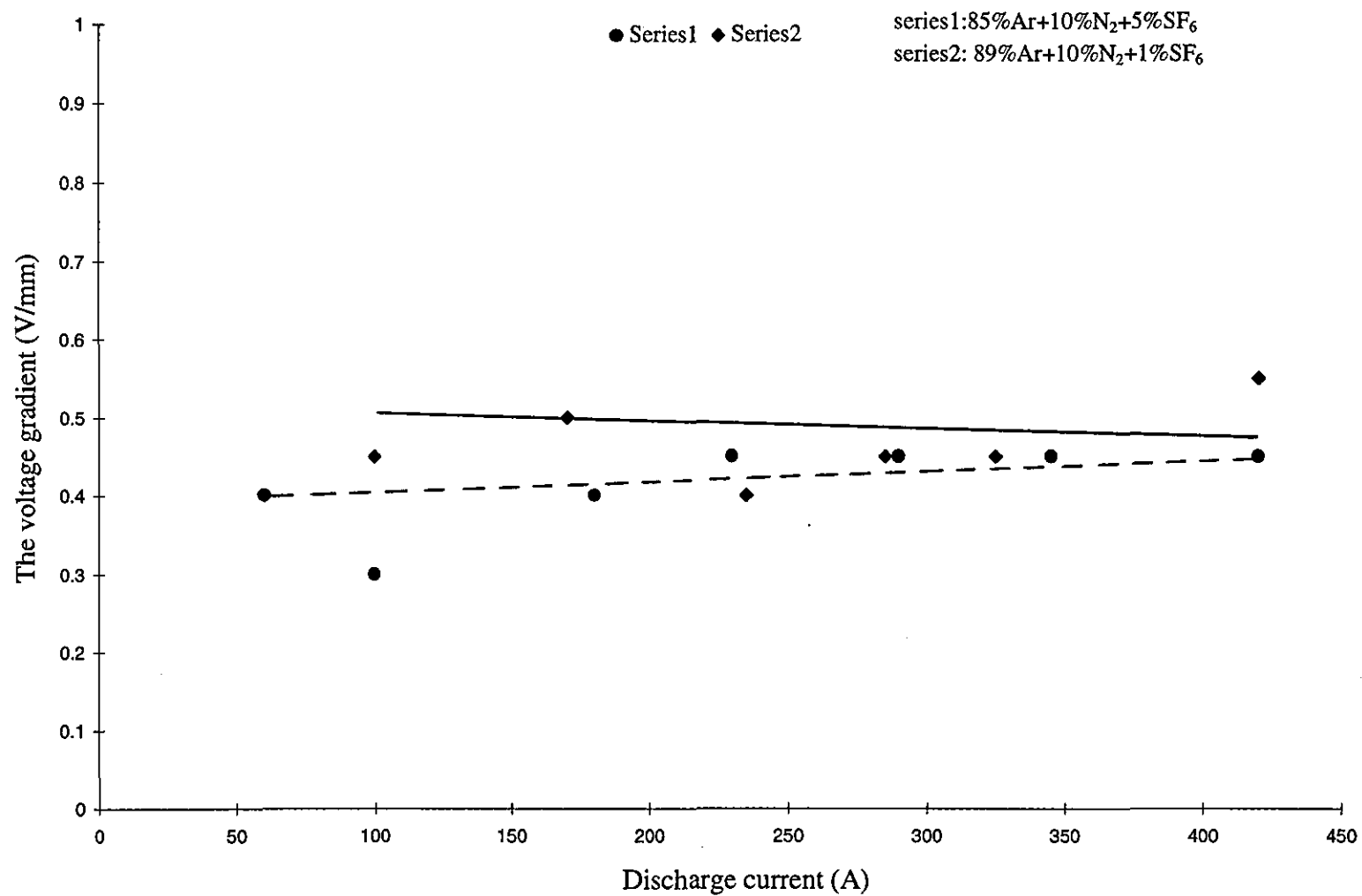


Fig. 5.15 Dependence of the discharge column voltage gradient and the discharge current in different mixtures of Ar, N<sub>2</sub> and SF<sub>6</sub>



is constant. However this voltage drop changes with change of gas or gas mixtures. The experimental results showed that the voltage drop across the electrodes for pure Ar and mixtures of Ar and  $N_2$  are around 20 V and 23 V respectively. Similarly the equivalent resistance  $R_h$  (Fig. 5.1) for the thermal conductivity of gases are constant. The equivalent resistance  $R_{ei}$  (Fig. 5.1) for the ionisation potential varied little because the first ionisation potentials of Ar (15.755 eV), N (14.5 eV) are close. The equivalent resistance  $R_{ds}$  (Fig. 5.1) for dissociation potential, however, varies dramatically with different gases. If an electronegative gas is used there is an equivalent resistance  $R_{neg}$  in series. From the point of view of increasing the discharge column voltage gradient the larger value for the equivalent resistances of  $R_{ei}$  and  $R_{ds}$  and  $R_{neg}$  are desired for a given discharge current and a separation of the electrodes.

The experimental results show that the discharge voltage in a transferred plasma torch using Ar surrounded by air at atmospheric pressure can be increased by addition of  $N_2$  to Ar. The discharge voltage was 8 V higher in Ar with only 5% addition of  $N_2$  however the corresponding voltage gradient (0.5 V/mm at 200 A) in the arc column is lower than that in pure Ar (1.0 V/mm). This is caused by the increase of the voltage fall across the cathode and the anode. The lower gradient of the discharge voltage in the mixture of Ar and  $N_2$  may be due to the dissociation of  $N_2$ , which was expected to constitute an energy loss and the lower ionisation potentials of  $N_2$  compared with that of Ar.

The small difference in the discharge column voltage gradients between pure Ar and the mixture of Ar and  $N_2$  is in good agreement with the theoretical calculation using the Saha equation. The number densities of electrons in the mixture of Ar and  $N_2$ , and in the pure Ar have no significant difference (Fig. 5.2). The mean free paths of Ar and  $N_2$  are

$62.6 \times 10^{-9}$  m and  $58.8 \times 10^{-9}$  m at atmospheric pressure respectively. Thus the discharge column voltage gradients are almost the same.

The discharge column voltage gradients in pure Ar and in the mixture of Ar and  $O_2$  surrounded by air show no significant difference. Ar with addition of  $O_2$  has no advantage in increasing the discharge column voltage gradient although  $O_2$  has a weak ability to attract electrons.

The mixture of Ar and  $SF_6$  has the most significant effect in increasing the discharge column voltage gradient because  $SF_6$  attracts electrons and forms negative ions, therefore the number density of electrons decreases and the voltage gradient increases.  $SF_6$  also decreases the velocity of electrons which are not attracted, then the mobility of electrons is decreased in the discharge column. This also leads to an increase of the voltage gradient.

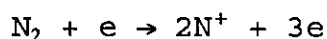
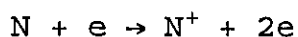
The best ratio of Ar and  $SF_6$  is 95% to 5%. Less than 5% of  $SF_6$  does not reduce the number density of electrons significantly. More than 5% of  $SF_6$  will not increase the voltage gradient proportionately because part of  $SF_6$  in the arc column does not take part in the reaction.

$SF_6$  has the best ability to reduce the number density of electrons,  $N_2$  has better ability to reduce the mobility of electrons while Ar keeps the discharge stable. Therefore this combination of 89% Ar + 10%  $N_2$  + 1%  $SF_6$  is best. The experimental results suggest that best results are obtained by choosing a gas which can reduce the number density of electrons and a gas which can reduce the mobility of electrons. By slowing down the electrons with  $N_2$ ,  $SF_6$  can attract the electrons more effectively because the effective cross section of  $SF_6$  is larger in the low electron volts region.

### §5.10.2 Collisions between electrons and atoms in mixtures of different gases

#### (1) The mixture of Ar and N<sub>2</sub>

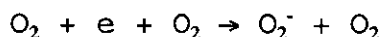
A decrease of the discharge column voltage gradient was observed in the mixture of Ar and N<sub>2</sub> (Fig. 5.9). This suggests that the ionisation of N<sub>2</sub> molecule and atom took place in the column of the discharge. The number density of electrons  $n_e$  in the mixture of Ar and N<sub>2</sub> was higher than that of pure Ar. The ionisation and the dissociation processes occurred commonly are



The experimental results suggest that the ionisation of N<sub>2</sub> atom and dissociation of N<sub>2</sub> molecules have more probability than ionisation of Ar because of the lower energy needed to excite the molecules and dissociate the molecules.

#### (2) The mixture of Ar and O<sub>2</sub>

Some of the chemical processes that happen in the mixture of Ar and O<sub>2</sub> can be written as follows



The experimental results showed that the discharge column voltage gradient with pure Ar and the mixture of Ar and O<sub>2</sub> have no significant difference. It suggested that the number density and the mobility of electrons did not change much even though O<sub>2</sub> was a weak electronegative gas. The number density of electrons was changed mainly by the charge transfer from Ar to O<sub>2</sub> and the following recombination of electrons and positive ions of O<sub>2</sub> molecules.

The high concentration of O<sub>2</sub> caused damage to the cathode and the orifice of the plasma torch although the addition of O<sub>2</sub> improved the stability of the discharge because of the lower ionisation potentials of O<sub>2</sub> (13.614 eV).

### §5.10.3 Temperature effect

#### §5.10.3.1. Power dissipation

The electrical power input per unit volume  $J E$  is given by

$$J E = \frac{I^2}{en_e \mu_e} \frac{1}{(\pi R^2)^2} \quad (5.41)$$

where  $R$  is radius of the discharge column.  $R$  changes with change of the gas velocity, discharge current and gas pressure and gas mixtures. Power dissipation is decreased with increases of the number density of electrons and the mobilities of electrons for a given discharge current. The relationship between the number density of electrons and the temperature is that the number density of electrons is increased with increase of the temperature below 16,000 K

(Fig. 5.2). At the higher temperature the electrical conductivity should be dependent on  $T_e^{3/2}$  primarily. The power input is decreased with increase of the temperature below 16,000 K.

The heat from the electric discharge is lost by radiation, convection and thermal conduction to the surrounding medium. The loss of heat from the radiation is only a small percentage (<10%) of the total energy losses. The loss of heat is dominated by the thermal conduction to the surrounding medium (>90%).

#### **§5.10.3.2. Thermal conductivity in the plasma column**

The addition of  $N_2$  to Ar in the plasma column can change the thermal conductivity of the arc. This is because

(a) the thermal conductivity of  $N_2$  is higher than that of  $O_2$  and Ar when the temperature is below 10,000 K. The peak value of the thermal conductivity of  $N_2$  is at about 7,000 K (Fig. 3.2),

(b) the recombination among electrons and positive ions and positive ions of molecules is occurred.

The energy absorbed by the vibrational excitation of  $N_2$  molecule also increased the effect of higher thermal conductivities. The experimental results showed, however, the discharge column voltage gradient in pure Ar and in the mixture of Ar and  $N_2$  in the air tight chamber have no significant difference. This indicates that the thermal conductivity of mixture of gases by adding small amount of  $N_2$  does not have much influence on the discharge column voltage gradients in these tests.

The discharge column voltage gradient in pure Ar surrounded by air is higher (1.0 V/mm) than that (0.3 V/mm)

in the airtight chamber. This big difference may be due to  $N_2$  in air, which helps to increase the gradient.  $N_2$  has lower ionisation potential (14.54 eV) than Ar (15.755 eV) but has a higher thermal conductivity than Ar (Fig. 3.2). The effect of the higher thermal conductivity results in the decrease of the diameter of the discharge column. This leads to the increase of the discharge voltage and the gradient.

#### **§5.10.3.3 Variation of temperature**

The thermal conductivity of  $N_2$  is increasing functions of the temperature ranging from 5,000 K-7,000 K. Combining the functions of the power dissipation and the thermal conductivity with temperature, the working temperature of the plasma column is determined by the intersection point of the functions.

The temperature ( $< 14,000$  K) leads to an increase of the number density of electrons which increases the electrical conductivity of the discharge gases. As a consequence, the power dissipation decreases on condition that the discharge current and the radius of the discharge column is kept constant. The discharge column voltage gradient is also decreased.

#### **§5.10.4 The discharge current density**

The discharge column voltage gradient depends on the discharge current density, the number density and the mobility of electrons. The change of the number density of electrons also causes the change of the current density. Table 3.3 shows the typical values of the density of the electric discharge current in some electric discharges applied in industry (Virens et al, 1982). The

relative range of the ratio of the discharge current and the number density of electrons ( $J/n_e$ ) is usually in the order of 10 except in a low pressure inert gas discharges. This suggests that the discharge column voltage gradient cannot be increased by a large amount.

#### §5.11. The summary

The mixtures of gases that contributed most to the increase of the discharge column voltage gradient is Ar + N<sub>2</sub> + SF<sub>6</sub>, which contains the strong electronegative gas. This mixture differs from pure Ar in two aspects, i.e.,

(1) the strong electronegative gas attracts electrons to form negative ions and prohibit further ionisation,

(2) N<sub>2</sub> decreases the velocity of electrons, which is in the lower electron energy region (<2 eV) that can be attracted effectively by SF<sub>6</sub>.

The second contribution to the increase of the discharge column voltage gradient was the choice of the best proportion for the mixture of the discharge gases. Small quantities of the strong electronegative gas (SF<sub>6</sub>) increased the discharge column voltage gradient significantly. The addition of N<sub>2</sub> also decreases the mobility of electrons. More electronegative gas increases the discharge column voltage gradient but causes the discharge to be unstable. The best mixture was shown to be 89% Ar, 10% N<sub>2</sub> and 1% SF<sub>6</sub>. The tests for the best mixture with the electric current varying from 60 A to 430 A showed the discharge was stable.

The mixture of Ar with addition of O<sub>2</sub> was unacceptable although O<sub>2</sub> improves the stability of the plasma column.

This was because that  $O_2$  damaged the cathode and the orifice of the plasma torch. The tests showed the cathode was totally oxidised after few minutes of running of the plasma torch with concentration of 10%  $O_2$  or more. The arc was very difficult to ignite and several ignitions were required.

Using the Saha equation gave the theoretical calculation of the number density of electrons and the discharge column voltage gradient on the assumption of the local thermal equilibrium in the plasma torch. The calculation showed that the number density of electrons did not change significantly with different additions of  $N_2$ ,  $O_2$  to Ar at the same temperature. This was verified by the test in which the discharge column voltage gradient with pure Ar, mixtures of Ar,  $N_2$  and  $O_2$  had no significant difference in an airtight chamber.

Analysis of the test results indicates that there is discrepancy between the theoretical calculation and the experimental results of measurement of the discharge column voltage gradient (Fig. 5.3, Fig. 5.11). This was due to two reasons:

(a) the mobilities of electrons was deduced at low pressure using average values calculated from the mean free path of atoms.

(b) the density of the discharge current in the calculation may be different from that in the test.

The thermal conductivity of a gas can influence the discharge column voltage gradient by changing the temperature of the electrons. The test results showed that the temperature of the discharge column, however, did not change much by addition of small amount of  $N_2$ . As a result the thermal conductivities of gases added have no significant influence on the number density of electrons



and the discharge column voltage gradient.

The ionisation potential of gases does influence the discharge column voltage gradient. The higher ionisation potential of gases used may increase the gradient of the discharge but results in the difficulty of arc ignition.

The Saha equation was modified to be used in the mixtures of different gases. The number density of electrons in the mixtures of diatomic gases can be calculated. The Saha equation can only be applied on the assumption of the local thermal equilibrium. The number density of electrons only depends on the gas temperature and gas pressure. The number density of electrons using the modified Saha equation applied for  $\text{SF}_6$ , however, was not suitable because the complete dissociation of  $\text{SF}_6$  is unknown.

## **Chapter Six**

**Distinction between a glow discharge and an arc discharge using spectroscopy**

## **§6.1 Introduction**

Spectroscopic measurements of the glow discharge and the arc discharge can provide information concerning the spatial and temporal variations of the electron density, the temperature of the electrons and the concentration of elements in the discharge column. The measurement of the spectral wavelength involves the successive measurement of the wavelength at wavelength intervals which are determined by the accuracy required.

There are extensive studies on the spectroscopic measurements applied to electric discharges (Maeker, 1956; King, 1965; Boumans, 1966; Chien et al, 1980). The analysis of the spectral data is discussed in detail by Griem (1964).

### **§6.1.1 Spectral lines used as a diagnostics for electric discharges**

The parameters of an electric discharge depend on the gas, gas pressure, electrode material and its geometry, the discharge current and the discharge voltage. A family of curves of the electric field strength exists even at the same discharge current and the discharge mode might be switched to a glow from an arc by varying other parameters such as gas or the discharge length.

The change of the discharge mode is associated with the change of the energy levels of ions, which in turn effect the emission of light. Two different modes of the electric discharge usually can be distinguished by its discharge current, voltage fall at the electrodes and the voltage between the electrodes, and the temperatures of the electrons and the discharge gases. The distinction is not easy however in some applications such as high power CO<sub>2</sub>

lasers or a Glydarc electric discharge because in the former it is difficult to measure the voltage fall at the electrodes and in the latter the voltage measured between the electrodes fluctuates due to the variation of the discharge length with time and position.

The emission lines from glow discharges can be used as a diagnostic method. These lines are used to calculate the number density of electrons in the discharge column and the temperatures of the electrons and the discharge gases.

The measurement of the electron temperature in the electric discharges is useful to distinguish the electric discharge mode because the electron temperature in a glow discharge is much greater than the average temperature of the electric discharge gases. The calculation of the electron temperature however involves complicated procedures.

Electrons gain energy from the applied electric field in an electric discharge. The atoms are excited or ionised by the energy transfer from collisions of electrons with atoms. The excited atoms or ions can return to the initial energy level giving up energy in de-excitation processes. This energy can be as emitted light or energy stored in metastable states. The ions and metastable atoms present in an inert gas discharge such as Ar are effective in exciting the emission lines because metastable states have a lifetime  $10^6$  -  $10^7$  times longer than other states (Wagatsuma, 1985).

The emission lines from glow discharges and arc discharges are governed by Plank's equation:

$$f = \frac{E_m - E_n}{h} = \frac{\Delta E}{h} \quad (6.1)$$

where  $E_m$  is excited energy at the m level and  $E_n$  excited energy at the n level, and h Plank's constant. The energy intervals in glow and arc discharges are different because they depend on excitation and ionisation levels in the electric discharge for example an arc must have a higher degree of ionisation to carry the higher discharge current density. The high temperature of electrons in a glow discharge produces excited lines that cannot be excited in an arc at atmospheric pressure. This provides a method determining the different discharge modes.

The initial objective was to measure the discharge column voltage gradient. The second objective was to identify the discharge mode by choosing the unique lines from an arc discharge and a glow discharge. These unique lines were used to identify the discharge mode applied to a Glydarc discharge. This chapter describes experiments to measure the emission lines from the arc and the glow discharges and applies the results to distinguish the electric discharge modes.

## **§6.2. Preliminary investigation**

The first attempt to measure the spectral lines from a glow discharge and an arc discharge was carried out using a scanning monochromator. The equipment was also used by Knight (1985) to determine the light intensity of an arc discharge using the multi-electrodes.

### §6.2.1 Silicon photodiode monochromator

The schematic diagram of the silicon photodiode monochromator (Rofin 6000 series) is shown in Fig. 6.1. The equipment is composed of a spectral analyser, a silicon photodiode detector, a sample and hold unit, and a wavelength marker. The light is gathered by a light guide which connected to the slit of the spectral analyser. The equipment was provided with a group of slits which were 0.2 mm, 0.5 mm, 1.0 mm, and 2.0 mm wide by 5.0 mm high. The spectral analyser is equipped with a rotating diffraction grating which is blazed at 300 nm with 1,200 grooves/mm. The grating is rotated in order to scan the wavelength from 300 nm to 1,100 nm. The frequency of the rotation of the grating can be varied from 10 Hz to 17 Hz. The light from the source is diffracted by the two Elbert mirrors and sensed by the silicon photo diode detector where the optical signal is converted into the electrical signal. This electrical signal is amplified by a built-in operational amplifier which has a voltage gain of  $10^8$ . The electrical signal is connected with an oscilloscope to display the spectral lines. At the same time the trigger signal for the oscilloscope and the wavelength marker are produced by an optical disk which is attached to the rotating shaft of the gratings.

The experiments showed that none of any spectral lines from a glow discharge could be recorded because the gain of the equipment ( $10^8$ ) was not high enough to detect the weak light emitted from the glow discharge even with the largest slit.

A series of tests were carried out to measure the spectral lines from the arc discharge. The sensitivity of the equipment was sufficient for the arc discharge even when the slit chosen was the narrowest (0.2 mm) however the spectral lines could not be separated because the

resolution of the equipment was too low. The equipment has the highest resolution of 5.0 nm at the full width half magnitude (FWHM). As a result the spectral lines on the oscilloscope were smooth continuous lines.

#### **§6.2.2 Rofin monochromator using a photomultiplier tube**

The first series of tests showed that the gain of monochromator using a silicon photodiode detector was too low to show any spectral lines from the glow discharge because the light from the glow discharge is very weak. The gain of the equipment was increased by replacing the silicon photodiode detector with a photomultiplier tube with a voltage gain up to  $10^6$  (Thorn EMI Electron Tubes, 9106B) So that the total gain of the modified equipment including the operational amplifier was increased to  $10^{14}$ . (Fig. 6.1).

Fig. 6.2 shows the spectral lines from a glow discharge using the photomultiplier tube. The graph showed the spectral lines as smooth continuous lines because the resolution of the equipment was low (5 nm) and exact reading of the spectral lines was difficult using the cursor on the oscilloscope which was controlled by the thumb wheel in the sample and hold unit. Once the recording of the spectral lines was finished the cursor was also recorded. The cursor cannot be moved. The exact reading was only relied on the relative calculation by the markers (10 nm/each) between the cursor and the interesting lines. This introduces an error which cannot be tolerated for the requirement of the accuracy of within 1.0 nm. The operational amplifier also introduced much more noise.

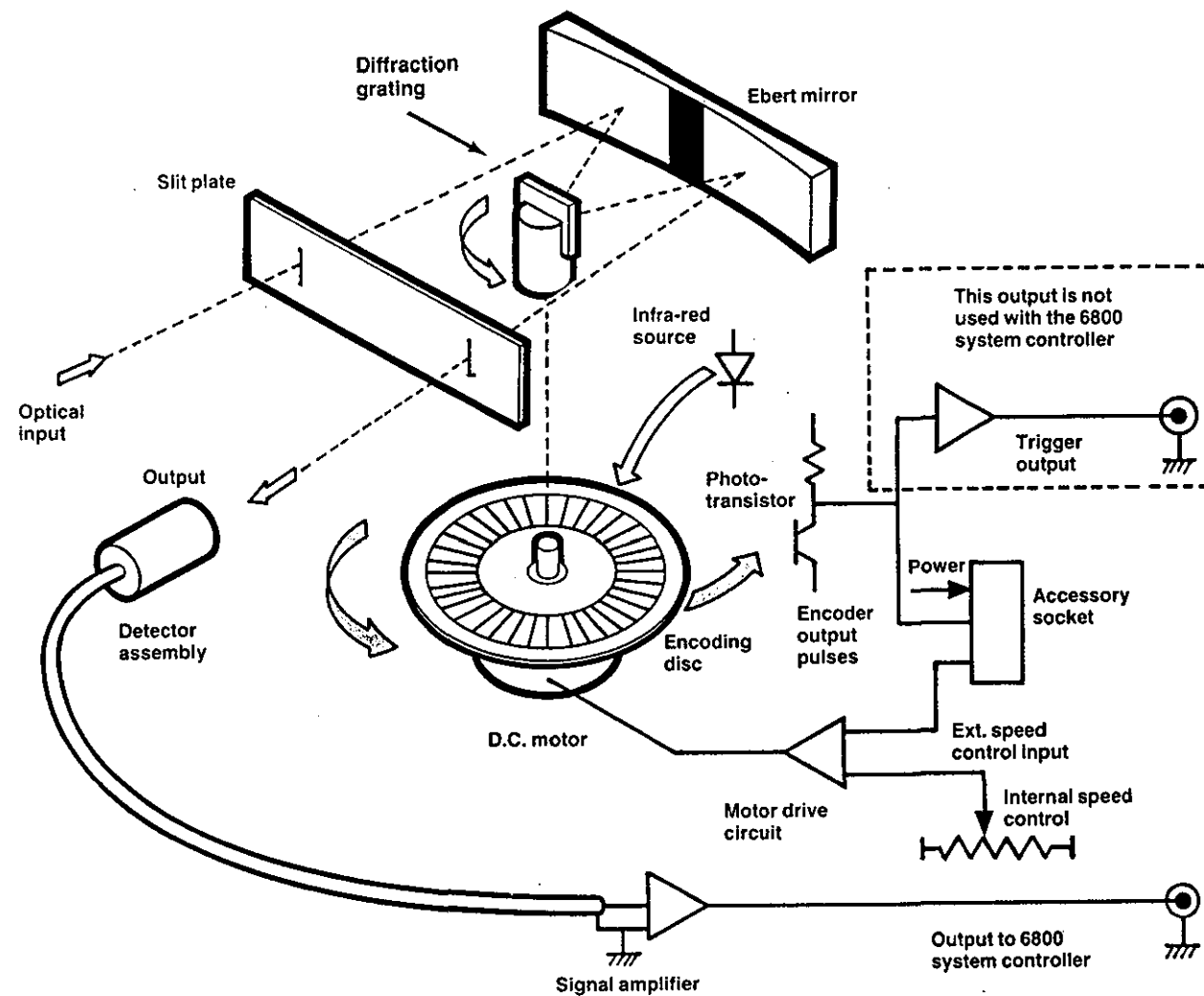
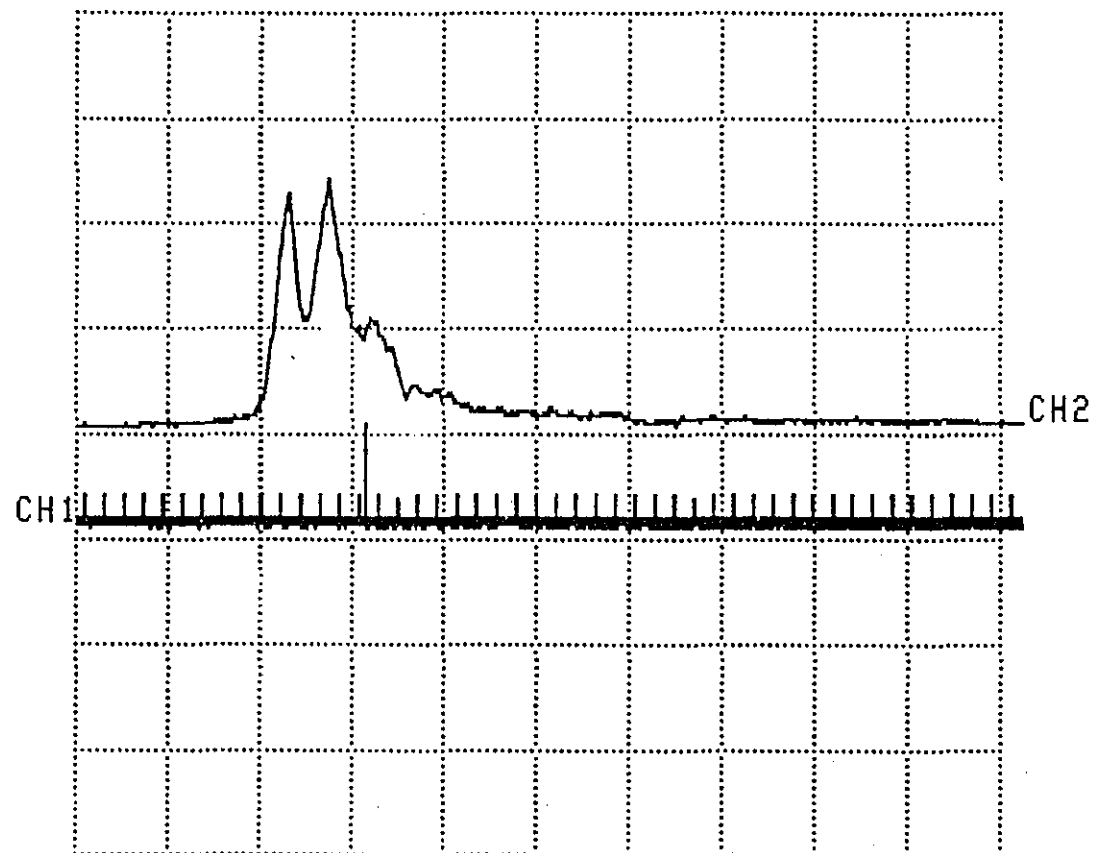


Fig. 6.1 Schematic diagram of the monochromator Rofin 6000 series





Cursor: 430 nm

CH1: Base marker (10nm/each)

CH2: Relative intensity

Fig. 6.2 Spectral lines from a glow discharge (discharge current of 100 mA at 500 Pa (5 mbar))

### §6.2.3 Photodiode array monochromator

An attempt was made to measure the spectral lines using a MultiSpec™ 1/8 M monochromator with 0.4 nm resolution which is shown in Fig. 6.3. (Model No. 77400, Specification in Appendix D). The equipment has an array of 1,024 photodiode cells with an effective detector of 25.0  $\mu\text{m}$  by 2,500.0  $\mu\text{m}$ . The light goes through the slit which is 25.0  $\mu\text{m}$  and is diffracted by the grating and impinges on the photodiode array. The small diode cell needs a minimum exposure time of 12.5 ms which corresponds to a maximum scan rate of 80 Hz. The difference between the photodiode array and the scanning monochromator is that the photodiode array senses the light without spinning diffraction grating and the light is processed into its spectral components more rapidly as it does not depend on the scanning spectrum.

The photodiode array spectral analyser is controlled by a laptop computer and the data acquisition program was coded according to the application. The equipment enabled the complete spectrum over the range of 300 nm to 850 nm.

A series of tests to measure the spectral lines from a glow discharge was carried out using the MultiSpec 1/8 M monochromator. The spectral lines still could not be observed due to the weak light even when the exposure time was increased to 5 minutes, which was the maximum exposure time allowed.

A test was also carried out to measure the spectral lines from an arc discharge. The spectral lines recorded could be distinguished because the equipment has a good resolution with the slit of 25.0  $\mu\text{m}$ . The results, however, could not be used for the distinction of the arc and the glow discharge because none of the spectral lines from a glow discharge could be measured using the same equipment.

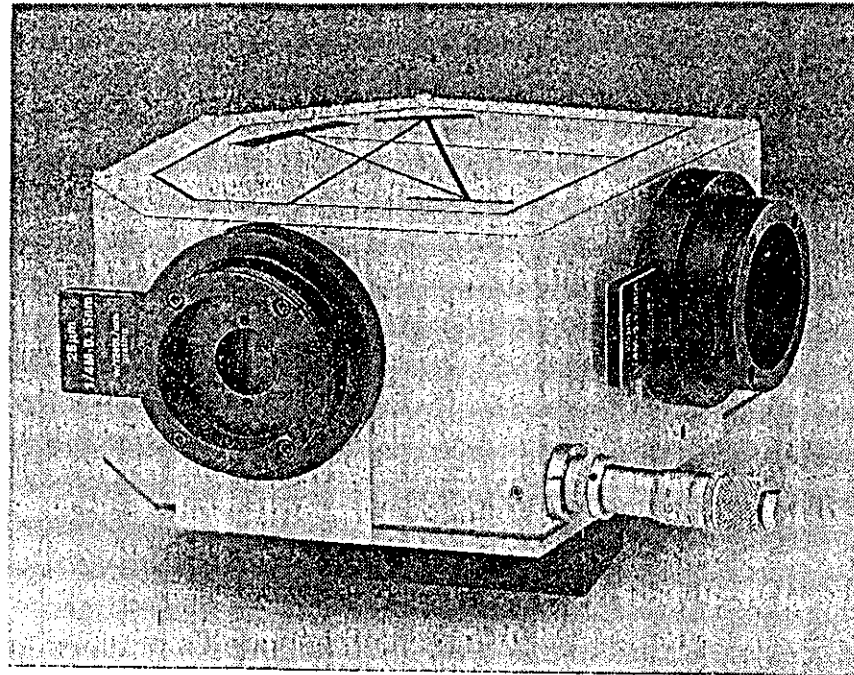


Fig. 6.3 MultiSpec™ 1/8 M monochromator

### **§6.3 Computer-based scanning monochromator with a photomultiplier tube detector**

This system was developed from the Rofin monochromator and is similar to the Rofin 6000 series except the detector, which was replaced by a photomultiplier tube (Fig. 6.4) which has a faster response and a narrower slit (0.18 mm). It comprises a spectral analyser, a data interface card, a photomultiplier tube unit with 9 dynodes and associated control software. The scanning time is 80 ms from 200 nm to 1,100 nm. One diffraction grating of 1,200 grooves/mm with blazed wavelength of 500 nm is used. The gain of the photomultiplier unit can be controlled in 6 steps from the minimum gain to the maximum gain in order to match the input density of the light. The spectral lines can be displayed, marked, and analysed on the screen of the computer and the whole data acquisition process is controlled by the computer. The use of a computer-based monochromator with a photomultiplier tube detector can achieve the high voltage gain ( $>10^6$ ) and low noise, high sensitivity of light (60 mA/W) and high resolution (1.4 nm) with the slit of 0.18 nm. The computer software provided easy analysis of the spectral lines measured.

### **§6.4 Calibration of the monochromator**

Calibration of the monochromator is necessary because the accuracy of the measurement of the wavelength is dependent upon how accurate the equipment is. Calibration of the computer-based monochromator with a photomultiplier tube was carried out by using a helium-neon laser. The software of the control system can calibrate automatically the band of wavelengths from 300 nm to 850 nm which was required for the test. Re-calibration of the wavelength is necessary when the slit is changed or the different

photomultiplier tube unit is used. The error of the measurement of the wavelength can be within 0.25 nm after calibration.

### §6.5 Experimental arrangement

Fig. 6.4 shows the experimental arrangement. The light guide was positioned at less than 10 mm from the discharge column, and at least 10 mm from the electrodes to avoid the spectrum from the fall regions in the glow discharge. When the spectrum was recorded for the arc discharge, the optical guide was positioned 10 mm away from the discharge column to avoid the damage of the optical guide caused by heat.

A spectrum from a glow discharge was recorded in a T-shape discharge tube made from quartz glass (Fig. 6.5). The discharge tube had an inner diameter of 25 mm and a length of 420 mm. The nearest distance from the central outlet to one end of the discharge was 160 mm. The electrodes used for the glow discharge were made of copper with the diameter of 6 mm.

The low current arc discharge (0.5 A to 2.0 A) was enclosed in a quartz tube with Ar filled at atmospheric pressure. The quartz tube had diameter of 96 mm, and length of 170 mm. The low current arc discharge was supplied from a power supply that could provide the maximum current of 2 A and the maximum voltage of 9 kV.

The high current arc discharge (50 A to 200 A) was operated using a TIG torch shielded by Ar at atmospheric pressure. The discharge electrode (cathode) in the arc discharge was tungsten ( $\phi$  2.5 mm) and the anode was a piece of mild steel.

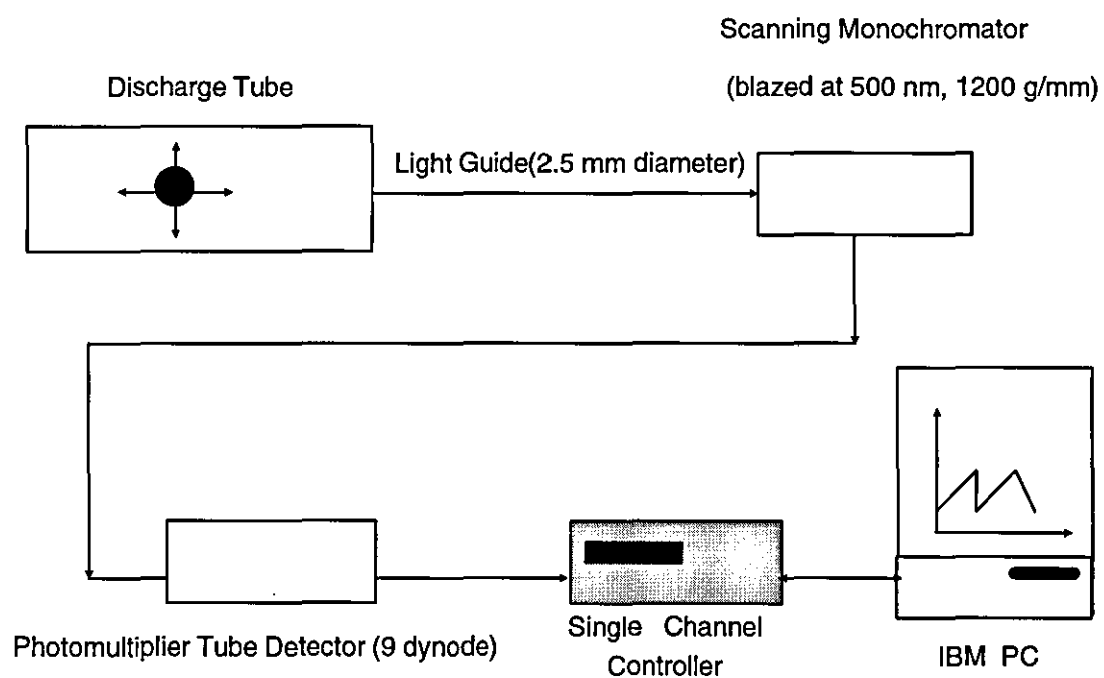


Fig. 6.4 Schematic of the experimental arrangement using the Rees 6800 series monochromator

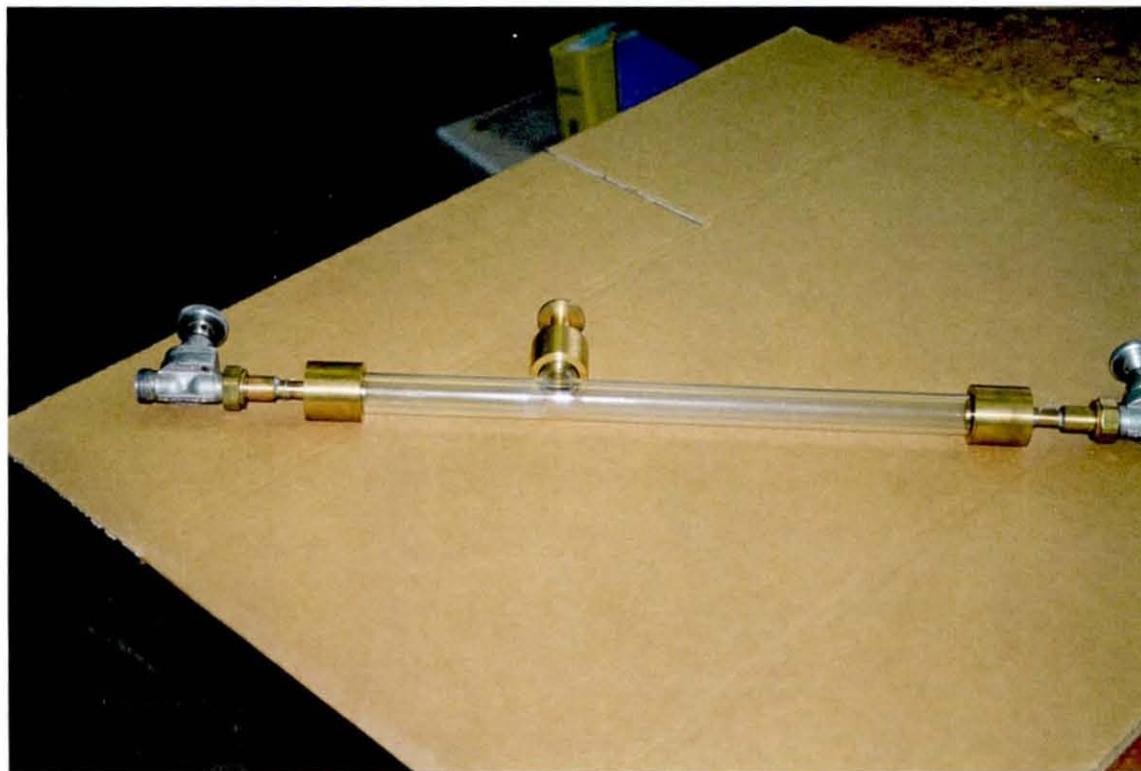


Fig. 6.5 Discharge tube used for a glow discharge

The vacuum system used a single stage rotary vacuum pump which evacuated the discharge cavity to 500 Pa. Ar of 99.95% purity was supplied from a cylinder. The discharge tube was pumped down and flushed with Ar at least 10 times to reduce contamination from residual air.

The glow discharge was supplied from the AC high voltage power supply which has been described in Chapter 4. The discharge current was measured by an oscilloscope using a shunt. The high current arc discharge was supplied by a commercial welding power supply, which could provide a maximum current of 350 A and a maximum open circuit voltage of 100 V.

A light guide with a diameter of 2.5 mm was used to increase the light input. It was examined by using the standard arc lamp. The spectral lines from the source were well shown in the equipment (300 nm to 1100 nm). It was verified that both the light guides and the equipment were in good working order.

## **§6.6. Experimental procedure**

A series of tests were carried out for a glow discharge, an arc discharge with low discharge current and high discharge current at atmospheric pressure. The test equipment was placed in a light-proof enclosure.

### **§6.6.1 Operating procedure for the glow discharge**

The experimental procedure for a glow discharge was first to pump the discharge tube down to 500 Pa and hold it for 15 minutes. The discharge tube was flushed with Ar at least 10 times to reach high purity of Ar in the tube. At a pressure of 500 Pa the inlet and the outlet valves were



closed. The power supply was switched on and the discharge voltage was increased until the breakdown occurred. The desired discharge current was set adjusting the voltage of the power supply. Once the discharge was stable the spectral analyser was operated and the spectral lines using the data acquisition programme were recorded after changing the magnitude of the spectral lines on the oscilloscope or on the screen of the computer to avoid the saturation of the amplifier by changing the gain of the spectral analyser.

#### **§6.6.2 Operating procedure for the arc discharge**

The low current arc discharge (0.5 A to 2.0 A) was operated in Ar in the discharge tube at atmospheric pressure. The tube was flushed with Ar first for at least 2 minutes and the discharge voltage was increased until the discharge occurred. The discharge current at the desired value was set increasing or decreasing the output discharge voltage or changing the stabilising resistors. The optical analyser programme for data acquisition was executed to view the spectral lines and adjust the gain of the photomultiplier tube unit and the software gain coefficient of the program to avoid the saturation or under gain of the spectral lines if necessary. The spectral lines were recorded and analysed.

Tests on the high current arc discharge (50 A to 150 A) with Ar as shield gas was carried out using a commercial TIG welding torch. The tip of the cathode was adjusted from 1 mm to 3 mm off the workpiece (as an anode). Pre-flush Ar for one minute was required before the power supply was switched on. The arc was initiated using the high-frequency high voltage supply, which was connected in parallel to the electrodes. The optical spectral analysis data acquisition program was operated to view the spectral lines and the

gain of the photomultiplier tube unit and the software gain coefficient of the program were adjusted to avoid the saturation or under gain if necessary. The spectral lines were recorded and analysed.

### **§6.6.3 Operating procedure for the Glydarc discharge**

The Glydarc discharge was carried out using the experimental arrangement described in Chapter 4. The procedure was the same as that of the arc discharge except the minimum separation of electrodes was fixed at 1 mm and the high frequency high voltage ignition supply was not used.

### **§6.7 Measurement of the discharge column voltage gradient**

The initial objective of the experiment was to measure the discharge column voltage gradient using the emission lines. The voltage gradient varies from the cathode fall region, positive column region and the anode fall region. The variation of the voltage gradient influences the energy of electrons and ions and the emission of light. The spectral lines should indicate the change of the voltage gradient in the discharge. This is known as the Stark effect which can be measured. A series of tests using a glow discharge was carried out to try to find the Stark effect but no difference could be measured.

The Stark effect can be used to measure the discharge voltage gradient, however the energy of atoms from collision with electrons and the energy of electrons gained by the acceleration of the electric field strength must be high enough to see this effect; Barbeau et al (1991) reported that the minimum electric field strength (120 V/mm) was required to observe the Stark effect in the

cathode fall of a glow discharge using a high resolution of spectral analyser (0.1 nm) at very low pressure ( $<10$  Pa). A pressure below 10 Pa is required so that the discharge column, the cathode fall region and the anode fall region can be easily separated naturally. The observation for one discharge region (e.g. the cathode fall region) is easily to be made to avoid the light emitted from other discharge regions. In order to increase the light output to the spectral analyser from the glow discharge, a lens as well as the optical light guide can be used. This will make high signal-noise ratio possible for the low luminance of the emitted light.

The observation of the change of the voltage gradient in the electric discharge cathode fall region, positive column region and the anode fall region at high pressure such as an arc at atmospheric pressure is difficult because the discharge column is constricted. This will cause difficulties in observing the Stark effect due to:

(a) the shorter discharge length will make it impossible separate the emitted light of one discharge region from the other regions of the source;

(b) The stronger emitted light of the discharge at high pressure will overlap the weak light emitted by the change of the voltage gradient which is indicated by the Balmer lines;

(c) the integration of emitted light is carried out by the spectral analyser. This means that it is difficult to tell the light emitted by the cathode fall region from the light emitted by the other regions.

### §6.8. Emission lines from a glow discharge

The emission lines from the positive column of the discharge in Ar at 500 Pa at three different discharge currents (50 mA, 100 mA and 150 mA) were measured by using the Rees Instruments monochromator. Fig. 6.6 shows the emission line from the glow discharge with the discharge current of 50 mA, 100 mA, and 150 mA. Intensities of neutral Ar lines at 420.1 nm, 434.8 nm, 521.0 nm, 696.5, 751.4 nm, 763.5 nm and 811.5 nm were strongly displayed. The peak value of intensity of spectral lines occurred at 656.75 nm. The energy levels of the corresponding spectral lines are shown in Fig. 6.7.

The wavelength of emission lines at three different discharge currents did not change although the intensities of these lines varied with the discharge current. At low discharge currents (50 mA) the intensities of the emission lines are distorted more by noise than that at high discharge current (150 mA).

The strong emission lines in the test were compared with those obtained by Wagatsuma et al (1985) who used a low pressure glow discharge lamp filled with Ar at pressure ranging from 400 Pa to 1,600 Pa. There is a good agreement with the results from 300 nm to 500 nm (Table 2.2). The emission lines above 500 nm could not be compared due to no corresponding experimental results from Wagatsuma et al (1985).

The effect of the second order of lines is the inherent disadvantage of using the ruled diffraction gratings (Fig. 6.8.). To ensure the highest accuracy from the monochromator, and to avoid the possibility of falsely interpreting the displayed spectra it is necessary to use an optical filter to avoid the effect of the second order of the light. A filter was used which has a band pass from

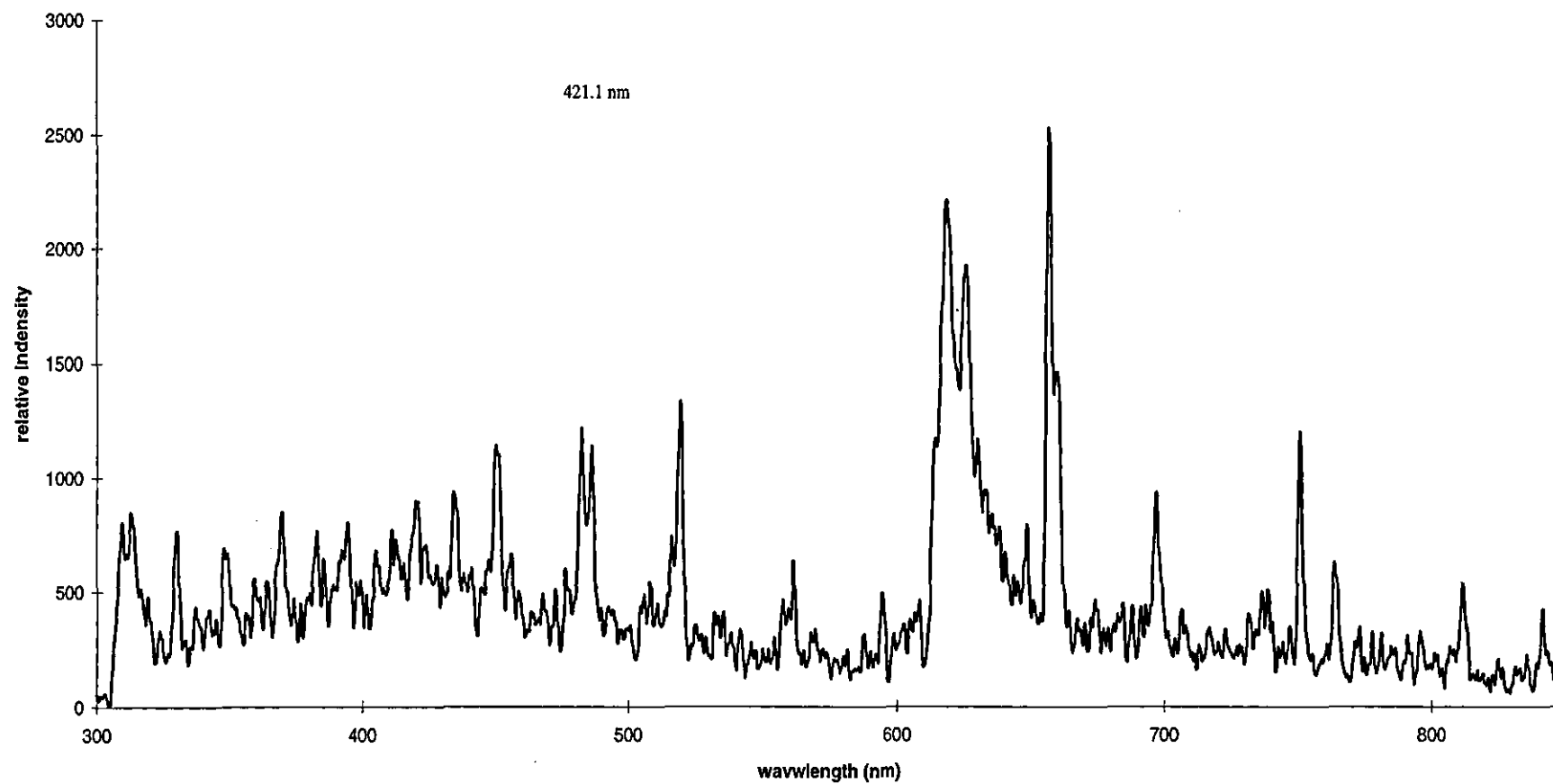


Fig. 6.6 Spectral lines from the glow discharge at discharge current 150 mA, 500 Pa ( 5 mbar )



580 nm to 1,100 nm positioned at the input slit (Model No. 6174, Rees Instruments Ltd.). Fig. 6.9 shows the spectral lines with this optical filter. The wavelengths of 618.25 nm, 625.75 nm were the second order of the light because they were not present when the filter was employed.

Measurements were also made to compare the emission lines at different positions along the discharge column. The test showed that there was no difference in wavelengths along the whole column. This was because the positive column of the discharge at low pressure (500 Pa) filled the discharge tube and hence the voltage gradient was not changed. The emission lines measured from the discharge column were identical when measurements were repeated.

#### **§6.9 Emission lines from an arc discharge with low discharge current**

A series of tests were carried out to measure the emission lines from the discharge at low discharge current (<2.0 A) in Ar at atmospheric pressure. The discharge

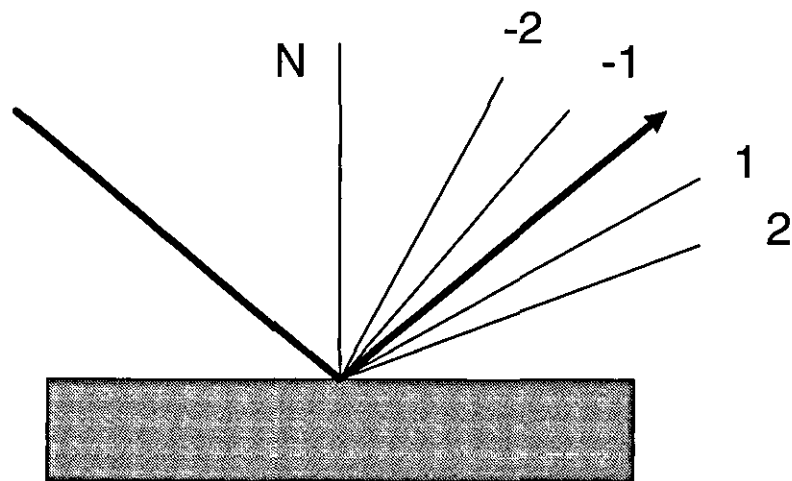


Fig 6.8 Different orders of light by a reflection grating

phenomenon is interesting because it is the region in which the transition of the glow to arc occurs. Saiepour et al (1990) and Yahya (1990) reported that the transition of the glow to arc discharge occurred at a discharge current of 0.5 A to 1.0 A with air at atmospheric pressure.

Fig. 6.10 shows the spectral lines from the discharge at different discharge currents (0.25 A, 0.5 A and 1.0 A). The spectral lines at discharge current 0.25 A were dominated by the lines from the infra-red region, whereas the spectral lines at a discharge current of 1.0 A was dominated by lines from the infra-red lines to the near ultraviolet lines.

The discharge at a discharge current of 0.25 A was believed to be a glow discharge because the discharge voltage measured was approximately 300 V whereas the discharge at discharge current 1.0 A was considered to be an arc discharge since the discharge voltage measured was only approximately 20 V.

The transition from the glow to arc occurred at the discharge currents from 0.6 A to 0.7 A, which could be observed from the unstable discharge. This was accompanied by fluctuation in the discharge voltage.

#### **§6.10 Emission lines from an arc discharge with high discharge current**

A series of measurements of discharge currents in an Ar arc at 50 A, 100 A, and 150 A were carried out using a TIG torch with separation of 1 mm to 3 mm between the electrodes. The emission lines are shown in Fig. 6.11 at 100 mm from the discharge column. The wavelengths of the strong emissions were 420.1 nm, 426.8 nm, 433.0 nm, 428.25 nm, 696.5 nm, 706.7 nm, 738.4 nm, 751.4 nm, 763.5 nm,



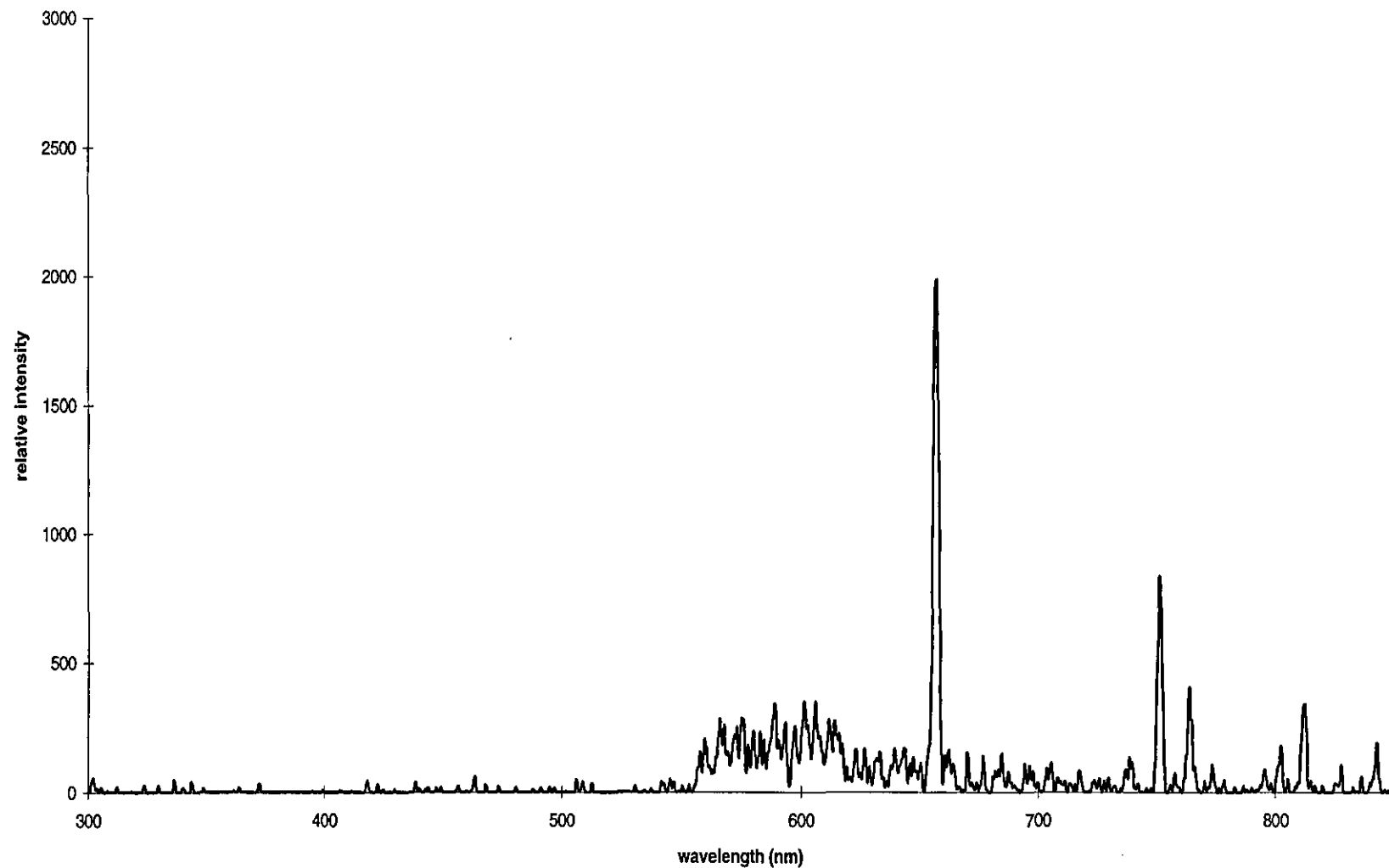


Fig. 6.9 Spectral lines from the glow discharge at discharge current 150 mA, 500 Pa (5 mbar)  
with the filter of OG570

Series1: 0.5 A, Series2: 0.25 A, Series3: 1.0A

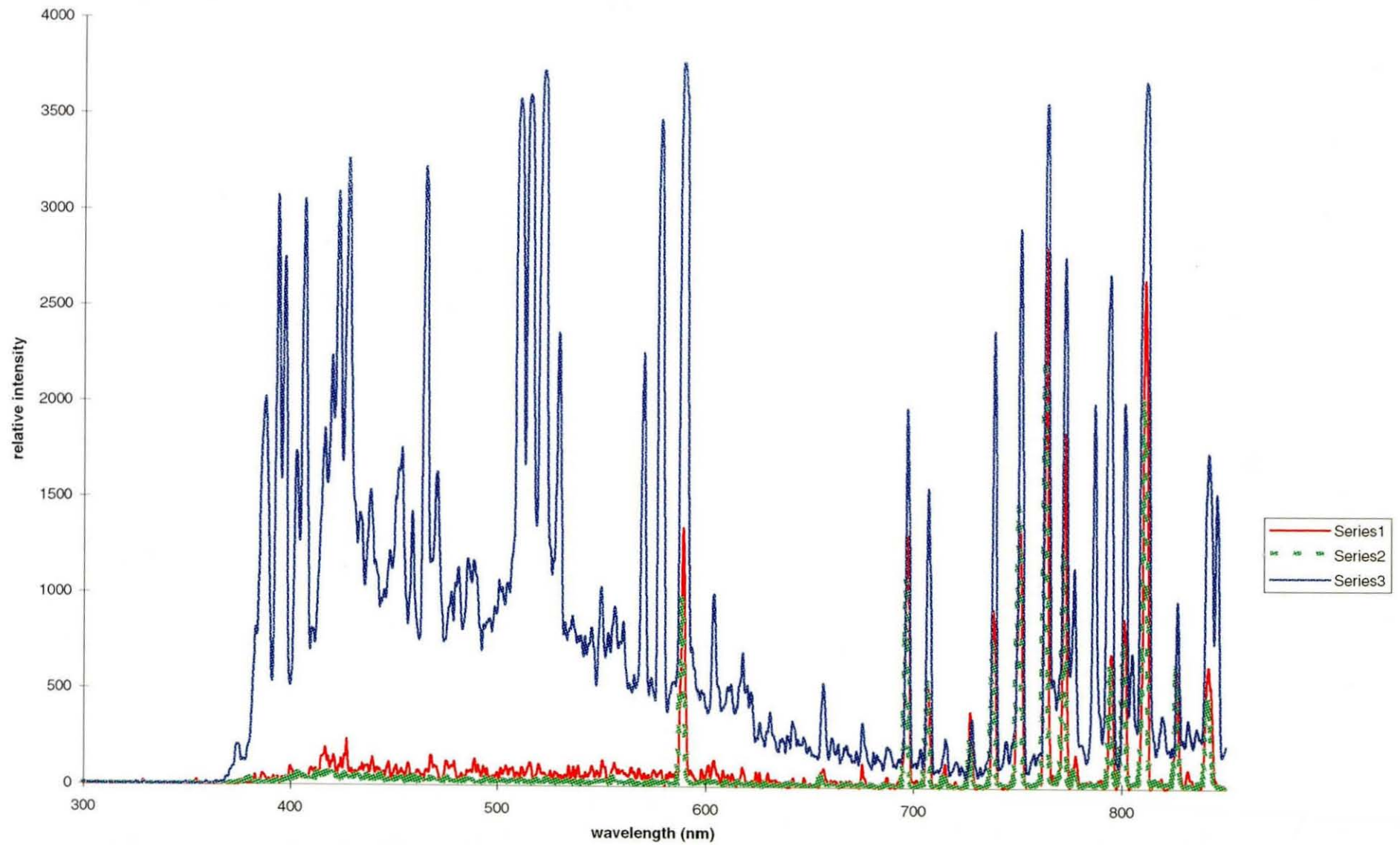


Fig. 6.10 Spectral lines from an arc with low discharge current 0.25 A, 0.5 A and 1.0 A

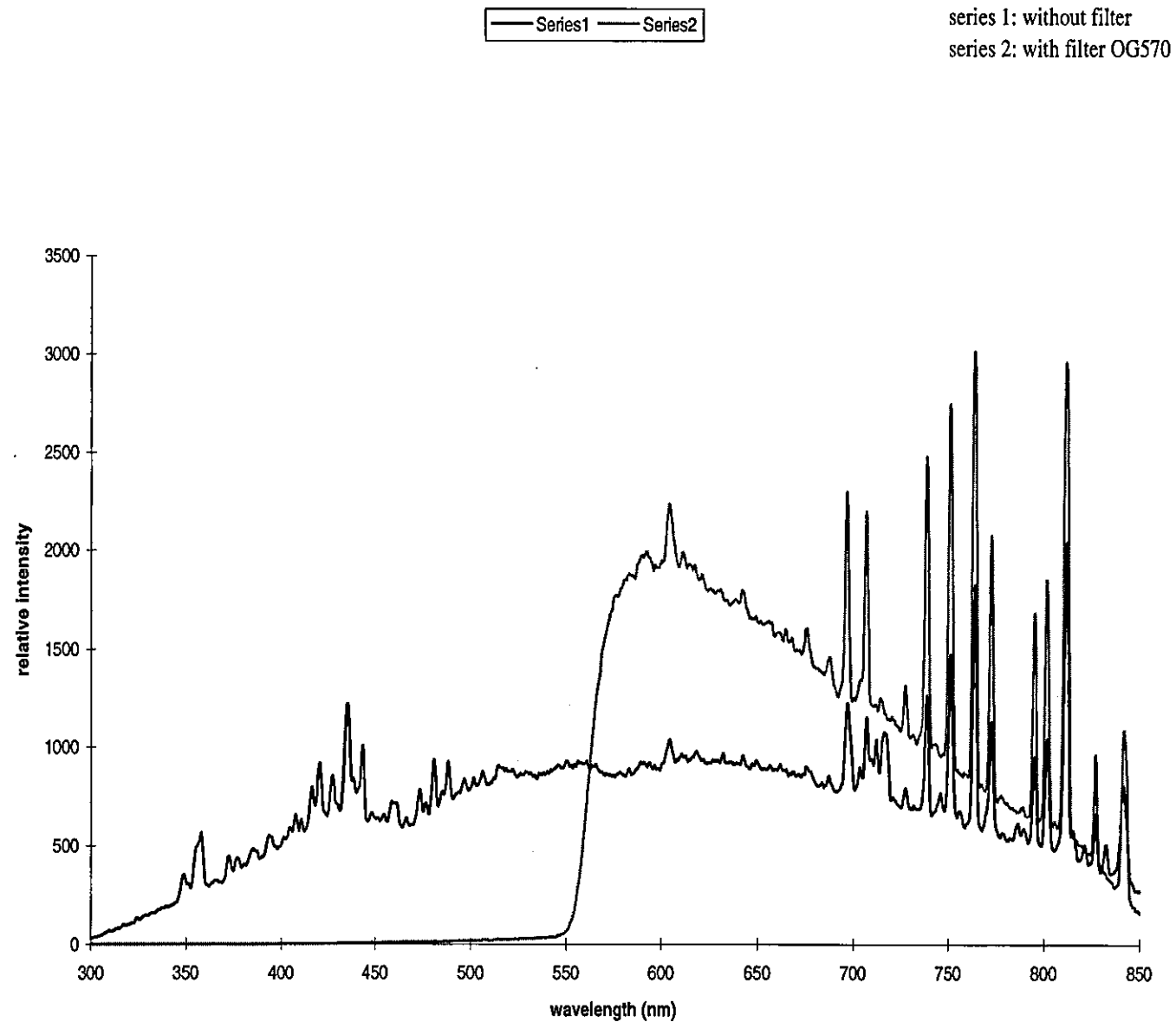


Fig. 6.11 Spectral lines from TIG arc at discharge current of 50 A

772.4 nm, 811.5 nm, and 840.8 nm. The peak intensity of the emission lines was shown at 763.5 nm. Fig. 6.11 also shows the spectral lines with the optical filter inserted. The spectral lines 716.50 nm and 688.0 nm were second order lines because they were not present when the filter was used.

When the distance between the sensor and the discharge column was varied between 150 mm and 250 mm, it showed that there was no significant difference except the intensity of the emission lines was reduced with increase of the distance. The results were also reproducible when the tests were repeated. There is a good agreement compared with those obtained by Thornton (1993).

#### **\$6.11. Emission lines from the Glydarc electric discharge**

A series of tests were carried out to measure the emission lines from the Glydarc electric discharge. Fig. 6.12 shows the emission lines with the sensor positions near the bottom, at the middle and at the top of the Glydarc electrodes. Spectral lines at 404.4 nm, 427.8 nm, 438.0 nm , 521.0 nm were observed. The peak intensities of these emission lines were 427.8 nm and 521.0 nm. The emission lines were less noisy at the middle position of the discharge compared with that at other positions. The emission lines were sampled and recorded 25 times at each position because of motion of the discharge column upwards.

Comparing the emission lines from the arc and the glow discharge, it was found that emission line 427.8 nm was only apparent in the arc discharge whereas the emission line 521.0 nm was only apparent in the glow discharge. The spectral lines from the Glydarc discharge shows that emission line 427.8 nm and 521.0 nm occurred. This suggested that the Glydarc was a mixture of the glow and

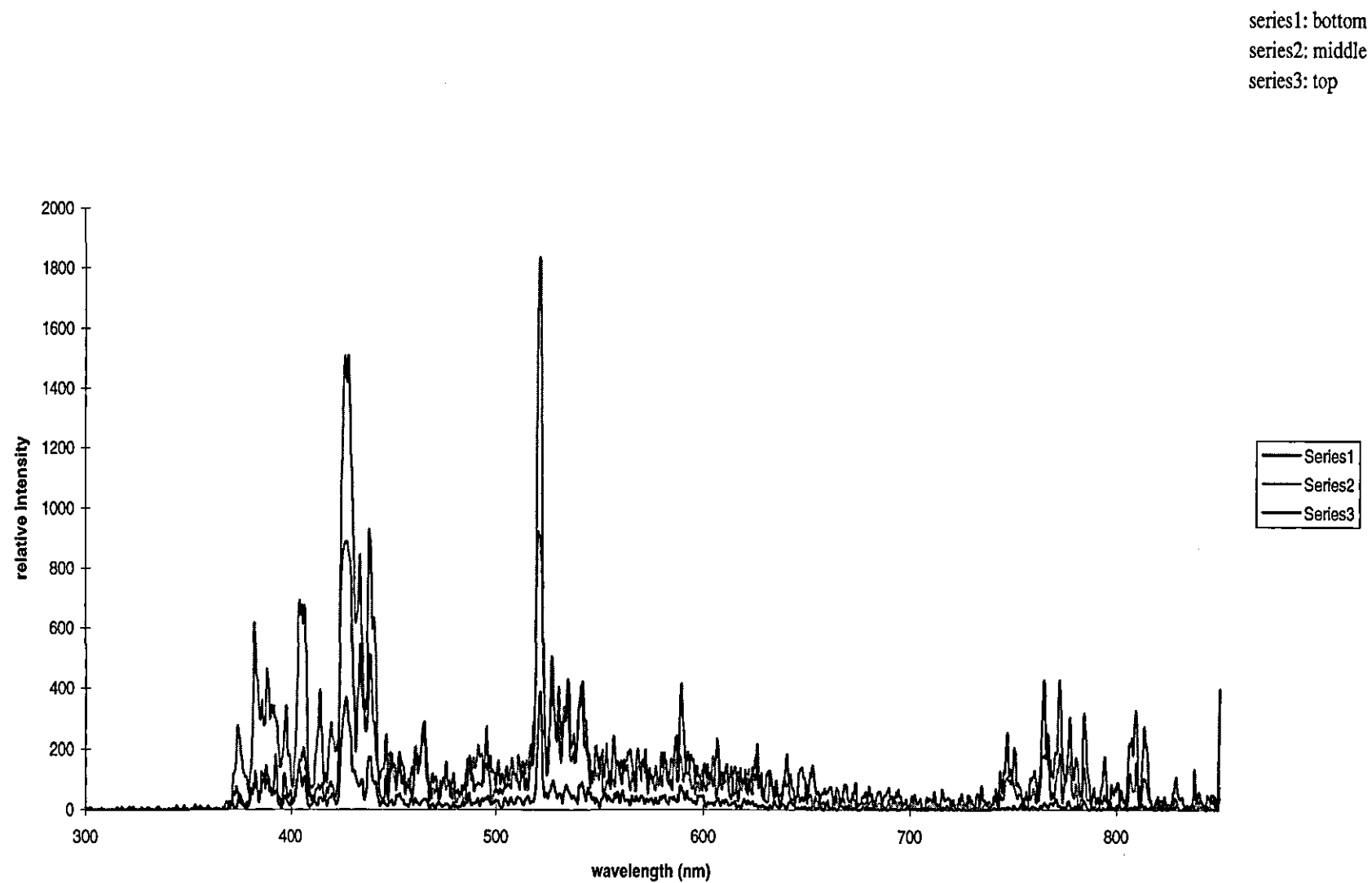


Fig. 6.12 Spectral lines from a Glydarc discharge with discharge current 1 A

the arc discharge. The emission line at the top position was slightly different from the other positions because the emission lines 750.4 nm, 763.5 nm were apparent.

#### **§6.12 Comparison of the emission lines**

Fig. 6. 13 is a schematic summary of the representative lines measured from the glow discharge and the arc discharge. The emission line 521.0 nm was only found in the glow discharge while the emission line 427.8 nm was only found in the arc discharge. A band of wavelengths in the near infra-red region were recorded for the arc discharge with a discharge current of 0.25 A at atmospheric pressure whereas the emission lines from the near infra-red to the near ultraviolet light were recorded for the arc discharge with a discharge current of 1.0 A. The emission lines 427.8 nm and 521.0 nm have been measured as characteristic of the arc discharge and the glow discharge respectively so that the Glydarc discharge was a mixture of the glow and the arc discharge because 427.8 nm and 521.0 nm existed simultaneously.

#### **§6.13 Discussion**

Several interesting points arise from the experimental results. Ar was employed in both glow and arc discharges because emission lines from Ar are well known (Table 2.2) (Wagatsuma, 1985). The emission line depends on the energy level, which is different in a glow discharge and an arc discharge according to Plank's equation. When Ar is used, the emission lines are from atomic emission lines and single ionised lines. The atomic emission lines correspond to energy differences between 11.55 - 11.83 eV and 12.90 - 13.48 eV. Fig. 6.7 shows part of the Ar energy level diagram (Bochkova et al, 1965). Among these atomic

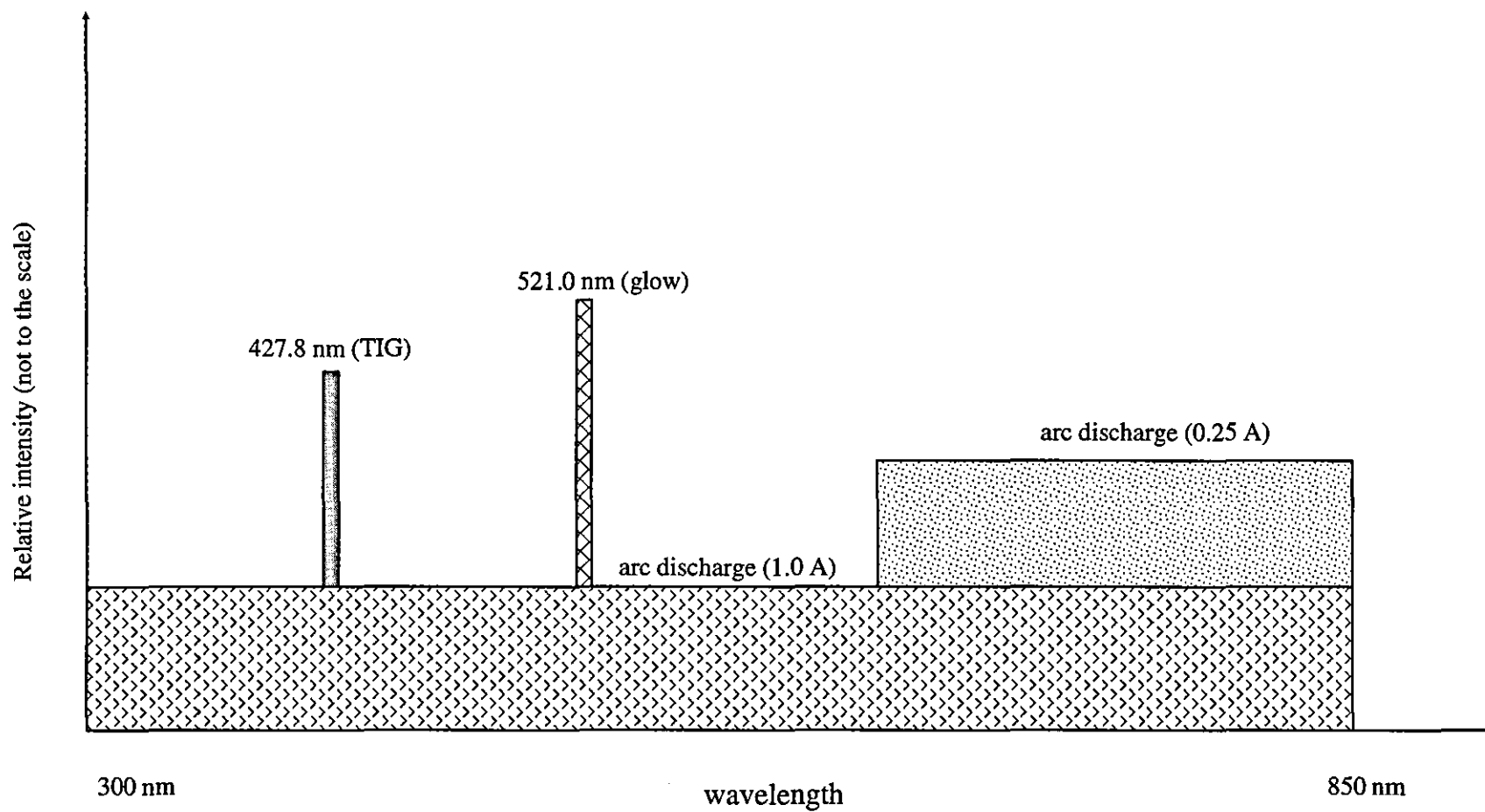


Fig. 6. 13 Schematic diagram of comprision of emission lines from the glow discharge and the arc discharge

lines Ar atomic line 415.9 nm and 420.1 nm are interesting because they have clear profiles and strong densities.

Glow discharges are effective in energy transfer among electrons and atoms and ions by electron collisions of the first and second kind. These collisions are helpful to create metastable states of atoms which will produce ionic emission lines. There are many electrons with energy of 11.5 - 11.8 eV in Ar glow discharges. This means that the atomic emission lines will be dominated from the source of the glow discharge. Ar atomic line is strongly shown. Arc discharges however produce many ions. The ions have electron energy more than 15.76 eV. This means that the ionic emission line will be dominated.

The emission lines from the Glydarc discharge show no difference with position of the discharge varied and the lines do not vary with time. This means that the emission lines from the Glydarc discharge are spatially and temporally independent i.e. the spectral lines are the same measured at any position and at any time.

Fig. 6.7 illustrates the energy level transitions for each of the emission lines measured in this series of experiments. The emission line involving  $3P_6 - 3P_4$  transitions at 521.0 nm was only apparent in the glow discharge while the emission line involving  $3P - 1S$  transition at 427.8 nm was only apparent in the arc discharge.

This suggests that the electron energy gained in the glow and in the arc discharge was different, governed by Plank's equation. These two lines are important because they are characteristic of the different discharge modes. The experimental results showed that 427.8 nm emission line and 521.0 nm emission line can be used to distinguish the discharge mode when Ar is used.



#### §6.14 Summary

A method for measurement of the spectral lines from a glow discharge and an arc discharge was developed. The experiment showed that the scanning monochromator using a slit of 0.18 mm with a photomultiplier tube provided a high resolution 1.4 nm and a high ratio of signal to noise, and a high sensitivity 60 mA/W.

The emission line 521.0 nm was only apparent from the glow discharge while the emission line 427.8 nm was only apparent from the arc discharge.

The spectral line measured from electric discharge with discharge currents (0.25 A, 0.5 A) at atmospheric pressure was dominated by the infra-red lines whereas the spectral line from a electric discharge current of 1.0 A was from near the infra-red region to the near ultraviolet lines.

The Glydarc electric discharge was the mixture of a glow discharge and an arc discharge because emission line 521.0 nm and 427.8 nm appeared.

## **Chapter Seven**

### **Conclusions and recommendations for further work**

## §7.1 Conclusions

Spectral lines from a glow discharge and an arc discharge have been investigated. The spectral lines were measured from the glow discharge in Ar at low pressure (500 Pa) and from the arc discharge with both low discharge current ( $< 2.0$  A) and high discharge current ( $> 50$  A) in Ar at atmospheric pressure. It was shown that the 427.8 nm line only occurred in the arc discharge whereas the 521.0 nm line only appeared in the glow discharge.

The transition of the glow to an arc in Ar at atmospheric pressure was studied over a range of discharge current from 0.1 A to 2.0 A. It has been shown that the spectral lines of the glow discharge was dominated by the lines from near infra-red, however the spectral lines from the arc covered all the wavelength ranging from the near UV to the near infra-red lines. The tests showed that the transition of the glow to the arc occurred at the discharge current of 0.6 A - 0.7 A.

The tests on the Glydarc electric discharge showed that both 427.8 nm and 521.0 nm lines occurred. Therefore the Glydarc electric discharge is believed to be a mixture of a glow discharge and an arc discharge. The relative calculation of the glow discharge and the arc discharge cannot be determined because of the integration of light that occurs using the scanning monochromator. The spectral lines from the Glydarc electric discharge were independent of the position of the sensor and did not vary with time.

The results indicated that in order to measure the low intensity of light from the glow discharge a spectral analyser which had a high gain ( $>10^6$ ) with low noise was required. This was achieved with a photomultiplier tube of

9 dynodes which provided high ratio of signal to noise ( $>1000$ ), a high resolution 1.4 nm and a high sensitivity of light (60 mA/W).

The effects of different gas and gas mixtures on the discharge column voltage gradient in a plasma torch have been investigated. The Saha equation has been modified for use with gas mixtures. The theoretical calculation for the electron number density and the voltage gradient was carried out for mixtures of Ar,  $N_2$  and  $O_2$  with the assumption of the local thermal equilibrium. Calculated values of the number densities of electrons in the mixtures of Ar with  $N_2$ , and Ar with  $O_2$  show no significant difference and therefore the voltage gradient with these mixtures should be approximately the same, which was shown by the experimental results. The modified Saha equation was not applied to the mixture of Ar with  $SF_6$  because the dissociation of  $SF_6$  into  $SF_5$ ,  $SF_6^+$  etc. at high temperature ( $> 5,000$  K) is not well understood and the relative amounts of  $SF_5$  and  $SF_6$  etc. can not be determined.

The experimental tests have shown that the gas mixture of Ar with  $SF_6$  has the most effect on the increase of the discharge column voltage gradient due to the strong electronegativity of  $SF_6$ . Ar with the addition of 5%  $SF_6$  by volume increased the voltage gradient to 0.5 V/mm compared with 0.3 V/mm for pure Ar. From the tests the best mixture was 89% Ar, 10%  $N_2$ , 1%  $SF_6$  based on the highest increase in voltage gradient and the lowest amount of the electronegative gas. The  $N_2$  slows down the velocity of electrons and enables  $SF_6$  which has a larger effective cross section in lower energy region ( $<2$  eV) to capture electrons more efficiently.

A mixture of Ar with N<sub>2</sub> may be used for more cost-effective where addition of N<sub>2</sub> is allowed. The results have shown that the voltage gradient with mixture of Ar and N<sub>2</sub> is 0.5 V/mm in the air tight chamber.

The simple resistance model was developed to show effects of excitation, dissociation, and ionisation and the cathode and the anode fall regions on the discharge column voltage gradient. The equation of mean free path for gas mixtures may provide a guideline when choosing the component of gases.

The characteristic of the Glydarc electric discharge in still and fast air flows has been investigated with discharge currents ranging from 100 mA to 2 A over a wide range of air flow rates (10 l/min. to 100 l/min.). The results show that the increase of the discharge voltage with increasing discharge current is due to the increase of the discharge column length which varies with time, position and the air flow rate rather than a positive V-I characteristic.

The discharge voltage between the Glydarc electrodes could not be measured directly because of the rapid fluctuation of the discharge voltage. A method was developed using measured rms values of the discharge current. The measurement error of the discharge voltage was within 10%.

Computer simulation of the Glydarc electric discharge using FLUENT has shown that the Glydarc electric discharge could interact with more of the air throughout using less divergent electrodes.

## §7.2 Further work

(1) Gas mixtures should be investigated experimentally to increase the discharge column voltage gradient further by considering the best effective cross section of different buffer gases, which can take advantage of the electronegativity of  $\text{SF}_6$ .

(a) Investigation of the relative amounts of the species such as  $\text{SF}_5$ ,  $\text{SF}_6^+$  etc. dissociated from mixture of Ar with  $\text{SF}_6$  using spectroscopy in the plasma torch.

(b) Study of the decrease of the number density of electrons with added gases in the discharge column using spectroscopy.

(2) Suitable spectral lines should be found to determine between a glow and an arc discharge in other gases such as  $\text{N}_2$ ,  $\text{O}_2$  and air at atmospheric pressure.

(3) Determination of the ratio of the glow discharge and the arc discharge in the Glydarc using non-scanning monochromator.

(4) Development of the spectral analyser using the existing equipment with a photomultiplier to study the voltage gradient of the electric discharge by Stark effect.

## References

Aarts, C. J. M. (1952). ' Investigation of an Arc Discharge which is Stabilized with a Screwshape Stream of Air '. Ph.D. thesis, University of Utrecht.

Aston, F. W. (1923). **Proceedings of Royal Society**. London.

Barbeau, J. and Jolly, J. (1991). ' Electric Field Measurement in the Cathode Sheath of a Hydrogen Glow Discharge '. **Applied Physics Letter**. 58(3), 237-239.

Bengston, R. D. (1963). Ph. D. thesis. University of Maryland, USA.

Beynon, J. (1972). **The Conduction of Electricity through Gases**. London, George G. Harrap & Co. Ltd.

Bhaumik, M. L.; Lacina, W. B. and Mann, M. M. (1972). ' Characteristics of CO Laser '. **IEEE Journal of Quantum Electronics**. QE8(2), 150-160.

Birdsall, C. K. and Langdon, A. B. (1985). **Plasma Physics via Computer Simulation**. New York, McGraw-Hill Book Company, Inc.

Bochkova, O. P. and Shreyder, E. YA. (1965). **Spectroscopic Analysis of Gas Mixtures**. New York, Academic Press.

Boumans, P. (1966). **Theory of Spectral Chemical Excitation**. London, Hilger & Watts Ltd.

Bricknell, A. C. and Patchett, B. M. (1985). ' GMA Welding of Aluminium with Argon/Freon Shielding Gas Mixtures '. **Welding Journal**. 64(5), 21-27

Bridge, T. J. and Patel, C. K. (1965). ' High-Power Brewster Window Laser at 10.6 Microns '. **Applied Physics Letter**. 7(11), 244-245.



Brown, S. C. (1967). **Basic Data of Plasma Physics, 1966 (2nd. ed. revised)**. Cambridge, Massachusetts, The M. I. T. Press.

Brunet, H. and Rocca-Serra, J. (1985). ' Model for a Glow Discharge in Flowing Nitrogen '. **Journal of Applied Physics**. 57(5), 1574-1581.

Bullis, R. H.; Nigham, W. L.; Fowler, M. C. and Wiegand, W. J. (1972), ' Physics of CO<sub>2</sub> Electric Discharge Lasers '. **AIAA Journal**. 10(4), 407-414.

Cambel, A. B. (1963). **Plasma Physics and Magnetofluid-mechanics**. New York, McGraw-Hill Book Company, Inc.

Chapman, S. and Cowling, T. G. (1970). **The Mathematical Theory of Non Uniform Gases(3rd edn.)**. Cambridge, Cambridge University Press.

Chaundy, C. F. J. (1954). ' The Anode Fall in a Glow Discharge '. **British Journal of Applied Physics**. 5, 255-256.

Chien, Y. K. and Benenson, D. M. (1980). **IEEE Transaction on Plasma Science**. PS-8, 441-471.

Christophorou, L. G.(1992). ' Breakdown Potential '. **McGraw-Hill Encyclopedia of Science & Technology (7th edn.)** 3, 45. New York, McGraw-Hill, Inc.

Christophorou, L. G. and Van Brunt, R. J. (1995). ' SF<sub>6</sub>/N<sub>2</sub> Mixtures '. **IEEE Transactions on Dielectrics and Electrical Insulation**. 2(5), 952-988

Corliss, C. H. (1970). ' Review of Oscillator Strengths for Lines of Cu I '. **Journal of Research of the National Bureau**

of Standards, Section A. Physics and Chemistry. 74A(6), 781-790.

Cormier, J. M.; Richard, F. and Chapelle, J. (1995). ' Gliding Arc Used as a Plasma Source '. **Proceedings of VDI Berichte**. 239-246

Czernichowski, A. and Lesueur, H. (1991). ' Low Temperature Incineration of Some Volatile Organic Compounds by Gliding Discharge under Atmospheric Pressure '. **Proceedings of 10th International Symposium on Plasma Chemistry**. Bochum, Germany.

Czernichowski, A. (1993). ' Gliding Discharge Reactor for H<sub>2</sub>S Valorization or Destruction '. In name of Penetrante, B. M.; and Schultheis, S. E. (ed.). **Non-Thermal Plasma Technologies for Pollution Control, Part B: Electron Beam and Electrical Discharge Processing**. New York, Springer-Verlag.

Czernichowski, A. (1994). ' Gliding Arc: Application to Engineering and Environment Control '. **Pure and Applied Chemistry**. 66(6), 1301-1310

DeMaria, A. J. (1973). ' Review of CW High-Power CO<sub>2</sub> Lasers '. **Proceedings of IEEE**. 61(6), 731-748.

Detusch, T. F.; Horrigan, F. A. and Rudko, R. I. (1969). ' CW Operation of High-Pressure Flowing CO<sub>2</sub> Lasers '. **Applied Physics Letter**. 15(3), 88-91.

Eberhagen, A. (1955). ' Eine quantitative Untersuchung der Lenardschen Hohlflammen '. **Zeitschrift fuer Physik**. 143, 312

Echer, G.; Kröll, W. and Zöllner, O. (1964). ' Thermal Instability of the Plasma Column '. **Physics of Fluids**. 7(12), 2001-2006.

Eckbreth, A. C. and Davis, J. W. (1972). ' The Cross-Beam Electric-Discharge Convection Laser '. **IEEE Journal of Quantum Electronics**. QE-8(2), 139-144

Eckbreth, A. C. and Owen, F. S. (1972). ' Flow Conditioning in Electric Discharge Convection Lasers '. **Review of Scientific Instruments**. 43(17), 995-998.

Evans, D. R.; Harry, J. E. and Yahya, Y. (1989). **Proceedings of Symposium on Plasma Processing and Synthesis of Material**, Italy

Finkelburg, W. and Maecker, H. (1956). ' Elektrische Bögen und thermisches Plasma '. **Handbuch Physik**. Berlin, Springer-Verlag.

**Fluent User's Manual(version 3.0)**

Flügge, S.(eds) (1956). **Encyclopedia of Physics (Vol. XXII)**. Berlin, Springer-Verlag.

Francis, G. (1956). ' The Glow Discharge at Low Pressure '. In Flügge, S.(eds) (1956). **Encyclopedia of Physics (Vol. XXII)**. Berlin, Springer-Verlag.

Fridman, A.; Chapelle, J.; Czernichowski, A.; Lesueur, H. and Stevefelt, J. (1993). ' Model of the Sliding Arc ---- Applications in Plasma Chemistry '. **Proceedings of 11th International Symposium on Plasma Chemistry**. 257-263

Fukui, T; Sugiyama, Y. and Terai, S. (1970). ' Effects of Nitrogen, Oxygen and Hydrogen Gases Added to Argon on MIG-

Welding of Aluminum alloys '. **Transactions of Japanese Welding Society**. 1(1), 19-27.

de Galan, L. (1965). ' Particle Distribution in the d.c. Carbon Arc '. Ph. D. thesis, University of Amsterdam.

de Galan, L. and Boumans, P. W. J. M. (1966). ' Theoretical Calculation of Transport of Metal Vapour through Discharge Column of Direct Current Arc '. **Analytical Chemistry**. 38(6), 674-681.

Galeev, I. G.; Goncharov, V. E.; Timerkaev, B. A.; Toropov, V. G. and Faskhutdinov, A. Kh. (1990). ' Special Features of a Glow Discharge in Supersonic Gas Flow '. **High Temperature**. 28(5), 623-626.

Gentle, K. W.; Ingard, U. and Bekefi, G. (1964). ' Physics Effect of Gas on Properties of a Plasma column '. **Nature**. 203(4952), 1369-1370.

Griem, H. (1964). **Plasma Spectroscopy**. London, McGraw-Hill.

Griffing, L. (1971). **Welding Handbook (6th ed.)**. New York, American Welding Society

Guile, A. E. (1986). ' The Electric Arc '. In Lancaster, J. F.(ed.). **The Physics of Welding**. Oxford, Pergamon Press.

Harry, J. E. (1965). ' Measurement of Electric Parameters of AC Arcs '. **IEEE Transactions on Industry and General Applications**. IGA-5(5), 594-599.

Harry, J. E. and Evans, D. R. (1987). ' A Large Bore Fast Axial Flow CO<sub>2</sub> Laser '. **IEEE Journal of Quantum Electronics**. QE-24(3), 503-506.

Harry, J. E. and Yahya, A. (1990). ' Chemical Synthesis and Waste Destruction Using High Power Glow Discharges '. **Proceedings of Plasma for Industry and Environment**. Oxford, British National Committee for Electroheat.

Harry, J. E. (1993a). ' The Destruction of Waste and Toxic Materials Using Electric Discharges '. **Engineering Science and Education Journal**. 2(4), 171-176.

Harry, J. E. (1993b). **Electric Discharges for Heating**. London, The British National Committee for Electroheat.

Harry, J. E. and Yuan, Q. (1993). ' Reduction of Breakdown Voltage of Atmospheric Pressure Arc Discharges in the Glydarc Process Using an Auxilliary Supply and Electrode '. **Proceedings of 11th International Symposium on Plasma Chemistry**.

Harry, J. E. and Yuan, Q. (1995). ' The Use of Gas Mixtures in a DC Plasma Torch to Increase the Operating Voltage, while Maintaining Stability, and Application to an Inflight Reactor '. **Proceedings of 12th International Symposium on Plasma Chemistry**.

Harry, J. E.; Yuan, Q. and M. Dubus (1995). ' Interaction Between Subsonic Gas Flow and a Glydarc Electric Discharge '. **Proceedings of 12th International Symposium on Plasma Chemistry**.

Hill, A. E. (1971). ' Uniform Electrical Excitation of Large-Volume High-Pressure Near-Sonic  $\text{CO}_2\text{-N}_2\text{-H}_2$  Flow Stream '. **Applied Physics Letter**. 18(15), 194-197.

Housby-Smith, C. and Jenkins, J. E. (1978). **Arc Research Report ULAP-T54**. University of Liverpool.

Hörman, H. (1935). ' Temperaturverteilung und Eleckronenedische in frei grennenden Lichtbögen '. **Zeitschrift fuer Physik.** 97, 539.

Huang, P. C. and Pfender, E. (1991). ' Study of a Transferred-Arc Reactor with a Converging Wall and Flow through a Hollow Cathode '. **Plasma Chemicals and Plasma Processes.** 11(1), 129-150.

Hughs, T.P. (1975). **Plasma and Laser Light.** London, Adam Hilger.

Ikeda, H.; Jones, G. R.; Irie, M. and Prsad, A. N. (1982). **Proceedings of VI International Conference on Gas Discharge and Their Applications.** 5-8. London.

Jones, G. R. (1988). **High Pressure Arcs in Industrial Devices.** Cambridge, Cambridge University Press.

Karditsas, P. J. (1990). ' A Helium Discharge with Neutral Gas Flow: Theoretical Calculation '. **Journal of Applied Physics.** 68(6), 2674-2686.

Kaufmann, W. (1900). ' Elektrodynamische eigentumlichkkeiten leitender gase '. **Ann. Phys.** 2(4), 158.

Kennedy, C. R. (1970). ' Gas Mixtures for Welding '. **Australian Welding Journal.** 2, 23-32.

Kock, M. and Richter, J. (1968). **Zeitschrift für Astrophysik.** 69, 180-192.

King, L. A. (1961). ' The Voltage Gradient of the Free Burning Arc in Air or Nitrogen '. **Proceedings of 5th International Conference on Ionisation Phenomena Gases.** Munich, Germany.

King, L. A. (1964). ' The Voltage Gradient of an Arc Column under Forced Convection in Air or Nitrogen '. **Research Report of the Electrical Research Association** (Report No. 5072), Surry, England.

King, L. A. (1965). **Colloquium on 'Spectrosc'**. International VI, Amsterdam, London, Pergamon Press.

Kirkpatrick, K. (1989). ' Welding with Lasers '. **Welding and Metal Fabrication**. 57(7), 294-298.

Knight, R. (1984). ' Multiple Electric Arc Discharge '. Ph.D. Thesis. Loughborough University of Technology.

Kuhlman, J. M.; Modlen, G. M. Srinivasan, S.; Nam, H. and Tiwari, S. N. (1986). ' Arc Generated Flow Phenomena in Repetitively Pulsed Gas-Flow Spark Gaps '. **IEEE Transactions on Plasma and Science**. PS-14(2), 228-233.

Lancaster, J. F. (ed.). (1986). **The Physics of Welding** (2nd edn.) Oxford, Pergamon Press.

Lapworth, K. C. (1974). **Journal of Physics E: Scientific Instrument**. 7, 413-420.

Largoche, G.; Orfeuill, M. and Caseau, P. (1991). **Les plasmas dans l'industrie**. Paris, Electricite De France.

Lesueur, H.; Czernichowski, A. and Chapelle, J. (1988). ' DC or AC High Pressure Discharges and Electroburner Applications '. **Proceedings of 9th International Conference on Gas Discharges and Their Applications**. 549-552

Little, P. F. and von Engle, A. (1952). **Proceedings of Physics Society**, London. 65, 459.

Maeker, H. (1956). **Annales de Physik**. 6, 441-446.

Mannkopf, R. (1943). ' Die Berechnung der Lichtbogentemperatur und das Stabilitätsproblem der Lichtbogensäule '. **Zeitschrift fuer Physik**. 70, 444.

McTaggart, F. K. (1967). **Plasma Chemistry in Electrical Discharges**. London, Elsevier Publishing Company.

Mierdel, G. (1929). **Handbuch der experimentalphysik**. Leipzig, Springer.

Moeller, G. and Rigden, J. D. (1965). ' High-Power Laser and in a Cold Discharge Action in CO<sub>2</sub>-He mixtures '. **Applied Physics Letter**. 7(11), 290-292.

Mondain-Monval (1973). ' The physical properties of fluids at elevated temperatures '. **International Institute of Welding Document**. 212-264.

Moore, C. E. (1948). **Atomic Energy Level**. Washington DC, National Bureau of Standards.

Müller, S. and Uhlenbush, J. (1987). ' Influence of Turbulence and Convection on the Output of a High-Power CO<sub>2</sub> Laser with a Fast Axial Flow '. **Journal of Applied Physics D: Applied Physics**. 20, 697-708.

Nighan, W. L. and Wiegand, W. J. (1964). ' Cause of Arcing in CW CO<sub>2</sub> Convection Laser Discharges '. **Applied Physics Letter**. 25(11), 633-636.

Norrish, J. (1974). ' High Deposition MIG Welding with Electrode Negative Polarity '. **Proceedings of 3rd Conference on Advances in Welding Processes**. Cambridge, England.

Raizer Yu. P. (1977). **Laser-induced Discharge Phenomena**. New York, Consultants Bureau.



Roberts, D. E. (1972). **Arc Research Report ULAP-T8**.  
Liverpool University.

Rubtsov, N. A. and Ourrechnikova, N. M. (1988). 'Calculation of Electric Arc Interaction with a Turbulent Gas Flow'. **Journal of Engineering Physics**. 54(4), 373-378.

Saha, M. M. (1920). 'Ionisation in the Solar Chromosphere'. **Philosophy of Magazine**. 40(238), 472

Saiepour, M. and Harry, J. E. (1991). 'Temporary Arc Discharges Resulting from Glow-to-Arc Transitions and Effect of Power Supply Parameters'. **International Journal of Electronics**. 70(2), 459-465.

Schwartz, M. M. (1969). **Modern Metal Joining Techniques**.  
New York, John Wiley

Seguin, V. A.; Capjack, C. E. and Seguin, H. (1987). 'Numerical Simulation of Gas Flow in a Magnetically Stabilized Coaxial Laser Discharge'. **Applied Physics B**, 42, 239-244.

Shepherd, W. and Zand, P. (1979). **Energy Flow and Power Factor in Nonsinusoidal Circuits**. Cambridge, Cambridge University Press.

Shirahata, H. and Fujisawa, A. (1973). 'Aerodynamically Mixed Electric CO<sub>2</sub> Laser'. **Applied Physics Letter**. 23, 80-81.

Shwartz, J. and Margalith, E. (1974). 'On the Gas Temperature in Coaxial Electric Discharge CO<sub>2</sub> Flow Lasers'. **Journal of Applied Physics**. 45(10), 4469-4476 .

Shwartz, J. and Lavie, Y. (1975). 'Effects of Turbulent on a Weakly Ionized Column'. **AIAA Journal**. 13(5), 647-652.

Smith, M. R.; Jones, G. R.; Housby-Smith, C.; Barrault, M. R. El-Menshawy, M. F. and Jenkins, J. E. (1978). **Arc Research Report ULAP-T61. University of Liverpool.**

Somers, P. J. and Smit, J. A. (1956). 'Measurements on Arc Discharge in Nitrogen at 1 atm and higher pressure'. **Applied Scientific Research.** 6, 75

Stein, R. P. (1953). **Physics Review.** 89, 134.

Stenbaka, N. and Person, K. A. (1987). 'Shielding Gases for Gas-Metal Arc Welding of Stainless Steel'. **Scandinavian Journal of Metallurgy.** 16(5), 229-232.

Stenbeng, W. (1931). **Ann. Phys.** 10, 296.

Suits, G. C. (1934). 'Experiments with Arcs at Atmospheric Pressure'. **Physics Review.** 46, 252

Suits, G. C. (1939). 'High Pressure Arcs'. **Physics Review.** 55, 561

Thomson, J. J. and Thomsom, G. P. (1933). **Conduction of Electricity through Gases (3rd edn.)**. Cambridge, Cambridge University.

Thornton, M. F. (1993). 'Spectroscopic Determination of Temperature Distributions for a TIG Arc'. **Journal of Physics D: Applied Physics.** 26, 1432-1438.

Tiffany, W. B. and Foster, J. D. (1969), 'Kilowatt CO<sub>2</sub> Gas-Transport Laser'. **Applied Physics Letter.** 15(3), 91-93.

Virens, L.; Smeets, A. H. M. and Cornelissen, H. J. (1982). 'Modelling of a Glow Discharge'. In Kunhardt, E. E. and Lussen, L. H. (ed.), **Electrical Breakdown and Discharges in**

**Gases: Macroscopic Processes and Discharges.** New York, Plenum Press

Von Engel, A. (1965). **Ionized Gases**(2nd. edn.). Oxford, Clarendon.

Von Engel, A. (1983). **Electric Plasmas: Their Nature and Uses.** London, Taylor & Francis Ltd.

Wagatsuma, K. and Hirokawa, K. (1985) ' Characterization of Atomic Emission Lines from Argon, Neon, and Nitrogen Glow Discharge Plasmas '. **Analytical Chemistry.** 57 (14), 2901-2907.

Wasserstrom, E.; Crispin, Y.; Rom, J. and Shwartz, J. (1978). ' The Interaction between Electrical Discharges and Gas Flow '. **Journal of Applied Physics.** 49(1), 81-86.

Wiese, W. L.; Smith, M. W. and Glenon, B. M. (1966). **Atomic Transition Probabilities** (Vol. 1). National Bureau Standards, Washington, D.C. USA.

Wilson, J. (1966). ' Nitrogen Laser Action in a Supersonic Flow '. **Applied Physics Letter.** 8(7), 159-161.

Wu, C. and Kunhardt, E. E. (1988). ' Formation and Propagation of Streamers in  $N_2$  and  $N_2$ - $SF_6$  Mixtures '. **Physics Review A.** 37(11), 4396-4406.

Yahya, A. (1990) Ph.D. Thesis, Loughborough University of Technology.

Yamamoto, T.; Mizuno, K.; Tamori, I.; Ogata, A.; Nifuku, M.; Michalska, M. and Prieto, G. (1996). ' Catalysis-Assisted Plasma Technology for Carbon Tetrachloride Destruction '. **IEEE Transaction on Industry Applications.** 32(1), 100-106.

Zemansky, M. W. (1957). **Heat and Thermodynamics**. New York, McGraw-Hill Book Company, Inc.

**Users guide to operating the photomultiplier tube accessory models 6030 A/B**, Rofin Ltd. 1982.

**Chart recorder interface model 6020 instruction manual**, Rofin Ltd. 1981.

**Users guide to operating the "UV-VIS" spectralyser model 6000/6000 LG**, Rofin Ltd. 1982.

**Users guide to operating the wavelength marker accessory (model 6001)**, Rofin Ltd. 1982.

**Sample and hold (Model No. 6003) instruction manual**, Rofin Ltd. 1980.

**Wavelength calibration charts for use with model 6000 monochromator and model 6001 wavelength marker unit**, Rofin Ltd. 1982.

# **Appendices**

## Appendix A

### The programme of the PSPICE simulation for an electric discharge

```
DISCHARGE CIRCUIT SIMULATION
VS 1 0 SIN(0 8500 50 0)
R1 1 2 2000
R2 3 0 1E6
L1 2 3 1H
D1 5 3 D1N7510
.MODEL D1N7510 D (IS=880.5E-18 RS=.25 IKF=0 N=1 XTI=3
EG=1.11 CJO=0
+ M=.5516 VJ=.75 FC=.5 ISR=1.859N NR=2 BV=1000 IBV=1M
NBV=1.6989
+ IBVL=1.9556M NBVL=14.976 TBV1=-21.277U)
D2 5 0 D1N7510
.TRAN 0.2M 60M
.PLOT TRAN V(3) I(VS)
.END
```

## Appendix B

### The program for the calculation of the number density of electrons and the electric field

```
*      PROGRAM FOR ELECTRON DENSITY IN THE MIXTURE OF ARGON
*      AND NITROGEN
*      USING C05NBF OF NAG MARK 14
*      .. PARAMETERS..
      INTEGER N, LWA
      PARAMETER (N=10, LWA=(N*(3*N+13))/2)
*      .. LOCAL SCALARS..
      DOUBLE PRECISION FNORM, TOL, ENE
      INTEGER I, IFAIL, J
*      .. LOCAL ARRAYS..
      DOUBLE PRECISION FVEC(N), WA(LWA), X(N)
*      .. EXTERNAL FUNCTIONS..
      DOUBLE PRECISION F06EJF, X02AJF
      EXTERNAL F06EJF, X02AJF
*      ..EXTERNAL SUBROUTINES..
      EXTERNAL C05NBF, FCN
      DOUBLE PRECISION U1(N), U2(N), PAI, P, EME, H, C, BKB, T, EE
      DOUBLE PRECISION DI, UE, E
      INTEGER IR, IS
      PARAMETER (IR=4, IS=IR+1)
      INTEGER IAG(IR, IS), ING(IR, IS)
      DOUBLE PRECISION ALAMB(IR, IS), NLAMB(IR, IS), U(IR, IS)
```

```

DOUBLE PRECISION D(IR,IS), Z(IR,IS)
DOUBLE PRECISION D11,D12,D21,D22,D31,D32
COMMON D11,D21,D12,D22,D32,D31
*   ..INTRINSIC FUNCTIONS..
INTRINSIC SQRT
*   .. EXCUTABE STATEMENTS..
WRITE(*,*) 'C05NBF EXAMPLE RESULTS'
*   THE FOLLOWING STARTING VALUES PROVIDE A ROUGH
SOLUTION
      DO 20 J=1, N
      X(J)=0.010
20    CONTINUE
      PAI=3.1415926
      P=1.013E5
      BKB=1.38E-23
      EME=9.108E-31
      T=5000.0
      H=6.63E-34
      C=2.998E10
      ALAMB(1,2)=93143.8
      ALAMB(1,3)=93750.639
      ALAMB(1,4)=94553.707
      ALAMB(2,3)=1432.0
      ALAMB(2,4)=108723.5
      ALAMB(3,4)=1112.4
      ALAMB(3,5)=1570.2
      ALAMB(4,5)=21090.0
      IAG(1,1)=1
      IAG(1,2)=5
      IAG(1,3)=3

```



```

      IAG(1,4)=1
      IAG(2,2)=4
      IAG(2,3)=2
      IAG(2,4)=2
      IAG(3,3)=5
      IAG(3,4)=3
      IAG(3,5)=1
      IAG(4,4)=4
      IAG(4,5)=4
      DO 30 III=1, 4
      DO 40 JJJ=III, 5
      IF (JJJ.EQ.III) U(III,JJJ)=0.0
      U(III,JJJ)=H*C*ALAMB(III,JJJ)
      write(*,*)'u(i,j)=' ,u(iii,jjj)
40    CONTINUE
30    CONTINUE
      DO 35 KK=1, 4
      Z(KK,1)=0.0
35    CONTINUE
      DO 50 K=1, 4
      DO 60 L=K, 5
      Z(K,1)=Z(K,1)+ IAG(K,L)*EXP(-U(K,L)/BKB/T)
60    CONTINUE
      write(*,*)'k=' ,k
      write(*,*)'z(k,1)' ,z(k,1)
50    CONTINUE
      U1(2)=15.755
      U1(3)=27.62
      U1(4)=40.9
      DO 70 II=1, 3

```

```

mm=II+1
D(II,1)=(2.0*PAI*EME/H/H)**(1.5)*(BKB*T)**2.5/
*P*2.0*Z(mm,1)/Z(II,1)*EXP(-U1(mm)*1.609E-19/(BKB*T))
write(*,*)'ii=',ii
write(*,*)'d(ii,1)=' ,d(ii,1)
70  CONTINUE
*   CALCULATE NITROGEN
NLAMB(1,2)=19223.0
NLAMB(1,3)=19231.0
NLAMB(1,4)=28840.0
NLAMB(2,3)=49.1
NLAMB(2,4)=131.3
NLAMB(3,4)=174.5
NLAMB(3,5)=57192.1
NLAMB(4,5)=67136.4
ING(1,1)=4
ING(1,2)=6
ING(1,3)=4
ING(1,4)=4
ING(2,2)=2
ING(2,3)=4
ING(2,4)=2
ING(3,3)=2
ING(3,4)=4
ING(3,5)=2
ING(4,4)=1
ING(4,5)=1
DO 80 I1=1, 4
DO 90 J1=I1, 5
IF (J1.EQ.I1) U(I1,J1)=0.0

```

```

        U(I1,J1)=0.0
        U(I1,J1)=H*C*NLAMB(I1,J1)
90      CONTINUE
80      CONTINUE
        DO 100 I2=1, 4
        Z(I2,2)=0.0
100     CONTINUE
        DO 120 I3=1, 4
        DO 130 J3=I3, 5
        Z(I3,2)=Z(I3,2)+ING(I3,J3)*EXP(-U(I3,J3)/BKB/T)
130     CONTINUE
        write(*,*)'i3=',i3
        write(*,*)'z(i3,2)=' ,z(i3,2)
120     CONTINUE
        U2(2)=14.54
        U2(3)=29.605
        U2(4)=47.426
        DO 140 I4=1, 3
        ii=i4+1
        D(I4,2)=(2.0*PAI*EME/H/H)**1.5*(BKB*T)**2.5/P*2.0*
*          Z(ii,2)/Z(I4,2)*EXP(-U2(ii)*1.609E-19/BKB/T)
        write(*,*)'i4=',i4
        write(*,*)'d(i4+1,2)=' ,d(i4,2)
140     CONTINUE
        D11=D(1,1)
        D12=D(1,2)
        D21=D(2,1)
        D22=D(2,2)
        D31=D(3,1)
        D32=D(3,2)

```

```

write(*,*)'d11=',d11
write(*,*)'d12=',d12
write(*,*)'d21=',d21
write(*,*)'d22=',d22
write(*,*)'d31=',d31
write(*,*)'d32=',d32
TOL=SQRT(X02AJF())
IFAIL=1
CALL C05NBF(FCN,N,X,FVEC,TOL,WA,LWA,IFAIL)
IF (IFAIL.EQ.0) THEN
  FNORM=F06EJF(N,FVEC,1)
  WRITE(*, 99999)'FINAL 2-NORM OF THE RESIDUALS=',FNORM
  WRITE(*,*)
  WRITE(*,*)'FINAL APPROXIMATE SOLUTION'
  WRITE(*,*)
  WRITE(*,99998)(X(J),J=1,N)
ELSE
  WRITE(*,99997)'IFAIL=',IFAIL
  IF (IFAIL.GT.1) THEN
    WRITE(*,*)
    WRITE(*,*)'APPROXIMATE SOLUTION'
    WRITE(*,*)
    WRITE(*,99998)(X(I),I=1,N)
  END IF
END IF
ENE=P/BKB*X(1)/T
WRITE(*,99996)ENE
UE=2.9*1.0E5/76.0
EE=1.602*1.0E-19
DO 150 JD=1, 10

```

```

E=JD*1.0E4/EE/ENE/UE
DI=JD*1.0E4
WRITE (*,99999) 'J=',DI
WRITE(*,99999) 'E=',E
WRITE(*,*)
150  CONTINUE
      STOP
99999 FORMAT(1X,A,E12.4)
99998 FORMAT(1X,3F12.9)
99997 FORMAT(1X,A,I2)
99996 FORMAT('Ne=',E16.10)
      END
*
      SUBROUTINE FCN(N,X,FVEC,IFLAG)
*
      ..PARAMETERS.. DEFINE VOLUME RATION..
      DOUBLE PRECISION DELTA2
      PARAMETER (DELTA2=0.250)
*
      ..SCALAR ARGUMENTS..
      INTEGER IFLAG,N
*
      ..ARRAY ARGUMENTS..
      DOUBLE PRECISION FVEC(N), X(N)
*
      ..EXECUTABLE STATEMENTS..
      DOUBLE PRECISION D11, D21, D12, D22, D32, D31
      COMMON D11,D21,D12,D22,D32,D31
      write(*,*) '*d11=',d11
      write(*,*) '*d12=',d12
      write(*,*) '*d21=',d21
      write(*,*) '*d22=',d22
      write(*,*) '*d31=',d31
      write(*,*) '*d32=',d32

```

```

FVEC(1)=X(1)-X(10)/(1+X(10))
write(*,*)'fvec(1)=',fvec(1)
FVEC(2)=X(1)*X(4)/X(2)-D11
write(*,*)'fvec(2)=',fvec(2)
FVEC(3)=X(1)*X(6)/X(4)-D21
write(*,*)'fvec(3)=',fvec(3)
FVEC(4)=X(1)*X(5)/X(3)-D12
write(*,*)'fvec(4)=',fvec(4)
FVEC(5)=X(1)*X(7)/X(5)-D22
write(*,*)'fvec(5)=',fvec(5)
FVEC(6)=X(1)*X(8)/X(6)-D31
write(*,*)'fvec(6)=',fvec(6)
FVEC(7)=X(1)*X(9)/X(7)-D32
write(*,*)'fvec(7)=',fvec(7)
FVEC(8)=1-(X(2)+X(4)+X(6)+X(8))
write(*,*)'fvec(8)=',fvec(8)
FVEC(9)=1-(X(3)+X(5)+X(7)+X(9))
write(*,*)'fvec(9)=',fvec(9)
FVEC(10)=X(10)-(X(4)+2.0*X(6)+3.0*X(8)+DELTA2*(X(5)+
*          2.0*X(7)+3.0*X(9)))/(1.0+delta2)
write(*,*)'fvec(10)=',fvec(10)
RETURN
END

```

## Appendix C

### Number density of electrons in a single ionised gas

The calculation of the number density of electrons in single ionised gas is a basis for multi-step ionised gases.

Assume  $n_1$  is the number density of single ionised particles; and  $n_0$  the number density of neutral particles and  $n_H$  the number density of heavy particles, there exists

$$n_H = n_0 + n_1$$

The number density of electrons is equal to the number density of single ionised particles

$$n_e = n_1$$

The degree of single ionisation is defined as

$$\alpha_1 = \frac{n_1}{n_H} = \frac{n_e}{n_H}$$

From the perfect gas equation, it follows

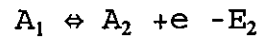
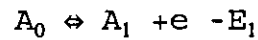
$$p = (n_e + n_H)kT$$

$$n_e = \frac{\alpha_1}{1 + \alpha_1} \frac{p}{kT}$$

Therefore the number density of electrons can be calculated if the degree of ionisation is known.

### Number density of electrons in single and double ionised gas and general formula

The ionisation reactions for both single and double ionised gas are written as:



Assume  $n_2$  is the number density of double ionised particles. Therefore the perfect gas equation is expressed as:

$$p = (n_e + n_0 + n_1 + n_2)k$$

For single and double ionisation of gas, the first and the second degrees of ionisation are

$$\alpha_1 = \frac{n_1}{n_H}$$

$$\alpha_2 = \frac{n_2}{n_H}$$

$$n_H = n_0 + n_1 + n_2$$



$$n_e = n_1 + 2n_2 = (\alpha_1 + 2\alpha_2)n_H$$

$$n_e = \frac{\alpha_1 + 2\alpha_2}{1 + \alpha_1 + 2\alpha_2} \frac{p}{kT}$$

In general  $n_e$  can be expressed as:

$$n_e = \frac{\alpha_e}{1 + \alpha_e} \frac{p}{kT}$$

$$\alpha_e = \sum_{i=1}^m i\alpha_i$$

$$\alpha_i = \frac{n_i}{n_H}$$

$$i = 1, 2, \dots, m$$

## Reference

Cambel, A. B. (1963). Plasma Physics and Magnetofluid-mechanics. New York, McGraw-Hill Book Company, Inc.

## Appendix D

### Specification of MultiSpec™ 1/8 M monochromator.

#### Specifications

Detector:	Photo diode array (25 mm length with 1,024 element arrays)
Focal length:	120 mm
Effective Aperture:	F/3.7
Usable Wavelength Range:	180 nm to 24 $\mu$ m
Wavelength Accuracy:	1 nm over the full range
Wavelength Reproducibility:	1 nm
Resolution:	0.4 nm with the slit of 25 $\mu$ m by 3 mm, 1200 l/mm grating
Dimension:	152 x 140 x 76 mm
Weight:	1.5 kg

